Reproduction and Seed Development in the Water Lily Nymphaea Thermarum – a New Perspective on the Evolution of Flowering Plant Seeds

Reproduction and Seed Development in the Water Lily *Nymphaea thermarum* – a New Perspective on the Evolution of Flowering Plant Seeds

A dissertation presented

by

Rebecca Ann Povilus

to

The Department of Organismic and Evolutionary Biology

In partial fulfillment of the requirements

for the degree of

Doctor of Philosophy

in the subject of

Biology

Harvard University

Cambridge, Massachusettes

July 2017

Dissertation Advisor: Professor William Friedman Rebecca Ann Povilus

Reproduction and Seed Development in the Water Lily *Nymphaea thermarum* –
a New Perspective on the Evolution of Flowering Plant Seeds

Abstract

Almost a century of research connects the origin of double fertilization, a major evolutionary innovation of flowering plants (angiosperms), to conflicting parental interests over offspring provisioning during seed development. Furthermore, work in a small handful of model systems has revealed that imprinting, an epigenetic phenomena based on chromatin methylation patterns, underlies key components of parent-of-origin effects on seed development. However, neither parent-of-origin effects on development nor genetic imprinting have been studied in any early-diverging angiosperm lineage – hindering our understanding of the evolutionary relationships between interparental conflict, parent-of-origin-effects, and chromatin methylation. For my dissertation I identified and leveraged the experimental tractability of the water lily *Nymphaea thermarum* (Nymphaeales) to perform reciprocal interploidy crosses and to document patterns of gene expression related to chromatin methylation during reproductive development.

In Chapter 1, we describe the floral biology, female reproductive development, fertilization, and seed ontogeny of *N. thermarum*, and thereby provide knowledge necessary for further experiments.

In Chapter 2, we create autotetraploid lines of *N. thermarum*, and perform reciprocal interploidy crosses to test for parent-of-origin effects on seed development. By measuring the size of seed components and rates of embryo development in different types of crosses, we provide the first evidence that parent-of-origin effects on offspring development may date to the evolutionary origin of flowering plants. We also demonstrate that that the evolutionary transfer of embryo-nourishing function from a genetically biparental endosperm to a genetically maternal storage tissue (perisperm) can function as a maternal strategy to recapture control of resource distribution among progeny.

In Chapter 3, we sequence transcriptomes of whole ovules and seeds from three key stages of reproductive development in *N. thermarum*. In particular, we examine the expression of genes associ-

ated with chromatin methylation – processes known to be essential for parent-of-origin effects on seed development in other angiosperms. We find evidence for a dynamic chromatin methylation landscape during reproductive development. However, genes involved in establishing, maintaining, and removing methylation marks associated with genetic imprinting show a mix of conserved and unique expression patterns between *N. thermarum* and other angiosperms, providing perspective on how the regulation of imprinting has changed throughout angiosperm evolution.

Table of Contents

Page	i	Title Page
	ii	Copyright Page
	iii	Abstract
	v	Table of Contents
	vi	Acknowledgements
	1	Dissertation
	1	Introductory Chapter
	15	Chapter 1
	51	Chapter 2
	72	Chapter 3
	111	Appendix: Supplementary Material
	112	Chapter 2 Supplementary Material
	124	Chapter 3 Supplementary Material

Acknowledgements

Beyond my coauthors, graduate committee members, and the individuals and entities mentioned in the acknowledgements at the end of each chapter, I would like to thank the many individuals who offered timely moral support and/or who were especially generous with their time in teaching me the techniques essential to completing my dissertation work. In particular, this includes Julien Bachelier, Robert L. Baker, Stephanie Conway, Michael Brent Hawkins, Laura Lagomarsino, Juan Losada, and Lachezar Nikolov. Finally, I would like to thank my husband, Jonathan Allen Kittel, for his relentless support during my graduate studies; I look forward to returning the favor.

Introductory Chapter

Seeds are complex structures that fulfill several functions - they house the embryo that is next sporophyte generation, contain nutrients to fuel germination and early seedling growth, and protect the embryo and nutrients until germination. Remarkably, these functions are carried out via the coordinated development of multiple seed components. The seeds of angiosperms (flowering plants) are particularly complex, in that they contain the products of two separate fertilization events: the embryo and the endosperm. Endosperm is a major evolutionary innovation of angiosperms; in the last common ancestor of flowering plants and non-flowering seed plants the embryo was surrounded by, and directly dependent on, the female gametophyte or sporophyte. The evolutionary origin of the endosperm fundamentally altered the dynamics of resource distribution in a seed, as nutrient flux is no longer simply a matter of flowing from the mother to an embryo. Endosperm is present in the vast majority of angiosperm lineages (having only been lost when selection favors an extreme reduction in seed size, as for the “dust seeds” of orchids), suggesting that the presence of endosperm is beneficial. Why endosperm, as an additional biparental seed component, should increase the fitness of either the parents or offspring has been question for botanists and evolutionary biologists ever since the discovery of double fertilization.

The theory of interparental conflict proposes that endosperm became an essential part of angiosperm seeds because parents (the maternal and paternal sporophytes) can have different interests in how maternal resources are distributed among offspring (Charnov 1979; Haig 1987; Smith and Fretwell, 1974;Trivers 1974; Queller 1983). If resources are limited and a mother supports the growth of multiple seeds that do not necessarily have the same father, then maternal fitness is maximized by distributing resources among a subset of most-fit offspring. Paternal fitness, in contrast, is maximized by encouraging resource investment into the seed it has contributed genetic material to. The origin of endosperm can therefore be interpreted as the insertion of paternal genome into a seed tissue that is able to mediate the flow of nutrients from a mother to the embryo, and thus provides an additional opportunity for the paternal interests to influence resource dynamics. Both the embryo and endosperm possess maternal and paternal genome complements, but the embryo is under high selective pressure to become a functional sporophyte and extreme perturbations to its development should be minimized. Thus, it has been

suggested that the evolutionary origin of endosperm is significant because it creates an arena for interparental conflict.

Much of the experimental evidence that provides the foundation for the central role of endosperm in interparental conflict comes from reciprocal interploidy crosses (Haig and Westoby, 1991)(Haig 2013). Interploidy crosses with genetically homogeneous lines are a way to alter the ploidy and the ratio of maternal and paternal genome complements of the embryo and endosperm, thereby making it possible to test for parent-of-origin effects on offspring development. Interploidy crosses have been performed using a phylogenetically wide sampling of angiosperms, and common suite of experimental phenotypes has emerged. In maternal excess crosses (mother is a tetraploid, father is a diploid), endosperm proliferation is suppressed, while in paternal excess crosses (mother is a diploid, father is a tetraploid), endosperm proliferation is promoted. Since endosperm influences embryogenesis (Hehenberger *et al.*, 2012; Lafon-Placette and Köhler, 2014), nutrient acquisition (Zhang *et al.*, 2007), and seed coat maturation (Ingouff *et al.*, 2006), changes to endosperm development can profoundly impact seed development as a whole.

Work in *Arabidopsis*, maize, and rice has revealed that genetic imprinting, via chromatin methylation marks on maternal or paternal alleles underlies key parent-of-origin effects on endosperm development (Haig and Westoby, 1991; Köhler *et al.*, 2012; Gehring and Satyaki, 2017). While the consistency of parent-of-origin effects on endosperm development across a phylogenetically broad sampling suggests that interparental conflict may be a fundamental component to endosperm development, the mechanisms by which imprinting occurs appears to vary between the relatively small number of monocots and eudicots which have been studied (Springer *et al.*, 2002; Butenko and Ohad, 2011; Gleason and Kramer, 2012; Köhler *et al.*, 2012; Haig 2013; Jiang and Ramachandran, 2016; Gehring and Satyaki, 2017). The question then becomes, what is the evolutionary relationship between interparental conflict, parent-of-origin effects on seed development, and imprinting via chromatin methylation?

Studies have begun to synthesize information from monocots and eudicots (Springer *et al.*, 2002; Butenko and Ohad, 2011; Köhler *et al.*, 2012; Haig 2013; Jiang and Ramachandran, 2016; Gehring and Satyaki, 2017), but information from the early-diverging angiosperm lineages (those whose origins predates the divergence of monocots and eudicots) is needed to provide an complete evolutionary perspective. However, parent-of-origin effects on seed development has not been studied in any member of an

early-diverging angiosperm lineage, either via interploidy crosses or by characterizing imprinting-related methylation dynamics. For my dissertation I identify and leverage the experimental tractability of the water lily *Nymphaea thermarum* (a member of the most ancient angiosperm lineages, the Nymphaeales) to address whether the relationships between interparental conflict, parent-of-origin-effects on seed development, and chromatin methylation predate the divergence of monocots and eudicots.

This Introductory Chapter describes key concepts in the development and diversity of angiosperm seeds, summarizes results from almost 100 years of reciprocal interploidy crosses, reviews the current model for how imprinting-related chromatin methylation patterns are regulated, and finally introduces *N. thermarum* as a new 'model organism' for studying angiosperm evolution. Chapter 1 provides a comprehensive description of floral biology, female reproductive development, and seed development in *N. thermarum* – providing a knowledge base for subsequent chapters. Chapter 2 involves the creation of autotetraploid lines of *N. thermarum* and their use (along with and diploid lines) to preform reciprocal interploidy crosses. Finally, in Chapter 3, RNA-seq datasets for three key stages of seed development in *N. thermarum* are generated and analyzed, with a particular focus on the activity of genes known to regulate chromatin methylation.

Typical ontogeny of endosperm and seed development in angiosperms, and other variations

Most flowering plants have triploid endosperm that undergoes free-nuclear development. For these species, the second fertilization event involves one haploid sperm nucleus fusing with the diploid central cell nucleus. The central cell is diploid due to the partitioning of two haploid nuclei into a single cell during female gametophyte development. Soon after double fertilization to create biparental embryo and endosperm, the endosperm begins to expand and undergo free-nuclear divisions. During this syncytial phase of endosperm development, embryo development is relatively quiescent. Also during this time, the surrounding maternal sporophytic tissues remaining from the ovule are either replaced by endosperm expansion (as can be true for the nucellus) or develop to accommodate the growing endosperm (as with the integuments). The syncytial phase of endosperm development is known to be important for drawing resources into the seed, with suggestions that the large central vacuole of the endosperm syncytium functions as a powerful nutrient sink (Zhang *et al.*, 2007).

However, at some point during development cell walls are formed and partition the endosperm

nuclei into separate cells. Besides marking the beginning of cellular endosperm divisions, endosperm cellularization is also known to be an important checkpoint for embryo development: where it has been studied, morphological development of the embryo does not procced past a certain stage until the endosperm has cellularized (Hehenberger *et al.*, 2012; Lafon-Placette and Köhler, 2014). During and after cellularization, the endosperm typically differentiates into distinct regions (such as micropylar and chalazal domains). Meanwhile, the expansion of the embryo begins to replace space previously occupied by the endosperm. The degree of embryo growth and development is highly variable, as is the further development of the endosperm. In species where the endosperm is the site of nutrient storage, embryo development is either arrested at an early stage and/or the embryo is relatively small, and the endosperm cells fill with nutrient reserves. In species where nutrients are stored in the embryo, continued growth and morphogenesis of the embryo eventually displaces the majority of the endosperm.

While this describes the most common mode of seed development in angiosperms, it by no means represents the full spectrum of structural and genetic variation in how seeds are constructed [Macheshwari 1950). In particular, both free-nuclear endosperm and triploid endosperm are understood to be derived characters for angiosperm (Floyd and Friedman, 2000; Geeta 2002; Williams and Friedman, 2002; Friedman and Ryerson, 2009)(Figure Intro.1). Most of the early-diverging lineages are characterized by diploid (Nymphaeales, Austrobaileyales) and/or cellular (*Amborella*, Nymphaeales, Austrobaileyales) endosperm. In addition, in these early-diverging lineages plus magnollids, it is more common for nutrients to be stored in either the endosperm or a tissue derived from the maternal sporophyte, but not in the embryo (Losada *et al.*, 2017). The Nymphaeales in particular is characterized by a unique suite of seed characters: a diploid, cellular endosperm, with nutrients stored in a tissue called the perisperm (which is derived from the maternal sporophyte).

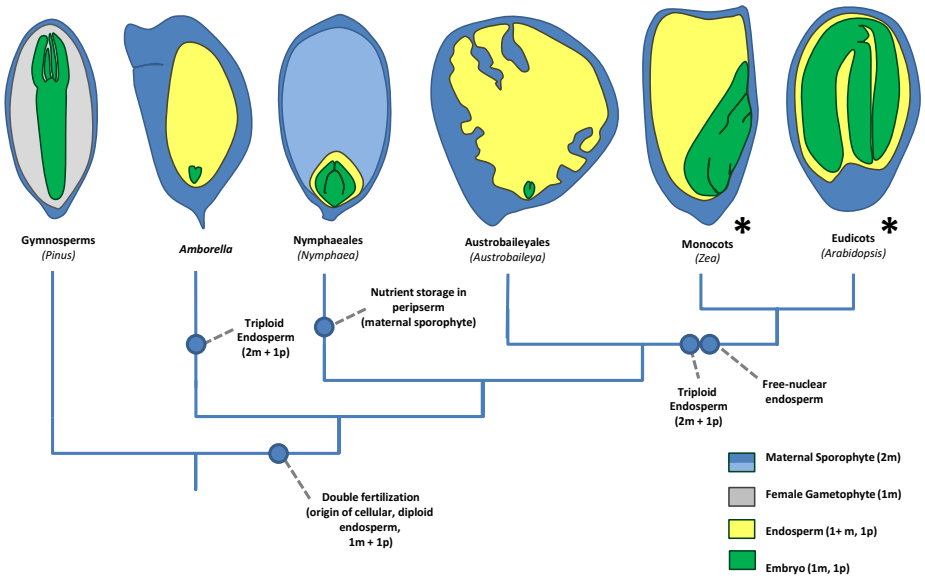

Figure Intro.1: Evolution of key characters of angiosperm seeds.

Diagrams show internal structure of seeds in several angiosperm lineages. While seed types typical of the lineages are shown, they do not represent the full diversity of seed bauplans that can be present within each lineage. Different seed components are color-coded, and the genetic composition of each component is noted. m = maternal genome complement, p = paternal genome complement. * indicates lineages which are represented in studies of either reciprocal interploify crosses or studies of genetic imprinting. Seeds are not drawn to a common scale.

Interploidy crosses in flowering plants – the importance of endosperm

The majority of reciprocal interploidy crosses have been performed for species with triploid and free-nuclear endosperm, although there is variation in whether nutrients are stored in endosperm or in the embryo (Haig and Westoby, 1991). In interploidy crosses, higher paternal ploidy (as in paternal excess crosses) produces seeds that are generally characterized by an accelerated rate of free nuclear divisions or a delayed transition from free-nuclear to cellularized endosperm (Haig and Westoby, 1991; von Wangenheim and Peterson, 2004). This yields more endosperm nuclei at the time of cellularization and hence more initial endosperm cells at the outset of cellular endosperm development - the result is a larger endosperm and a larger seed. In these paternal excess crosses, endosperm development is often

so perturbed that seed filling is disrupted or seeds are aborted. Conversely, the effect of relatively higher maternal ploidy is precocious endosperm cellularization or a slower rate of nuclear division, leading to fewer initial endosperm nuclei and cells at the onset of cellular development. Ultimately, this produces smaller endosperm and smaller seeds. Studies in maize have explicitly demonstrated that it is changes to the ratio of maternal to paternal genome complements, rather than total ploidy, that triggers these developmental responses (Lin 1984). The evolutionary transition from free-nuclear to cellular endosperm can therefore been viewed as an important character for how the effects of altered parental genome dosage become apparent during seed development (Haig and Westoby, 1991; Gehring and Satyaki, 2017).

Changes to the ontogeny of the endosperm then echo throughout the rest of seed development. For example, endosperm cellularization is important for the advancement of embryo development in *Arabidopsis* (Hehenberger *et al.*, 2012; Lafon-Placette and Köhler, 2014), as embryo development is often impaired or altogether arrested in paternal-excess crosses (Scott *et al.*, 1998). In other species, early endosperm cellularization in maternal-excess crosses appears to trigger early advancement of embryo morphogenesis (rice (Zhang *et al.*, 2016), *Brassica* (Stoute *et al.*, 2012)). These developmentally advanced embryos can, counterintuitively, be smaller at the time of seed maturity (Scott *et al.*, 1998); in some seeds, the maximum size of the endosperm (which would be smaller due to early cellularization) is an important determinant of maximum embryo size. Unfortunately, embryo growth (changes to size) and morphogenesis (changes to form) are not always reported separately in interploidy-cross studies, which can lead to inconsistencies in how effects on the embryo are discussed.

Interploidy crosses have also been performed for a few taxa with either diploid or cellular endosperm, but none have been performed for any species with both diploid and cellular endosperm, nor for any species with perisperm (Haig and Westoby, 1991; von Wangenheim and Peterson, 2004). *Oenothera hookeri* has diploid, free-nuclear endosperm, and both positive effects of higher paternal ploidy and negative effect of higher maternal ploidy were found for endosperm nuclei/cell number (von Wangenheim 1962). *Galeopsis pubescens* (Håkansson 1952), *Datura stramonium* (Sansome *et al.*, 1942), *Solanum pimpinellifolium* (Cooper and Brink, 1945), and *S. acaule* (von Wangenheim 1957) have cellular endosperm, and paternal-excess seeds in these interploidy crosses were characterized by high rates of endosperm failure and seed abortion during early development. Interestingly, von Wangenheim (von

Wangenheim 1957) observed an initial free-nuclear phase of endosperm development in paternal-excess crosses in *S. acaule*. Seed set was typically less severely impacted in the maternal-excess crosses, in which endosperm proliferation was consistently repressed. Altogether, the effects of higher maternal and paternal ploidy in these crosses (with diploid or cellular endosperm) are fundamentally similar to crosses in species with triploid, free-nuclear endosperm. This suggests that endosperm development is still the primary arena of the relationship between parental genome complements in species with diploid or cellular endosperm, and that neither free-nuclear endosperm development nor triploid endosperm is actually required for parent-of-origin effects on offspring development to occur. If true, then it is possible that interparental conflict could be influencing seed development in the early-diverging angiosperm lineages, whose origins predate the evolution of free-nuclear or triploid endosperm (Figure Intro.1).

Imprinting via chromatin methylation underlies parent-of-origin effects on seed development

Interploidy crosses with genetically homogenous lines make it clear that parent-of-origin of genetic material matters for development, and so there must be an underlying molecular mechanism that allows otherwise identical parental alleles to be transcriptionally distinguished from one another (Haig and Westoby, 1991). Studies of *Arabidopsis* and a small number of monocots have revealed that genetic imprinting is the underlying mechanism of parent-of-origin effects on seed development. Imprinting involves the establishment, maintainance, and removal of DNA and histone methylation marks during gamete development, which are carried through fertilization (Gehring and Satyaki, 2017). Importantly, patterns or levels of DNA methylation differ between gametes – for example, the egg cell is globally hypermethylated while the central cell is globally hypomethyled (Gutiérrez-Marcos *et al.*, 2006). Methylation patterns also differ between male and female gametes (Trasler, 2006). After fertilization, the establishment and editing of histone methylation marks can occur at specific loci. Since methylation of DNA and histones at a locus can affect the expression of that locus, an otherwise identical allele can be expressed differently, depending on whether it came from a male or female gamete (Zilberman *et al.*, 2006). Interestingly, some of the components of processes that control histone methylation are themselves imprinted, often such that they are expressed only from the maternal allele (Gehring and Satyaki, 2017).

The genes and processes involved in chromatin methylation during reproductive development

are best understood in *Arabidopsis*. DNA methylation occurs in different contexts, via the action of different DNA cytosine methyltransferases (Sharma *et al.*, 2009; Gehring and Satyaki, 2017). CHROMOMETHYLASE proteins (CMT) establish and maintain methylation in the CNG context, while members of the DNA METHYLTRANSFERASE family (MET) maintain CG methylation. In balance with maintenance of methylation marks, the DNA glycosylase DEMETER (DME) removes methylation established by MET1 [35]. Members of these three families are active during gamete formation, and through the early stages of seed development [34]. The POLYCOMB REPRESSIVE COMPLEX 2 (PRC2) is comprised of MEDEA (MEA), FERTILIZATION-INDEPENDENT SEED2 (FIS2), FERTILIZATION-INDEPENDENT ENDOSPERM (FIE), and MULTICOPY SUPRESSOR OF IRA1 (MSI1), and trimethylates histone H3 on lysine 2 (a mark primarily associated with transcriptional silencing). PRC2 activity is important for regulating the expression of genes during endosperm development and function. For example, in Arabidopsis PHERES (PHE1) is under the control of both DME-mediated DNA methylation and PRC2-mediated histone methylation, and controls the onset of the free-nuclear to cellular transition during endosperm development (Köhler *et al.*, 2012; Gehring and Satyaki, 2017) – a key aspect of the experimental phenotypes observed during reciprocal interploidy crosses.

While chromatin methylation dynamics are associated with genetic imprinting and parent-of-origin effects on gene expression, DNA and histone methylation are involved in other processes during reproductive development. For example, the RNA-directed DNA methylation (RdDM) is responsible for repressing transposon activity in the egg cell and embryo (Ingouff *et al.*, 2017), but has not been shown to be important for genetic imprinting (Köhler *et al.*, 2012). However, our understanding of how imprinting-related chromatin methylation is regulated during reproductive development is far from complete in any model system. Additional, yet undiscovered, genes and processes may be important – a point highlighted by some of the differences between PRC2 activity in Arabidopsis, other eudicots (Gleason and Kramer, 2012), and monocots like *Oryza sativa* (rice; Nallamilli *et al.*, 2013; Furihata *et al.*, 2016). There is little evidence that PRC2 as a whole is important for seed development in rice, yet imprinting occurs via histone-methylation marks in monocots, and impacts endosperm development (Luo *et al.*, 2009; Nallamilli *et al.*, 2013). Beyond building more complete models of how chromatin methylation is regulated in these model systems, understanding methylation dynamics in other species can help identify the evolutionarily conserved, and therefore functionally essential, components of these mechanisms.

***Nymphaea thermarum* as a model system from within an early-diverging angiosperm lineage.**

The study of early-diverging lineages is necessary to understand the evolution of angiosperm reproductive biology. A recent resurgence in descriptive work among these lineages has already provided new perspectives on how reproductive characters evolved in angiosperms (Floyd and Friedman, 2001; Friedman *et al.*, 2003a; Friedman and Williams, 2003b; Friedman 2006; Friedman *et al.*, 2008; Friedman and Ryerson, 2009; Rudall *et al.*, 2009; Endress 2010; Bachelier and Friedman, 2011; Friedman *et al.*, 2012; Losada *et al.*, 2017). However, the vast majority of species within the Amborellales, Nymphaeales, and Austrobaileyales are not amenable to being used as experimental or genetic model systems. Most are long-lived trees, shrubs, lianas, or aquatic plants that are difficult to maintain in large numbers and under conditions necessary for performing controlled pollinations. In addition, genome size within these lineages can be dauntingly large (for example, the genome of *Austrobaileya scandens* is estimate to be >9 Gbp (Leitch and Hanson, 2002)), few genetic resources exist, and no protocols for transient or stable transformation have been developed for any constituent species. A few species have been suggested for their potential as model systems (Rudall *et al.*, 2009; Vialette-Guiraud *et al.*, 2011; Bliss *et al.*, 2013), but they have yet to be adopted for wide-spread use.

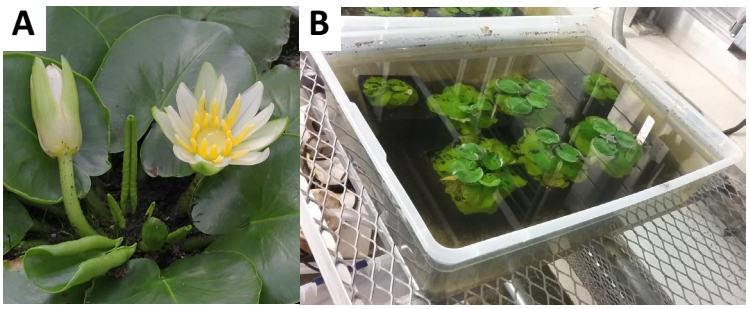

Figure Intro.2: *Nymphaea thermarum* as a tractable model system

Images of *N. thermarum*, showing habit and reproductive features, as well as growth in a greenhouse. A) *N. thermarum* individuals support only a single open flower at a time, but flowering continuously throughout the year. In this image, one open flower, one older (fertilized) flower (top left), and one pre-anthesis floral bud (bottom, middle) are evident. B) Multiple individuals can be grown in individual pots, in a single 7-gallon plastic tub - no other specialized equipment is necessary.

Nymphaea thermarum, however, is a minute water lily that displays remarkable potential as an experimental/genetic model system (Figure Intro.2). It requires only shallow water (and thus little specialized equipment to grow), and is small enough that dozens to hundreds can be grown on a single greenhouse bench. We show that *N. thermarum* is pre-disposed to self-fertilization (Chapter 1), yet it can be emasculated and out-crossed in a controlled manner. Hundreds of seeds with high germination rates are produced in a single fruit, and plants flower continuously throughout the year. The generation time is 4-5 months, but individual plants can live for 5+ years - making it possible to maintain genetic lines without constant propagation. Finally, *N. thermarum* has one of the smallest genomes yet found within an early-diverging lineage: ~500 Mbp (Pellicer *et al.*, 2013)(which is on par with other model systems, such as *Aquilegia*). A project is underway to sequence, assemble, and annotate the genomes of *N. thermarum*, and transcriptomes of several tissues have already been produced.

The importance of organismic biology

While *N. thermarum* certainly shows potential as a model system, it was only recently described as a species relatively recently (Fischer 1988) and has been little studied since. Therefore, before any experiments are preformed, it is necessary to precisely understand the biology of the characters in question in this particular system. The ultimate aim of this dissertation is to provide a new perspective on how interparental conflict, parent-of-origin effects on seed development, and the regulation of chromatin methylation have been connected during the evolution of seed development in angiosperms. It is only appropriate then, that this dissertation begins with a study of how reproduction and reproductive development occurs in this species.

References

Bachelier JB, Friedman WE (2011) Female gametophyte competition in an ancient angiosperm lineage. *Proc Natl Acad Sci U S A* 108(30):12360-12365.

Bliss BJ, Wanke S, Barakat A, Ayyampalayam S, Wickett N, Wall PK, Jiao Y, Landherr L, Ralph PE, Hu Y, Neinhuis C, Leebens-Mack J, Arumuganathan K, Clifton SW, Maximova SN, Ma H, dePamphilis CW (2013) Characterization of the basal angiosperm *Aristolochia fimbriata*: a potential experimental system for genetic studies. *BMC Plant Biol* 13:12.

Butenko Y, Ohad N (2011) Polycomb-group mediated epigenetic mechanisms through plant evolution. *Biochim Biophys Acta, Gen Regul Mech* 1809(8):395-406.

Charnov EL (1979) Simultaneous hermaphroditism and sexual selection. *Proc Natl Acad Sci U S A* 76: 2480-2484.

Cooper DC, Brink RA (1945) Seed collapse following matings between diploid and tetraploid races of *Lycopersicon pimpinellifolium*. *Genetics* 30(4):376-401.

Endress PK (2010) The evolution of floral biology in basal angiosperms. *Phil Trans Royal Soc Lond B Biol Sci* 365:411-421.

Fischer E (1988) Beiträge zur Flora Zentralafrikas I. Eine neue Nymphaea sowie ein neuer Streptocarpus aus Rwanda. *Feddes Repert* 99:385-390.

Floyd SK, Friedman WE (2000) Evolution of Endosperm Developmental Patterns among Basal Flowering Plants. *Int J Plant Sci* 161(S6)S57-S81.

Floyd SK, Friedman WE (2001) Developmental evolution of endosperm in basal angiosperms: evidence from *Amborella* (Amborellaceae), *Nuphar* (Nymphaeaceae), and *Illicium* (Illiciaceae). *Plant Syst Evol* 228:153-169.

Friedman WE (2006) Embryological evidence for developmental lability during early angiosperm evolution. *Nature* 41:337-340.

Friedman WE (2008) Hydatellaceae are water lilies with gymnospermous tendencies. *Nature* 453:94-97.

Friedman WE, Bachelier JB, Hormaza JI (2012) Embryology in *Trithuria submersa* (Hydatellaceae) and relationships between embryo, endosperm, and perisperm in early-diverging flowering plants. *Am J Bot* 99:1083-1095.

Friedman WE, Gallup WN, Williams JH (2003a) Gametophyte development in *Kadsura*: implications for Schisandraceae, Austrobaileyales, and the early evolution of flowering plants. *Int J Plant Sci* 164:S293-305.

Friedman We, Ryerson KC (2009) Reconstructing the ancient female gametophyte in angiosperms: insights from Amborella and other ancient lineages of flowering plant. *Am J Bot* 96:129-143.

Friedman WE, Williams JH (2003b) Modularity of the angiosperm female gametophyte and its bearing on the early evolution of endosperm in flowering plants. *Evolution* 57:216-230.

Furihata HY, Suenaga K, Kawanabe T, Yoshida T, Kawabe A (2016) Gene duplication, silencing, and expression alteration govern the molecular evolution of PRC2 genes in plants. *Genes Genet Syst* 91(2):85-95.

Geeta R (2002) The origin and maintenance of nuclear endosperms: viewing development through a phylogenetic lens. *Proc R Soc Lond B Biol Sci* 270:29-35.

Gehring M, Satyaki PR (2017) Endosperm and imprinting, inextricably linked. *Plant Physiol* 173:143-154

Gleason EJ, Kramer EM (2012) “Characterization of Aquilegia Polycomb Repressive Complex 2 Homologs Reveals Absence of Imprinting.” *Gene* 507(1):54–60.

Gutiérrez-Marcos JF, Costa LM, Dal Prà M, Scholten S, Kranz E, Perez P, Dickinson HG. (2006) Epigenetic asymmetry of imprinted genes in plant gametes. *Nat Genet* 38(8):876-878.

Haig D (1987) Kin conflict in seed plants. *Trends Ecol Evol* 2(11):337–340.

Haig D (2013) Kin conflict in seed development: an interdependent but fractious collective. *Annu Rev Cell Dev Biol* 29:189-211.

Haig D, Westoby M (1991) Genomic imprinting in endosperm: its effects on seed development in crosses between species and between different ploidies of the same species, and its implications for the evolution of apomixis. *Phil Trans R Soc Lond B Biol Sci* 333:1–13.

Håkansson A (1952) Seed development after 2x,4x crosses in *Galeopsis pubescens*. *Hereditas* 38:425-448.

Hehenberger E, Kradolfer D, Köhler C (2012) Endosperm cellularization defines an important developmental transition for embryo development. *Development* 139(11):2031-2039.

Hsieh TF, Shin J, Uzawa R, Silva P, Cohen S, Bauer MJ, Hashimoto M, Kirkbride RD, Harada JJ, Ziberman D, Fischer RL (2012) Regulation of imprinted gene expression in *Arabidopsis* endosperm. *Proc Natl Acad Sci U S A* 108(5):1755-1762.

Ingouff M, Jullien PE, Berger F (2006). The female gametophyte and the endosperm control cell proliferation and differentiation of the seed coat in *Arabidopsis*. *Plant Cell* 18(12):3491-3501.

Ingouff M, Selles B, Michaud C, Vu TM, Berger F, Schorn AJ, Autran D, Van Durme M, Nowack MK, Martienssen RA, Grimanelli D (2017) Live-cell analysis of DNA methylation during sexual reproduction in *Arabidopsis* reveals context and sex-specific dynamics controlled by noncanonical RdDM. *Genes Dev* 31(1):72-83.

Jiang SY, Ramachandran S (2016) Expansion mechanisms and evolutionary history on genes encoding DNA glycosylases and their involvement in stress and hormone signaling. *Genome Biol Evol* 8(4):1165-1184.

Köhler C, Wolff P, Spillane C (2012) Epigenetic mechanisms underlying genomic imprinting in plants. *Annu Rev of Plant Biol* 63:331-352.

Lafon-Placette C, Köhler C (2014) Embryo and endosperm, partners in seed development. *Curr Opin Plant Biol* 17:64-69.

Leitch IJ, Hanson L (2002) DNA C-values in seven families fill phylogenetic gaps in the basal angiosperms. *Bot J Linn Soc* (2002) 140(2):175-179.

Lin BY (1984) Ploidy barrier to endosperm development in maize. *Genetics* 107(1):103-115.

Losada JM , Bachelier JB, Friedman WE (2017) Prolonged embryogenesis in *Austrobaileya scandens* (Austrobaileyaceae): its ecological and evolutionary significance. *New Phytol* 215(2):851-864.

Luo M, Platten D, Chaudhury A, Peacock WJ, Dennis ES (2009) Expression, imprinting, and evolution of rice homologs of the polycomb group genes. *Mol Plant* 2:711–723.

Maheshwari P (1950) *An Introduction to the Embryology of Angiosperms* (McGraw-Hill Book Company, New York).

Nallamilli BRR, Zhang J, Mujahid H, Malone BM, Bridges SM, *et al.* (2013) Polycomb group gene OSFIE2 regulates rice (*Oryza sativa*) seed development and grain filling via a mechanism distinct from *Arabidopsis*. *PLoS Genet* 9(3): e1003322.

Pellicer J, Kelly LJ, Magdalena C, Leitch IJ (2013) Insights into the dynamics of genome size and chromosome evolution in the early diverging angiosperm lineage Nymphaeales (water lilies). *Genome* 56:1-13.

Queller DC (1983) Kin selection and conflict in seed maturation. *J Theor Biol* 100(1):153–172.

Rudall PJ,Eldridge T, Tratt J, *et al.* (2009) Seed fertilization, development, and germination in Hydatellaceae (Nymphaeales): implications for endosperm evolution in early angiosperms. *Am J* Bot 96:1581–1593.

Sansome ER, Satina S, Blakeslee AF (1942) Disintegration of ovules in tetraploid-diploid and in incompatable species crosses in *Datura*. *Bull Torrey Bot Club* 69(9):405-420.

Scott RJ, Spielman M, Baily J, Dickinson HG (1998) Parent-of-origin effects on seed development in *Arabidopsis thaliana*. *Development* 125:3329-3341.

Sharma R, Mohan Singh RK, Malik G, Deveshwar P, Tyagi AK, Kapoor S, Kapoor M (2009) Rice cytosine DNA methyltransferases - gene expression profiling during reproductive development and abiotic stress. *FEBS J* 276(21):6301-6311.

Smith CC, Fretwell, SD (1974) The optimal balance between size and number of offspring. *Am Nat* 108:499-506.

Springer NM, Danilevskaya ON, Hermon P, Helentjaris TG, Phillips RL, Kaeppler HF, Kaeppler SM (2002) Sequence relationships, conserved domains, and expression patterns for maize homologs of the polycomb group genes *E(z)*, *esc*, and *E(Pc)*. *Plant Physiol* 128(4):1332-1345.

Stoute AI, Varenko V, King GJ, Scott RJ, Kurup S (2012) Parental genome imbalance in *Brassica oleracea* causes asymmetric triploid block. *Plant J* 71(3):503-516.

Trasler JM (2006) Gamete imprinting: setting epigenetic patterns for the next generation. *Reprod Fertil Dev* 18(1-2):63-69.

Trivers RL (1974) Parent-offspring conflict. *Am Zool* 14:249-264.

Vialette-Guiraud AC, Alaux M, Legeai F, Finet C, Chambrier P, Brown SC, Chauvet A, Magdalena C, Rudall PJ, Scutt CP (2011) *Cabomba* as a model for studies of early angiosperm evolution. *Ann Bot* 108(4):589-598.

von Wangenheim KH (1957) Untersuchungen über den Zusammenhang zwischen Chromosomenzhal und Kreuzbarkeit bei Solanum-Arten. *Z induct Abstamm u Vererb Lehre* 88:21-37.

von Wangenheim KH (1962) Zur Ursache der Abortion von Samenanlagen in Diploid-Polyploid-Kreuzungen: II. Untershiedliche Differenzierung von Endospermen mit glechem Genom. *Z Vererb Lehre* 93:319-334.

von Wangenheim KH, Peterson HP (2004) Aberrant endosperm development in interploidy crosses reveals a timer of differentiation. *Dev Biol* 270(2)277-289.

Williams JH, Friedman WE (2002) Identification of diploid endosperm in an early angiosperm lineage. *Nature* 415(6871):522-526.

Zhang H, Luo M, Johnson SD, Zhu X, Liu L, Huang F, Liu Y, Xu P, Wu X (2016) Parental genome imbalance causes post-zygotic lethality and deregulates imprinting in rice. *Rice* 9:43-55.

Zhang WH, Zhou Y, Dibley KE, Tyerman SD, Furbank RT, Patrick JW (2007) Nutrient loading of developing seeds. *Funct Plant Biol* 34:314-331.

Zilberman D, Gehring M, Tran RK, Ballinger T, Henikoff S (2006) Genome-wide analysis of Arabidopsis thaliana DNA methylation uncovers an interdependence between methylation and transcription. *Nat Genet* 39:61-69.

Chapter 1

Title: Floral biology and ovule and seed ontogeny of *Nymphaea thermarum*, a water lily at the brink of extinction with potential as a model system for basal angiosperms

Authors: Rebecca A. Povilus[1,3]*, Juan M. Losada[1,3], William E. Friedman[1, 2]

[1] Department of Organismic and Evolutionary Biology, Harvard University, 26 Oxford Street, Cambridge, Massachusetts 02138 USA; [2] Arnold Arboretum of Harvard University, 1300 Centre Street, Boston, Massachusetts 02131 USA; [3]Contributed equally

Published as:

Povilus, R. A., J. M. Losada, and W. E. Friedman. 'Floral Biology And Ovule And Seed Ontogeny Of Nymphaea thermarum, A Water Lily At The Brink Of Extinction With Potential As A Model System For Basal Angiosperms'. *Annals of Botany* 115.2 (2014): 211-226

Abstract

Background and Aims: Nymphaea thermarum is a member of the Nymphaeales, of one of the most ancient lineages of flowering plants. This species was only recently described and then declared extinct in the wild, so little is known about its reproductive biology. In general, the complete ontogeny of ovules and seeds is not well documented among species of *Nymphaea*, and has never been studied in the subgenus *Brachyceras*, the clade to which *N. thermarum* belongs.

Methods: Flowers and fruits were processed for brightfield, epifluorescence, and confocal microscopy. Flower morphology, with emphasis on the timing of male and female functions, was correlated with key developmental stages of the ovule and the female gametophyte. Development of the seed tissues and dynamics of polysaccharide reserves in the endosperm, perisperm, and embryo were examined.

Key Results: Pollen release in *N. thermarum* starts before the flower opens. Cells walls of the micropylar nucellus show layering of callose and cellulose in a manner reminiscent of transfer cell wall patterning. Endosperm development is ab initio cellular, with micropylar and chalazal domains that embark on distinct developmental trajectories. The surrounding maternal perisperm occupies the majority of seed volume, and accumulates starch centrifugally. In mature seeds, a minute but fully developed embryo is surrounded by a single persistent layer of endosperm.

Conclusions: Early male and female function indicate that *N. thermarum* is predisposed towards self-pollination, a phenomenon that is likely to have evolved multiple times within *Nymphaea.* While formation of distinct micropylar and chalazal developmental domains in the endosperm along with a copious perisperm, characterize the seeds of most members of the Nymphaeales, seed ontogenies vary between and among the constituent families. Floral biology, life history traits, and small genome size make *N. thermarum* uniquely promising as an early-divergent angiosperm model system for genetic and molecular studies.

Key words: embryo, endosperm, female gametophyte, flower biology, megagametogenesis, megasporogenesis, *Nymphaea thermarum*, Nymphaeales, perisperm, protogyny, seed development, stigma.

Introduction

Nymphaea thermarum, a member of one of the most ancient lineages of flowering plants, is a remarkable species from many perspectives. This annual, miniature water lily was originally described from a restricted hot-spring habitat in Rwanda (Fischer, 1988), and was recently declared as extinct in the wild (Fischer and Magdalena-Rodriguez, 2010). With little known about its physiology or reproductive biology, germplasm is currently maintained in just a few botanical collections worldwide. Far from being written off as a botanical curiosity and evolutionary dead-end, however, we propose that *N. thermarum* is uniquely poised to help unravel many long-standing questions about the origin and early evolution of angiosperms, the clade which includes the majority of land plant diversity.

Early diverging angiosperm lineages are particularly poor in species amenable to genetic experimentation. Most taxa are woody and perennial (e.g. *Amborella*, Austrobaileyales, Chloranthales and the vast majority of magnoliids), and even the aquatic and typically perennial life history of most members of Nymphaeales make them difficult to maintain in large numbers in a controlled environment. *Nymphaea thermarum*, while aquatic, requires only shallow water, has a relatively short generation time of 5-6 months, and is small enough that hundreds of individuals can be grown in a single greenhouse room. Like *Arabidopsis thaliana*, *N. thermarum* self-fertilizes, is also capable of outcrossing, and reproduces prolifically by seed. Finally, *N. thermarum* has a genome size that is on a par with other established flowering plant model systems (roughly twice as large as the genome of *A. thaliana*) (Pellicer *et al.*, 2013). Any attempt to develop this species into a model system, including creation of isogenic lines and development of stable transformation protocols, would benefit from a detailed knowledge of its reproductive biology. In addition, such information will be invaluable for conservation efforts, such as propagation and maintenance of remaining genetic diversity, with the potential to reintroduce this species into its native habitats.

Nymphaeales is one of the most ancient angiosperm lineages, either sister to all flowering plants except *Amborella* or sister to *Amborella* and together forming the sister group to all other flowering plants (Maia *et al.*, 2014; Ruhfel *et al.*, 2014). While all members of Nymphaeales are aquatic, there has nonetheless been considerable evolutionary diversification over the nearly 125 million years of history documented in the fossil record (Qiu *et al.*, 1999; Friis *et al.*, 2001; 2006; 2011; Magallon *et al.*, 2013; Doyle and Endress, 2014; Iles *et al.*, 2014). Recent molecular dating studies corroborate the ancient

age of Nymphaeales, with Hydatellaceae diverging from its sister group Nymphaeaceae plus Cabombaceae roughly 127 million years ago (Saarela *et al.*, 2007; Iles *et al.*, 2014). Thus, studies within the clade present a unique opportunity to examine how reproductive characters have diversified in these aquatic plants since the Early Cretaceous.

Fortunately, the historical popularity of *Nymphaea* flowers for ornamental and cultural uses means that the macroscopic (morphological) aspects of reproductive biology have been documented for many taxa (Moseley, 1961; Wiersema, 1988 and references herein; Endress, 2010). Protogyny (female receptivity occurring before shedding of pollen within the same flower) is the norm in *Nymphaea* flowers (Schneider and Chaney, 1981; Schneider, 1982; Capperino and Schneider, 1985; Williams *et al.*, 2010), as is true of the vast majority of hermaphroditic basal angiosperms. For *Nymphaea*, the separate female and male phases are punctuated by floral movements – the flower opens one day or evening as functionally female, closes, and reopens as functionally male. Intriguingly, many of the exceptions to protogyny that have been documented among basal angiosperm lineages with hermaphroditic flowers involve taxa within *Nymphaea* (Endress, 2010). *Nymphaea thermarum* is a member of the *Brachyceras* subgenus (Borsch *et al.*, 2011), a pan-tropical clade that is often referred to as the tropical day-blooming water lilies, while the several other subgenera in *Nymphaea* are circumscribed according to biogeography and whether flowering is nocturnal or diurnal. There are about 46 extant species in *Nymphaea*, making it is the largest genus in Nymphaeaceae, which with 58 species is by far the largest family within Nymphaeales, compared to 10 species in Hydatellaceae and 6 in Cabombaceae (Stevens, 2001 onwards).

The developmental morphology of flowers and fruits within Nymphaeales has been documented in most genera and subgenera (Chifflot, 1902; Heslop-Harrison, 1955a,b; Moseley, 1961; Khanna, 1964b; Ramji and Padmanabhan, 1965; Schneider, 1976; 1982; 1983; Schneider and Moore, 1977; Schneider and Chaney, 1981; Moseley *et al.*, 1984; Williamson and Moseley, 1989; Schneider *et al.*, 2003; Endress 2001; 2005; Grob *et al.*, 2006; Rudall *et al.*, 2007; Zhou and Fu, 2007; Hu *et al.*, 2009; Rudall *et al.*, 2009; Sokoloff *et al.*, 2009; 2010; Vialette-Guiard *et al.*, 2011). Features of female gametophyte development, fertilization, and seed development have also been studied, but are scattered across a century of embryological literature (Cook, 1902; 1906; 1909; Conard 1905; Seaton 1908; Martin, 1946; Meyer, 1960; Khanna, 1964a,b; 1965; 1967; Valtzeva and Savich, 1965; Schneider, 1978; Schneider and Ford, 1978; Batygina *et al.*, 1980, 1982; Schneider and Jeter, 1982; Winter and Shamrov 1991; Van Miegroet and

Dujardin, 1992; Orban and Bouharmont, 1998; Bonilla-Barbosa *et al.*, 2000; Floyd and Friedman, 2000; 2001; Yamada 2001; Williams and Friedman, 2002; Baskin and Baskin 2007; Friedman, 2008; Zhou and Fu, 2008; Rudall *et al.*, 2008, 2009; Friedman *et al.*, 2012). An integrative approach to the ontogenies of the gametophyte, embryo, endosperm, and perisperm in *Nymphaea thermarum* will fill a conspicuous gap in our knowledge of ovule and seed development within Nymphaeales.

In this study, we document reproductive development of *N. thermarum*, from floral bud emergence through fertilization and seed development, up to germination. The goals are to correlate the timing of key events during floral and ovule development with pollination and seed development in order to provide an integrated view of the reproductive biology of *N. thermarum.* This, we hope, can be used as a reference for future experimental and genetic work and/or conservation efforts. In addition, we seek to document in detail the ontogeny and nutritional status of the endosperm, embryo, and maternal tissues during seed development. In turn, these embryological features of *N. thermarum* are used to examine the evolutionary-developmental history of a suite of reproductive characters within the broader comparative context of the Nymphaelaes. As will be seen, heterochronic alterations in floral development have been an important force in the evolutionary history of the clade and specifically in the origin of a set of apomorphic features in *N. thermarum*.

Materials and Methods

Plant material

Nymphaea thermarum seeds from the Botanische Gärten der Universität Bonn (Bonn, Germany) were sown and plants grown at the greenhouses of the Arnold Arboretum of Harvard University, according to the guidelines of Fischer and Magdalena-Rodriguez (2010). To study female gametophyte development, flowers were collected at different developmental stages from flower bud to flower opening. Flowers were measured over the 12 days between floral bud emergence and first day of anthesis in order to generate a correlation between bud length and number of days until anthesis. To evaluate seed development, self-fertilized flowers and fruits were collected at daily intervals after first flower opening until seed set and release. Seeds were allowed to germinate in a petri dish filled with water and kept at room temperature and collected at regular intervals until the emergence of the first leaf. Collected material was fixed in 4% v/v acrolein (Polysciences, New Orleans, Louisiana, USA) in 1X PIPES buffer (50

mmol/L PIPES, 1 mmol/L MgSO4, 5 mmol/L EGTA) pH 6.8, for 24 hours. Fixed material was then rinsed three times one hour each with 1X PIPES buffer, dehydrated through a graded ethanol series, and stored in 70% ethanol.

Microscopy

Samples for sectioning were dehydrated though a graded ethanol series up to 100% ethanol, then infiltrated with and embedded in glycol methacrylate (JB-4 Embedding Kit, Electron Microscopy Sciences, Hatfield, Pennsylvania, USA). Embedded materials were serially sectioned at 4 µm thick ribbons with a Leica RM2155 rotary microtome and mounted onto slides. Sections were stained with a periodic acid-Schiff's (PAS) reagent for insoluble polysaccharides (Feder & O´Brien, 1969), counterstained with Toludine Blue for general tissue structure (Feder & O´Brien, 1969). To detect the β-glucan callose, 0.1% aniline blue in 0.1N K_3PO_4 (Currier, 1957). To visualize cellulose and other polysaccharides in cell walls, slides were stained with an aqueous solution of 0.07% calcofluor white (Hughes and McCully, 1975).

Bright field and differential interference contrast images were recorded with a Zeiss Axio Imager Z2 microscope equipped with a Zeiss HR Axiocam digital camera (Zeiss, Oberkochen, Germany). Imaging of callose was done with a Zeiss Axiophot microscope with epifluorescence (HBO 100) connected to a MRC Axiocam Zeiss digital camera and a cube filter with 365nm excitation, and 465nm long pass barrier emission wavelengths. Calcofluor-stained sections were imaged on a Zeiss LSM700 Confocal Microscope, equipped with an AxioCam HRc camera (Zeiss, Oberkochen, Germany), excitation at 405nm and a emission-detection at 465nm wavelength.

Whole-mount samples for confocal microscopy were dissected to less than 2mm in any dimension. Samples were rehydrated though a graded ethanol series to 100% aqueous, and stained for the Fuelgen reaction according to Barrell and Grossniklaus (2005), with incubation times adjusted for size of the samples. Samples were then dehydrated in a graded ethanol series to 100% ethanol. In the case of pre-fertilization and early post-fertiliztion ovules, samples were cleared by graded infiltration with Immersol 518f (Zeiss, Oberkochen, Germany). For older fertilized ovules and seeds, samples were infiltrated with and embedded JB-4 glycol methacrylate (Electron Microscopy Sciences, Hatfield, Pennsylvania, USA). Blocks were cut by hand with razor blades to remove superfluous tissue layers. Samples were mounted in a drop of Immersol 518f on custom well-slides and imaged with a Zeiss LSM700 Confocal

Microscope, equipped with an AxioCam HRc camera (Zeiss, Oberkochen, Germany). A two-pass, three-channel acquisition mode was used to maximize histochemical information: Pass one = excitation at 405 and 488 nm, emission detection between 400-520 nm (Channel 1) and 520-700 (Channel 2). Pass two = excitation at 638 nm, emission detection between 520-700 nm (Channel 3).

Digital Image Processing

Pictures, line drawings, and figures were processed using either Image J (http://rsbweb.nih.gov/ij/index.html)or Adobe Creative Suite 5 (Adobe Systems, San Jose, California, USA). For light microscopy, image manipulations were restricted to operations that were applied to the entire image. For confocal z-stacks, loss of signal with tissue depth was compensated for by using the Stack Contrast Adjustment Plugin for Image J (Čapek *et al.*, 2006). In the cases where uneven thickness of overlying tissue resulted in uneven signal brightness within an optical section, channels were adjusted manually to compensate, resulting in even signal levels across an optical section.

Maximum projections of confocal z-stacks were generated in Image J using the 3D-Project tool. 3-D surface models were created with the 3D-Viewer plugin in Image J, using the "Surface" setting on z-stacks in which each zone of interest had been manually outlined from each optical slice.

Results

Floral and ovule morphogenesis

Flowers of *Nymphaea thermarum* are hermaphroditic (Fig. 1.1). Floral buds emerge from the ground-level shoot apical meristem about twelve days before anthesis. At this stage, the outermost tepals are green and the immature inner tepals have a white/cream coloration. Two ranks of anthers surround 6-11 separate carpels. Stigmatic surfaces are delimited by upturned carpel tips and are oriented towards the ventral side of the gynoecium. Carpels are characterized by parietal placentation with numerous ovule primordia per carpel (data not shown). At six days before anthesis, anthers develop a light yellow coloration, carpel walls begin to fuse, and their tips reflex. Ovules enlarge, with both integuments present and the inner integument extends beyond the outer. Two days before flower opening, anthers increase in yellow pigmentation and papillate stigmatic surfaces are completely exposed. Ovule growth continues and an endostomic micropyle is formed.

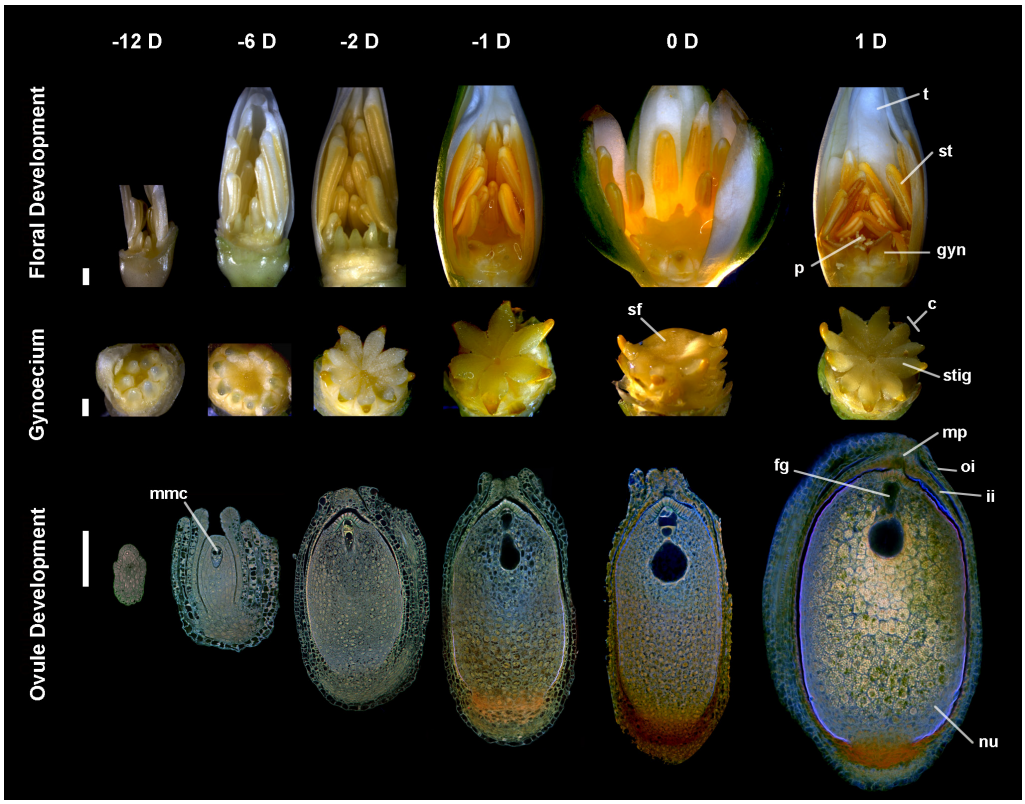

FIGURE 1.1: Flower and ovule morphogenesis in *Nymphaea thermarum*. Stages in floral biology, gynoecium development, and ovule morphogenesis are depicted at 12, 6, 2, and 1 days before anthesis, as well as the first and second day of anthesis (noted as -12 D, -6 D, -2 D, -1 D, 0 D, and 1 D, respectively). Stereomicroscope images of floral buds (first row, some perianth removed to show all floral organs) and gynoecia (second row, all other floral organs removed), along with confocal optical sections of *N. thermarum* ovules pretreated with Feulgen reaction and cleared (third row, whole ovules). *First row:* Outer ranks of anthers dehisce and some stigmatic fluid is secreted at -1 D. Flowers then open for two consecutive days (0 D, 1 D), with a prominent drop of stigmatic fluid present on 0 D and fully dehisced anthers evident at 1 D. *Second row:* carpels begin to fuse at -6 D and stigmatic surface is revealed by -2 D. Stigmatic fluid present on -1 D and prominent on 0 D. *Third row:* endostomic micropyle formed by -2 D. Mature female gametophyte, with hour-glass shape, present on -1 D. By 1 D, starch accumulation in nucellus (perisperm) is apparent. c = carpel, fg = female gametophyte, gyn = gynoecium, ii = inner integument, mmc = megaspore mother cell, mp = micropyle, nu = nucellus (perisperm), oi = outer integument, p = pollen, sf = stigmatic fluid, st = stamen, stig = stigma, t = tepal. *Scale bars*: 100 µm.

One day before flower opening, the outer rank of anthers dehisces and stigmatic fluid is secreted from the suture of each carpel. On the first day of anthesis, flowers usually open in the morning and copious stigmatic fluid is present on the surface of the gynoecium. Ovules are mature, and are anatropous, bitegmic, and crassinucellate. Flowers close in the afternoon. On the second morning of anthesis, flowers re-open and the remaining anthers dehisce to release loosely aggregated pollen, while the stigmatic surface is dry and discolored. Fertilized ovules show a dramatic increase in size and starch content. Flowers re-close typically in the afternoon of the second day. Flowers may open for one or more additional days with continued pollen release. After that, the pedicel curls to draw the closed flower down to the soil level, often partially burying the developing fruit.

Female gametophyte development

The megaspore mother cell is distinguished from other cells of the nucellus by its larger size, large nucleus, and prominent starch grains (Fig. 1.2A). Concurrent with micropyle formation, the first meiotic division occurs at the micropylar end of the megaspore mother cell (Fig. 1.2B). A tetrad of megaspores is formed at the completion of meiosis. (Fig. 1.2C). The three micropylar-most megaspores degenerate, while the chalazal-most megaspore persists and features a centrally-positioned nucleus surrounded by starch grains (Fig. 1.2D). The first mitosis of the functional megaspore produces two nuclei surrounded by a mass of cytoplasm and starch (Fig. 1.2E). By this time, the nucellar tissue between the female gametophyte and the nucellar epidermis has degenerated or been crushed by expansion of the female gametophyte, leaving the female gametophyte in direct contact with the thickened walls of the nucellar epidermis. The female gametophyte then undergoes a second round of mitosis and cellularizes into three starch-filled small cells at the micropylar end (egg apparatus), and a larger starchless cell that occupies the rest of the female gametophyte (Fig. 1.2F). The mature egg apparatus consists of two synergids and one egg cell at the micropylar end. The large central cell nucleus resides at a circumferential constriction in the central cell, giving the female gametophyte an hour-glass shape (Fig. 1.2G). Prior to fertilization, the absence of nutrient reserves in the mature gametophyte contrasts with some starch accumulation in both the nucellus surrounding the chalazal end of the female gametophyte, and in the micropylar nucellar epidermis.

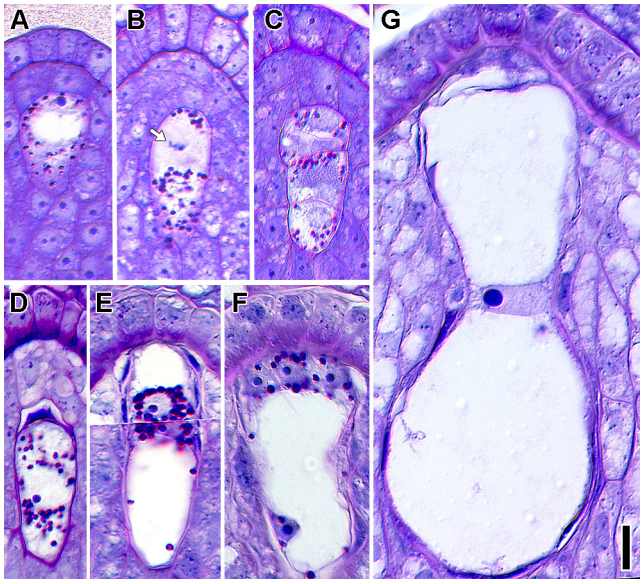

FIGURE 1.2: Female gametophyte development in *Nymphaea thermarum*. Material embedded in JB-4 resin, sectioned at 4 µm, and stained with Periodic acid Shiffs-PAS reagent and toluidine blue. (A) Megaspore mother cell, starch granules present in cytoplasm. (B) First meiotic division showing chromosomes (arrow) at the micropylar pole and starch granules at the chalazal pole. (C) Linear tetrad of four cellular megaspores. (D) Functional megaspore, formed from the chalazal-most megaspore, with degenerating micropylar megaspore. (E) Two nucleate female gametophyte, with starch surrounding the nuclei. This image represents a composite of two sequential sections. (F) Immature 4-celled female gametophyte, with three cells at the micropylar end and one (the central cell) that occupies the rest of the female gametophyte. (G) Mature female gametophyte, devoid of starch and showing an hour glass shape. Scale bar: 10 µm.

Cells of the micropylar nucellar epidermis feature a highly elaborated inner face of the chalazal-most, periclinal wall, with discrete layers of cellulose and callose. The nucellar epidermis begins to form this distinct layer about six days before anthesis (Fig. 1.3A). The inner periclinal walls, which contact or flank the developing female gametophyte, thicken and develop a convoluted appearance that persists through fertilization (Fig. 1.3B-D). This wall does not stain strongly with toluidine blue. Cellulose deposition coincides with elaboration of the inner periclinal wall six days before anthesis (Fig. 1.3E). Cellulose continues to accumulate up to anthesis (Fig. 1.3F-G). After fertilization, cellulose is absent from the site of pollen tube penetration (Fig. 1.3H, arrow). A discrete layer of callose is present on the micropylar-most face of this transfer cell-like wall approximately three days before anthesis (Fig. 1.3J-K), but is conspicuously absent after fertilization (Fig. 1.3L).

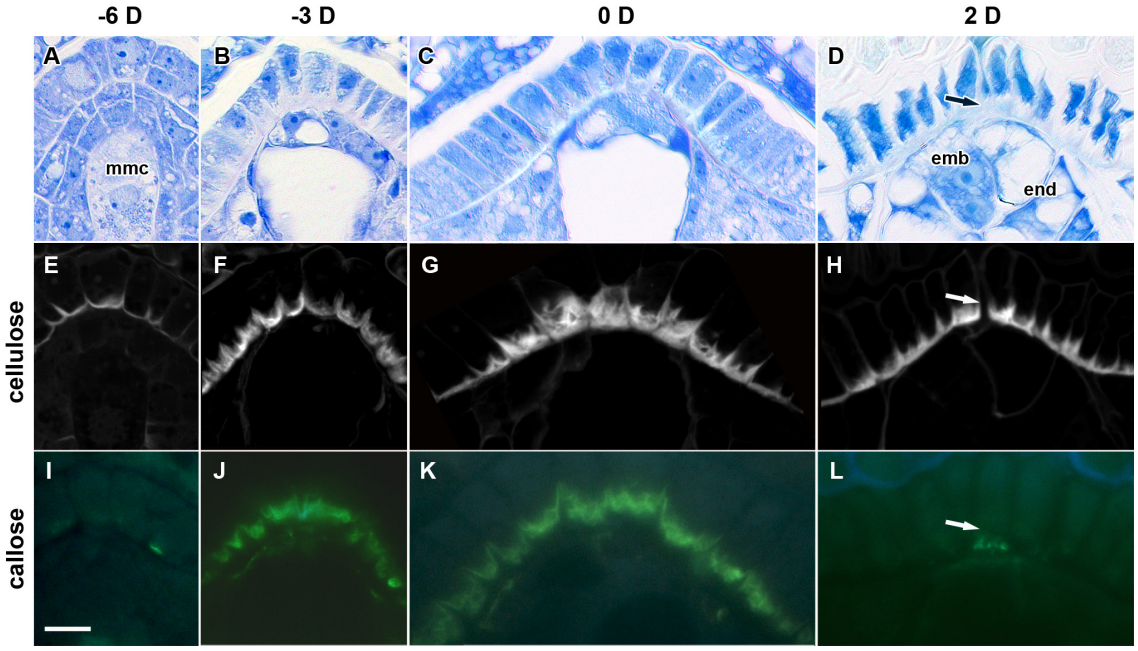

FIGURE 1.3: Micropylar nucellar epidermis in *Nymphaea thermarum* developing ovules. Ovules from 6 days before anthesis ("-6 D", megaspore mother cell stage; A, E, I), 3 days before anthesis ("-3 D", immature 4-celled female gametophyte stage; B, F, J), first day of anthesis ("0 D", mature female gametophyte stage; C, G, K), and two days after anthesis ("2 D", post-fertilization; D, H, L). Material was embedded in JB-4 resin, sectioned at 4 µm, and stained for general structure (toluidine blue; A-D), cellulose and other polysaccharides (calcofluor white; E-H), or callose (aniline blue; I-L). The inner tangential wall of the nucellar epidermis did not stain strongly with toluidine blue throughout ovule development (A-D), but did stain strongly for cellulose starting at the megaspore mother cell stage (E) with cell wall elaboration reaching a maximum by 0 D (G). After fertilization, cellulose was absent at the site of pollen tube penetration (arrowhead) (H). Callose did not accumulate until -3 D (I), but subsequently formed a discrete layer just interior to the cellulosic wall convolutions of the inner tangential wall (J-K). This callose layer was not present after pollination (L). Scale bar: 10 µm.

Pollination, double fertilization, and early endosperm differentiation

Prior to pollen deposition on the stigma surface, subdermal tissue beneath the multicellular stigmatic papillae show intense starch accumulation (Fig. 1.4A). These starch reserves decrease dramatically upon pollen tube emergence from the pollen grains (Fig. 1.4B). Strikingly, pollen grains and pollen tubes also contain copious starch reserves through the time of fertilization. Starch presence in pollen grains may be related to pollination syndrome and/or metabolic activity (Baker and Baker 1979), but significant quantities of starch in pollen tubes are rare among angiosperms. By the second day of anthesis, stigmatic cells are devoid of starch (Fig. 1.4C).

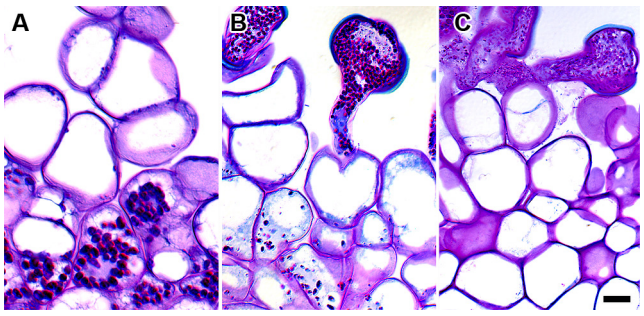

FIGURE 1.4: Pollen-stigma interactions in *Nymphaea thermarum*. Material embedded in JB-4 resin, sectioned at 4 µm, and stained with Periodic acid-Schiffs reagent and toluidine blue. (A) Starch presence in subdermal stigmatoid layer, prior to pollination (-2 D). (B) Pollen grains with high starch content one day before anthesis (-1 D), with reduction in stigmatoid starch reserves. (C) Absence of starch in stigmatic tissue, second day of anthesis (1 D). Scale bar: 10 µm.

After entering the micropyle, the pollen tube penetrates the nucellar cap and female gametophyte. Two sperm cells are discharged into one of the synergids (Fig. 1.5A). Interestingly, at the time of sperm cell discharge the central cell nucleus is located next to the egg cell apparatus (Fig. 1.5B). This migration is temporary, and shortly after fertilization the central cell nucleus, now the primary endosperm nucleus, is located at its former position at the point of female gametophyte constriction.

On the first day of anthesis, the primary endosperm nucleus divides and a transverse wall is formed in the region of the central constriction of the former female gametophyte (Fig. 1.5B, 5C). Thus, two endosperm domains are created: a micropylar endosperm domain and a chalazal endosperm domain. Two nucleoli are present in the chalazal domain endosperm nucleus (Fig. 1.5B), but after migration to the chalazal-most end, a single nucleolus is present (Fig. 1.5C). The chalazal cell is cytoplasmically dense and develops a finger-like projection into the nucellus. Two days after anthesis, the two-celled embryo has accumulated starch, and the micropylar endosperm domain has undergone multiple rounds of cell division (Fig. 1.5D). The chalazal endosperm nucleus greatly enlarges in size, suggesting multiple rounds of endoreduplication. Starch content in the surrounding nucellar tissue dramatically increases. The formation of a cell wall during the primary endosperm division, as well as the subsequent creation of a multicellular micropylar domain and a unicellular chalazal domain, demonstrates that endosperm development in *Nymphaea thermarum* is *ab intio* cellular as well as highly bipolar.

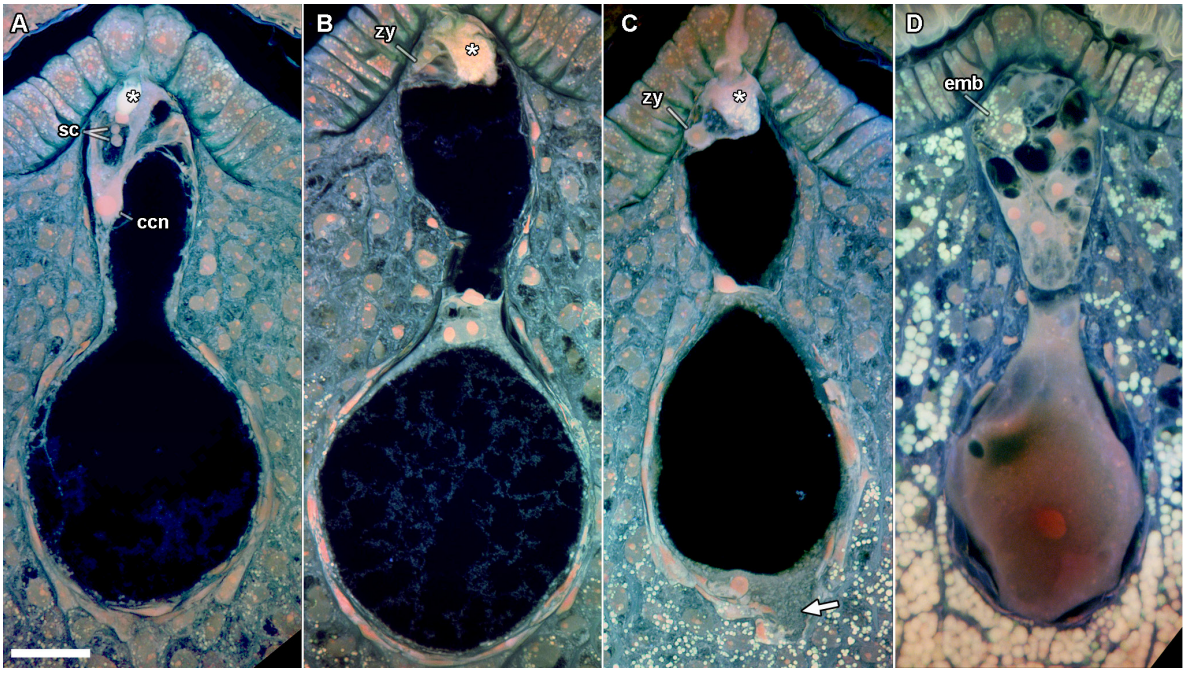

FIGURE 1.5: Fertilization and endosperm differentiation in *Nymphaea thermarum*. Confocal images shown are maximum projections of 20 or more optical sections. Material pretreated with Feulgen reaction and embedded in JB-4 resin. (A) Pollen tube penetration of the nucellar cap, and delivery of two sperm cells. The central cell nucleus is located next to the egg apparatus. (B) Primary endosperm nucleus migration and cellular division. Two endosperm domains are present: a micropylar endosperm domain, and a chalazal endosperm domain. (C) Migration of chalazal endosperm domain nucleus to the chalazal pole and extension of a finger-like projection into the nucellus (arrow). The zygote and micropylar endosperm domain remain undivided. (D) Chalazal endosperm domain nucleus enlarges but does not divide. The micropylar endosperm domain has undergone several rounds of cellular division, while the embryo is two-celled and has accumulated starch. Starch reserves were also present in the nucellus. asterisk = pollen tube discharge; ccn = central cell nucellus; emb = embryo; sc = sperm cells; zy = zygote. Scale bars: 10 µm.

Seed development

After fertilization, volumetric increase of the developing seed is accompanied by changes in the color of the seed coat: fertilized ovules progress from colorless, to bright red, and then brown in mature seeds (Fig. 1.6, top row). At maturity (and until germination) a floating aril encompasses the micropylar half of the seed.

To examine the rate and pattern of volumetric increase of the embryo, endosperm and perisperm during seed maturation, whole seeds were evaluated with confocal imaging (Fig. 1.6, bottom row). Maternal tissue (perisperm and seed coat) accounts for the greatest proportion of seed volume throughout seed development. The micropylar endosperm domain reaches its maximum area by eight days after anthesis. The outermost layer of the micropylar endosperm begins to differentiate at this time, with the rest of the micropylar endosperm cells becoming more vacuolate. The outer micropylar endosperm layer persists though seed maturity (around 22D), while the rest of the space is eventually occupied by the expanding embryo. Eight or more days later (30D), seed germination begins with the fracturing of the seed coat near the micropyle and subsequent emergence of the root apical meristem. Cotyledon expansion drives epicotyl emergence. The cotyledon tips remain in the seed and in direct contact with the single persistent layer of endosperm cells throughout germination.

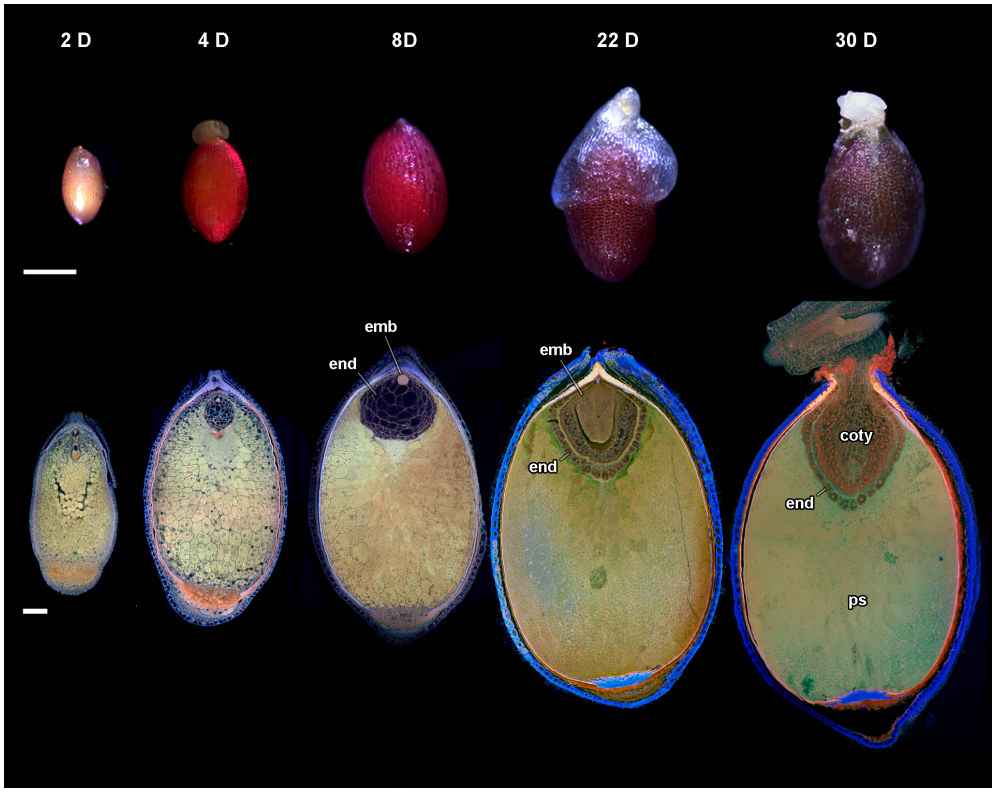

FIGURE 1.6: Seed development in *Nymphaea thermarum*. Stereomicroscope images of seeds (top row) and single confocal optical sections or maximum projections of twenty or more optical sections, material treated with Feulgen reaction (bottom row). *Top row*: External volumetric changes in developing seeds of *Nymphaea thermarum* accompanied a continued browning of the exotesta up to maturity (22 D) and through germination (30 D). *Bottom row*: Whole-mount imaging of seeds revealed that perisperm accounted for the majority of seed volume throughout development, and that perisperm accounted for the majority of volumetric seed enlargement. The endosperm reached a maximum volume at eight days after anthesis (8 D). After this point, the growing embryo displaced most of the endosperm, leaving only the outermost layer of endosperm cells. This layer persisted through germination. coty = cotyledons, end = endosperm, SAM = shoot apical meristem, ps = perisperm. Scale bars: 100 µm.

While the micropylar endosperm persists and physically separates the embryo from direct contact with maternal tissues throughout seed maturation, the chalazal endosperm domain embarks on a distinct developmental trajectory (Fig. 1.7). Immediately after the first endosperm cell division that establishes the micropylar and chalazal domains, the chalazal domain/cell is larger than the micropylar domain (1D) but undergoes a reduction in volume by two days after anthesis (2D). Growth of the micropylar domain and shrinkage of the chalazal domain (4D) continue until about eight days after anthesis, at which point the micropylar endosperm has expanded to its maximum volume (8D). By seed maturity (20D), the embryo has undergone dramatic growth, mostly at the expense of the micropylar endosperm, and the chalazal domain is difficult to detect.

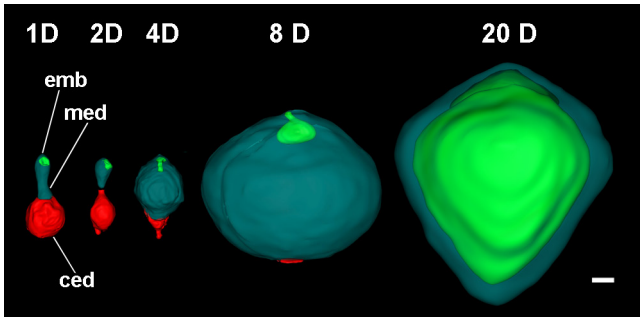

FIGURE 1.7: Embryo-endosperm volumetric relationships in *Nymphaea thermarum*. 3D surface renderings of the developing offspring tissues reconstructed from Z-stacks of whole mount ovules. Offspring tissues depicted on the second day of anthesis, and at 2, 4, 8, and 20 days after anthesis (noted as 1 D, 2 D, 4 D, 8 D, and 22 D, respectively). Immediately after fertilization, the chalazal endosperm domain was slightly larger than the micropylar domain. Growth of the micropylar domain occurred through 8 D, partly at the expense of the chalazal endosperm domain. The expansion of the embryo was comparatively negligible, until after the micropylar endosperm reached its maximum volume. The chalazal domain was rarely evident after 8 D. By the time of seed maturity (20 D), the embryo had expanded into space previously occupied by the micropylar endosperm, displacing all but a single layer peripheral endosperm cells. ced = chalazal endosperm domain, emb = embryo, med = micropylar endosperm domain. Scale bar: 10 µm.

Insoluble polysaccharides during seed development

Reserves of insoluble polysaccharides accumulate in different offspring tissues at different times throughout development. Initially, all cells of the filamentous embryo contain starch (Fig. 1.8A), but these reserves become restricted to the suspensor with differentiation of the globular embryo proper (Fig. 1.8B), and subsequent initiation of the cotyledonary ridges by eight days after fertilization (Fig 8C). Starch grains are very rarely observed in the chalazal endosperm domain/cell (arrow) or the adjacent micropylar endosperm (Fig. 1.8 D, E). However, beginning eight days after fertilization, small aggregations of starch are present in the outermost layers of the micropylar endosperm (Fig. 1.8F).

Starch accumulates centrifugally in the perisperm immediately after fertilization, with the area adjacent to the chalazal endosperm domain acting as the focal point. Three perisperm zones are readily distinguished: the endosperm adjacent zone, the transition zone, and the peripheral zone. The endosperm-adjacent zone is an amorphous mass that is present throughout seed development (Fig. 1.8 D-F). Distinct cells or cellular structures, such as nuclei and cell walls, are not evident. The transition zone is characterized by polygonal perisperm cells that transition from containing discrete starch aggregations and having identifiable nuclei (Fig. 1.8G), to being so full of starch that cellular structures become severely distorted (Fig. 1.8H, I). Finally, the peripheral zone is the outermost area of the perisperm, which is last to accumulate starch (Fig. 1.8 J-L). Cells of the peripheral zone are elongated, rather than polygonal, and the accumulated aggregations of starch are smaller than found elsewhere in the perisperm.

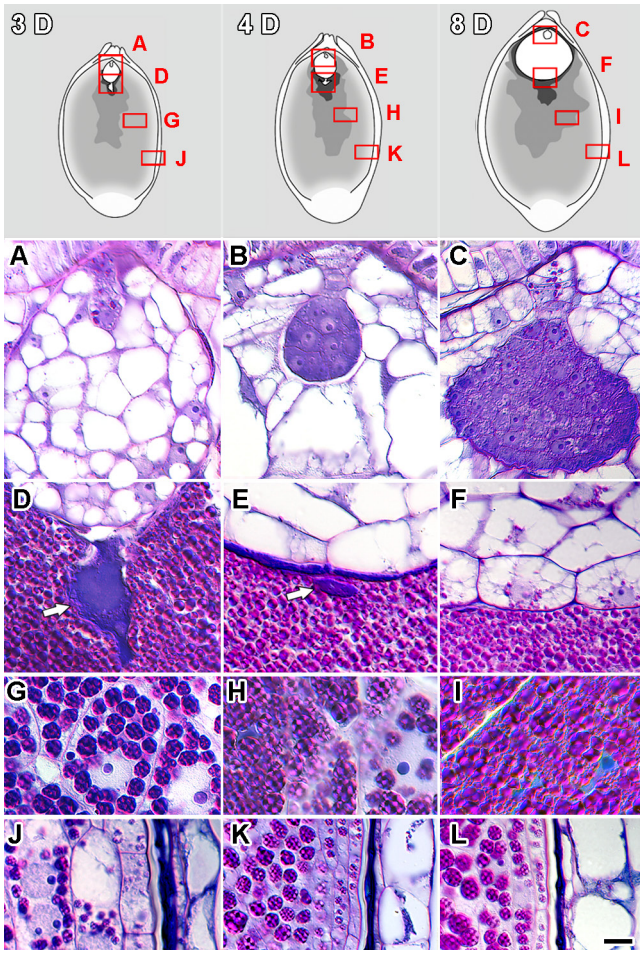

FIGURE 1.8: Insoluble polysaccharides zonation in *Nymphaea thermarum* developing seeds. Material embedded in JB-4 resin, sectioned at 4 µm, and stained with Periodic acid Shiffs-PAS reagent and toluidine blue. *N. thermarum* seeds, examined at 3 (A, D, G, J), 4 (B, E, H, K), and 8 (C, F, I, L) days after anthesis (noted as 3 D, 4 D, and 8 D, respectively). (A) Initially, starch is present throughout the filamentous embryo, but is later restricted to the suspensor and nascent root pole in the late-globular embryo (B). Inception of the cotyledonary ridges (C). (D) Early and dense accumulation of starch in the endosperm adjacent zone of the perisperm. (D-F) Starch is consistently absent from the chalazal endosperm (arrow), but is present in the peripheral layers of the micropylar endosperm at 8 days after anthesis. (G-I) Perisperm transition zone, in which cells progressively accumulate starch. (J) Perisperm peripheral zone with some multinucleate cells. (J-K) Starch accumulation is delayed relative to other perisperm zones. (L) Starch aggregations remain discrete, even at 8 days after anthesis. Scale bar: 10 µm

When the two cotyledons (asterisks) are initiated during embryo development (Fig. 1.9A), the cells of the micropylar endosperm adjacent to the embryo become increasingly vacuolate and appear to degenerate. Starch density is reduced in the perisperm adjacent to the endosperm, relative to its density in this zone at earlier stages. At seed maturity (20 days after anthesis), starch is present in the cotyledons (asterisks) of the expanded embryo and in the single layer of remaining endosperm (Fig. 1.9B). The rest of the perisperm is completely full of starch, to the point of making individual cells difficult to distinguish, thus blurring the boundary between the endosperm adjacent zone and the peripheral zone.

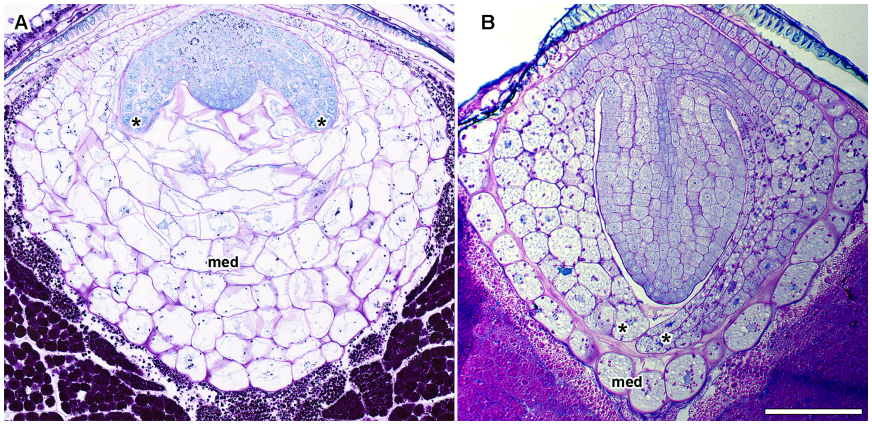

FIGURE 1.9: Seed maturation in *Nymphaea thermarum*. Material embedded in JB-4 resin, sectioned at 4 µm, and stained with Periodic acid Schiffs-PAS reagent and toluidine blue. (A) Prior to seed maturation, two cotyledons are initiated. The cells of the micropylar endosperm near the embryo become increasing vacuolate and distorted as the cotyledons expand. Starch is present in the micropylar endosperm domain. (B) In mature seeds, the embryo has expanded, displacing the majority of the micropylar endosperm. Starch is present in the persistent endosperm and throughout the cotyledons of the embryo. In the perisperm transition zone, discrete cells are no longer readily apparent. Scale bar: 100 µm.

Discussion

Flower and pollination biology of *Nymphaea thermarum*

The majority of extant basal angiosperm lineages with hermaphroditic flowers are protogynous (Thien *et al.*, 2009; Endress, 2010). In most members of the Nymphaeaceae and Cabombaceae, protogyny is manifest as a discrete temporal separation between female and male phases, punctuated by the closing and re-opening of the flower each day or night of anthesis (reviewed in Wiersema 1988). In the day-blooming subgenus *Brachyceras* (of which *Nymphaea thermarum* is a member), this sequence occurs over two or more days: the flower opens on the first day as functionally female, with stigmatic secretion present and the stigmatic surface receptive, and then closes in the evening. The following morning, the flower reopens for one or more days as functionally male, as the anthers dehisce to disperse pollen (Heslop-Harrison, 1955a; Prance and Anderson 1976; Wiersema 1988; Orban and Bouharmont, 1995; Thien *et al.*, 2009; Williams *et al.*, 2010). Although flowers of *N. thermarum* open, close, and reopen as is typical for water lilies with separate female and male phases, they are incompletely protogynous. The overlap of female and male function in *N. thermarum* is a consequence of the dehiscence of the outermost whorl(s) of anthers prior to anthesis, contemporaneous with the onset of stigmatic secretion. This advancement of male development relative to other floral ontogenetic events creates overlap between female and male function. Furthermore, *N. thermarum* resembles other hermaphroditic members of Nymphaeales in that it is capable of self-pollination (Wiersema, 1988). Since pollen is released before the flower opens, and thus before the opportunity for the flower to receive out-crossing pollen, *N. thermarum* is not only capable of self-pollination, but is very likely predisposed to it.

Pollen release in bud has been described in three genera of Nymphaeaceae (Borsch *et al., 2008*): the monotypic genus *Euryale* (Okada and Otaya, 1930; Okada, 1938; Kadono and Schneider 1987), *Barclaya* (Williamson and Schneider, 1994), and several species of *Nymphaea*, including *N. capensis* Thunb. var. *zanzibarensis* (Prance and Anderson, 1976; Orban and Bouharmont 1995), *N. ampla* (Prance and Anderson, 1976), *N. minuta* (Landon *et al.*, 2007), and *N. thermarum*, as shown in the current work. The four *Nymphaea* species all belong to the tropical subgenus *Brachyceras* (Borsch, 2011), suggesting that acceleration of male development may be a trait that evolved in a common ancestor of this group. Overlap between female and male function has been reported in other species of *Nymphaea (N. alba, N. amazonum, N. conardii, N. jamesoniana, N. ligulata, N. rudgeana)* , but in contrast to what we found

in *N. thermarum*, can be due to late or prolonged female function, rather than necessarily early male function (Wiersema 1988). Assuming that protogyny is plesiomorphic for Nymphaeaceae, the partial breakdown of this dichogamous pattern appears to have evolved independently several times within the family, and can involve different heterochronic mechanisms that affect the relative timing of either or both female and male development events.

A biological predisposition towards self-pollination can have profound effects on population dynamics, and thus the evolutionary history of a species. On one hand, self-compatibility can be advantageous in guaranteeing fruit production under unfavorable conditions such as pollinator scarcity or in fragmented populations with few individuals in small patches (Pang and Saunders, 2014). Since *N. thermarum* is extinct in the wild, pollinator interactions are unknown, but populations were known to be fragmented (Fischer, 1988; Fischer and Magdalena-Rodriguez, 2010). On the other hand, widespread selfing may have actually played a role in the demise of the species. Generations of inbreeding can decrease the amount of genetic, and thus phenotypic, variation in small populations, leading to decreased times to population extinction (Brook *et al.*, 2002; Frankham, 2005; Reed, 2005; Dornier *et al.*, 2012). This effect, compounded by the fact that population size was already constrained by specialization for a limited habitat (hot springs), may have rendered *N. thermarum* unable to cope with rapid habitat loss. Understanding how the floral biology of *N. thermarum* may have factored into its near-extinction can help conservation efforts and prevent a similar fate for other tropical and non-tropical water lilies (Nierbauer *et al.*, 2014). Other members of the subgenus *Brachyceras* that are similarly inclined towards self-pollination and found within limited ranges, such as the Madagascar endemic *N. minuta* (Landon *et al.*, 2007), are therefore of particular concern.

Ovule development in *Nymphaea thermarum*

Development of the female gametophyte and ovule of *N. thermarum* is generally in accordance with what is known from other members of the Nymphaeales. The female gametophyte of *N. thermarum* is of the Nuphar/Schisandra type, in that it is monosporic and four-nucleate, four-celled at maturity. This type of female gametophyte is characteristic of the most ancient flowering plant lineages described to date (Nymphaeales: Orban and Bouharmont, 1998; Williams and Friedman, 2002; Friedman, 2006; 2008; Rudall *et al.*, 2008. Austrobaileyales: Williams and Friedman, 2004; Friedman *et al.*,

2003; Tobe *et al.*, 2007; Bachelier and Friedman, 2011), with the exception of *Amborella trichopoda* which has a unique nine-nucleate, eight-celled female gametophyte (Friedman and Ryerson, 2009). Our observations of *N. thermarum* provide further support for the hypothesis that the Nuphar/Schisandra-type female gametophyte is the only type to be found among the Nymphaeales, despite decades of earlier reports that described occurrence of the more complex and ubiquitous Polygonum type. These reports have been shown to almost certainly be erroneous (Williams and Friedman, 2002; Friedman and Williams, 2003).

During the free-nuclear stages of female gametophyte development in *N. thermarum*, simultaneous enlargement of the female gametophyte and degeneration of the micropylar nucellus puts the female gametophyte in direct contact with the single persistent layer of nucellar epidermis. The interior periclinal cell walls of this nucellar epidermal layer thicken and become convoluted in a manner reminiscent of transfer cell morphology. Similarly differentiated tissue in the micropylar part of the ovule has been referred to as epistase, but this phenomena appears to be unusual and is poorly understood in terms of both development and function (Maheshwari, 1950). Wall thickening of the nucellar epidermis has been described in three additional species within *Nymphaea* (*N. advena*, *N. gigantea*, *N. odorata*), and in *Victoria amazonica*, (Nymphaeaceae) (Cook, 1902; 1906; Winther and Sharmov, 1991), but was (likely mistakenly) attributed to sclerification. Cytological examination of N. thermarum reveals that these prominent convoluted cell walls are distinct from the filiform apparatus, and are composed of different layers of cellulose and callose that accumulate throughout ovule maturation.

Prolonged cellulose synthesis to create wall invaginations increases surface area of the plasmalemma, and thus capacity for solute transfer, and is a common feature of transfer cell walls (Talbot *et al.*, 2007). Callose is also associated with a number of transfer cell types: the gametophyte/sporophyte interface in mosses (Ofler *et al.*,2003), nodules of legumes (Dahiya and Brewin 2000), and endosperm tissue in cereal grains (Zheng and Wang, 2011; Thiel *et al.*, 2012; Thiel, 2014). The dramatic disappearance of callose from this layer of nucellus upon pollen tube penetration in *N. thermarum* suggests that this layer might have a discrete function associated with pollen tube attraction, fertilization, and/or early offspring growth. Our examination of the broader literature on angiosperm ovules indicates that this type of cell wall patterning in the nucellus adjacent to the egg apparatus (and separate from the filiform apparatus) is either unique to water lilies or significantly under-reported (see Maheshwari 1950).

Seed ontogeny in *Nymphaea thermarum*

Studies of seed development in Nymphaeales are scattered across the last century of embryological research (Cook, 1902; 1906; 1909; Conard 1905; Seaton 1908; Martin, 1946; Meyer, 1960; Khanna, 1964a,b; 1965; 1967; Valtzeva and Savich, 1965; Schneider, 1978; Schneider and Ford, 1978; Batygina *et al.*, 1980, 1982; Schneider and Jeter, 1982; Floyd and Friedman, 2000; 2001; Yamada 2001; Williams and Friedman, 2002; Friedman *et al.*, 2008; Friedman *et al.*, 2012). Nevertheless, the more recent evaluations and reviews, which take advantage of taxonomic revisions, have revealed a number of common features of seed development Nymphaeales: a perisperm (maternally-derived storage tissue) that comprises the majority of seed volume, a small diploid endosperm, and a minute embryo.

Comparison of seed ontogenies among the three extant families of Nymphaeales (Hydatellaceae, Cabombaceae and Nymphaeaceae) indicates that details of endosperm development vary between, and even within, these families. Members of Hydatellaceae have a cellular endosperm that remains fairly undifferentiated (Friedman *et al.*, 2012; Rudall *et al.*, 2009). In Nymphaeaceae and Cabombaceae, division of the primary endosperm cell into two cells gives rise to a bipolar endosperm with two distinct domains: the micropylar domain which surrounds the embryo, and the chalazal domain which faces (and often penetrates) the maternal tissues of the perisperm (Cook, 1902; 1906; 1909; Seaton, 1908; Khanna, 1964b; 1965; 1967; Floyd and Friedman, 2000 and 2001; Yamada, 2001; Schneider and Jeter, 1982). While the chalazal domain remains uninucleate, the divisions that take place in the micropylar domain can be either free nuclear (Cabombaceae) (Cook, 1906; Floyd and Friedman, 2000) or cellular (Nymphaeaceae) (Cook, 1902 1906, 1909; Khanna, 1967; Schneider 1978; Schneider and Ford, 1978; Seaton 1908; Floyd and Friedman, 2001) and will ultimately create the majority of endosperm tissue within the seed. The *ab initio* endosperm development in *N. thermarum* is fundamentally similar to what has been described in other members of the Nymphaeaceae.

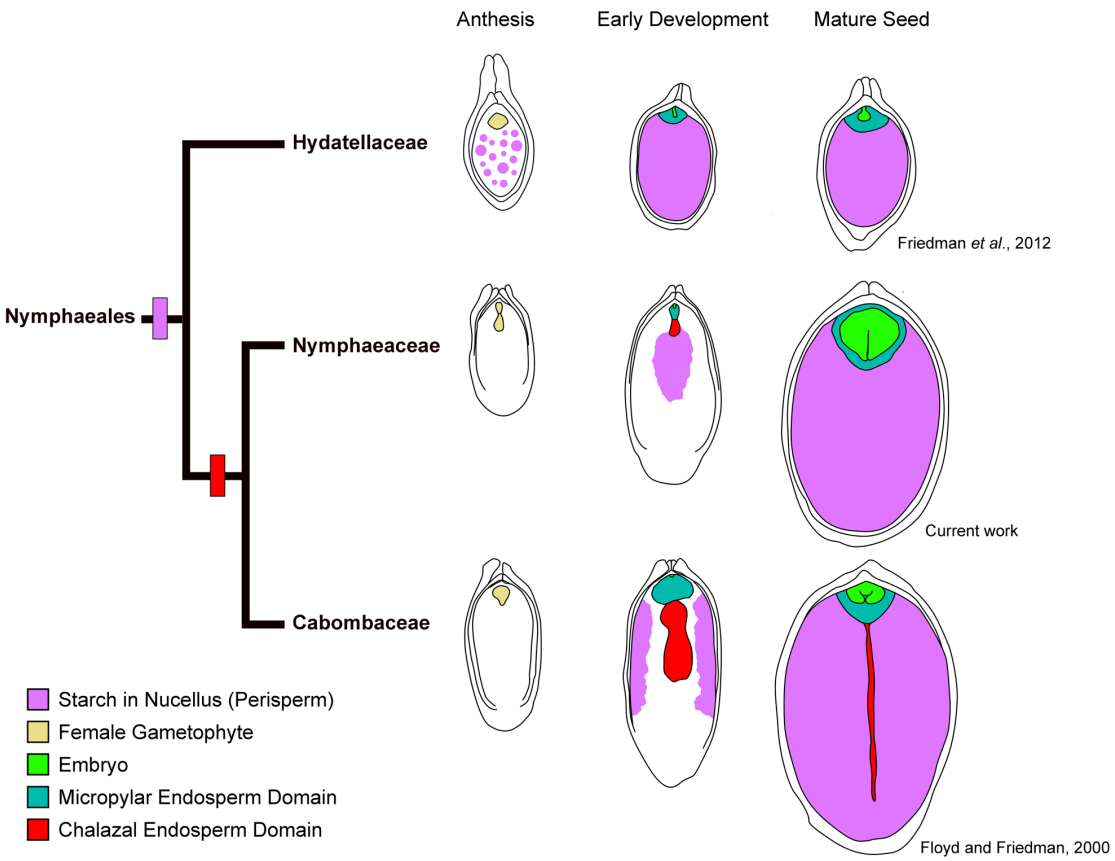

Figure 1.10. Patterns of starch accumulation in the maternal tissues during seed development of Nymphaeales. While members of the Hydatellaceae show starch accumulation (pink) throughout the perisperm before fertilization, in *Nymphaea* (Nymphaeaceae) starch accumulates centrifugally in the perisperm after fertilization, and the chalazal endosperm (red) has an ephemeral nature. In turn, *Cambomba* (Cambombaceae) shows centripetal starch accumulation in the perisperm, and the chalazal endosperm protrudes into the perisperm and persists at seed maturity. Teal: micropylar endosperm domain; Green: embryo; Beige: female gametophyte

Studies of seeds in *Nymphaea* typically have not recorded the complete ontogeny of the different tissues (Cook, 1902, 1906, 1909; Seaton, 1908; Khanna, 1964a, 1967; Batygina, 1980; Valtzeva and Savich, 1965; Rudall *et al.*, 2009), and many have overlooked the development of the ephemeral chalazal endosperm domain. Our study of *N. thermarum* provides the most complete ontogeny of the chalazal endosperm domain in any species of *Nymphaea*. Notably, while the domain remains unicellular and uninucleate, it produces a single, minute projection that protrudes into the perisperm. The presence and extent of development of a chalazal endosperm protrusion varies across Nymphaeales (Fig. 1.10). In Hydatellaceae, the chalazal endosperm domain is not apparent and is in fact difficult to distinguish at all (Friedman *et al.*, 2012). In Cabombaceae and *Nuphar* (Nymphaeaceae), the chalazal endosperm domain (protrusion) forms a large tube-like structure that penetrates through the perisperm, almost to the chalazal end of the seed, and persists at seed maturity (Cook, 1902; 1906; 1909; Seaton, 1908; Khanna, 1964b; 1965; 1967; Schneider and Jeter 1982; Floyd and Friedman, 2000 and 2001; Yamada 2001).

The chalazal endosperm domain of several members of the Nymphaeales has been referred to as a haustorial structure, based primarily on its proximity to and apparent interaction with the perisperm tissue (Cook 1902, 1906; Khanna, 1965; 1967; Valtzeva and Savich, 1965; Schneider and Jeter, 1982; Floyd and Friedman 2000). We note that throughout Nymphaeales the degree of protrusion of the chalazal endosperm appears to correlate inversely with the presence of starch in the immediately adjacent perisperm at the time of chalazal endosperm development. Patterns of perisperm starch accumulation vary both spatially and temporally, and may contribute to variation in chalazal endosperm development. Before fertilization in Hydatellaceae, the entire perisperm is filled with starch (Friedman, 2008: Friedman *et al.*, 2012). In Cabombaceae, post-fertilization starch accumulation in the perisperm is centripetal (Figure 10). In *Nymphaea* (this study), starch first accumulates after fertilization at the center of the perisperm and proceeds in a centrifugal pattern. While we cannot establish a causal link between centrifugal perisperm filling and 'stunted' chalazal endosperm development in *N. thermarum* compared with centripetal perisperm filling and prolonged chalazal development in *Cabomba*, our observations support the idea that chalazal endosperm development, and probably function, is intimately linked to nutrient dynamics within the seed.

***Nymphaea thermarum* as a Model System for Illuminating Early Evolution of Key Angiosperm Traits**

Extensive study of eudicot and monocot "model" taxa has revealed much about the molecular biology and gene interactions that underlie flower and seed development (reviewed, for example, in Zanis 2007; Litt and Kramer 2010; Ruan *et al.*, 2012; Dresselhaus and Doughty, 2014; Lafon-Placette and Köhler, 2014; Ó'Maoiléidigh *et al.*, 2014). However, we know relatively little about how these processes operate in early-diverging angiosperm lineages (Soltis *et al.*, 2007; Chanderbali *et al.*, 2010). Consequently, it has not been possible to reconstruct the molecular development of flowers and reproductive processes during the earliest phases of angiosperm evolution.

The lack of genetic and molecular studies in the most ancient angiosperm lineages is not without good reason: the majority of taxa in these clades are woody and long-lived, which makes them unsuitable as subjects for molecular and genetic experiments. During the last five years, three herbaceous members of basal angiosperm lineages have been suggested as possible model systems: *Trithuria* (Hydatellaceae) (Rudall *et al.*, 2009), *Cabomba caroliniana* (Cabombaceae) (Vialette-Guiraud *et al.*, 2011), and *Aristolochia fimbriata* (Aristolochiaceae, Piperales) (Bliss *et al.*, 2013). As of now, none of these taxa has been embraced as a major "model" system. We suggest that *Nymphaea thermarum* has a unique potential for development into a model system. Many of its growth requirements have already been established (Fisher and Magdalena Rodriguez, 2010). The diminutive size of *N. thermarum* means that large numbers of individuals can be maintained in greenhouses or growth chambers, and although they are "aquatic," these plants can be raised in individual pots placed in shallow tanks or tubs. Importantly, *N. thermarum* has a short life cycle of 5-6 months from seed germination to seed production, a generational timeframe that is exceedingly rare among basal angiosperms. Each flower can produce hundreds of seeds following either self-pollination or, if the maternal flower is emasculated at least one full day before anthesis, cross-pollination. A small genome size (1 C = 0.51 pg, only about twice the size of *Arabidopsis thaliana*) further makes this system tractable for genetic experimentation (Pellicer *et al.*, 2013). Indeed, work is underway to 1) produce transcriptomes from a variety of tissues, 2) generate isogenic lines, and 3) develop stable transformation protocols. An annotated genome would complete the package of creating a model system taxon rooted deeply at the base of the flowering plant phylogeny.

Finally, the results from this study establish a timeline for female reproductive development, floral biology, and seed development. A firm understanding of the reproductive biology of *N. thermarum*,

combined with information on remaining genetic diversity maintained in ex situ collections, will be essential for any attempt to reintroduce populations into the wild and conserve this remarkable species.

References

Bachelier JB, Friedman WE (2011) Female gamete competition in an ancient angiosperm lineage. *Proc-Natl Acad Sci U S A* 180: 12360–12365.

Baker HG, Baker I (1979) Starch in angiosperm pollen grains and its evolutionary significance. *Am J Bot* 66: 591–600.

Barrell P, Grossniklaus U (2005) Confocal microscopy of whole ovules for analysis of reproductive development: the *elongate1* mutant affects meiosis II. *Plant J* 43: 309-320.

Baskin CC, Baskin JM (2007) Nymphaeaceae: a basal angiosperm family (ANITA grade) with a fully developed embryo. *Seed Sci Res* 17: 293–296.

Batygina TB, Kravtsova TI, Shamrov II (1980) The comparative embryology of some representatives of the orders Nymphaeales and Nelumbolales. *Botanicheskii Zhurnal* 65: 1071–1086.

Batygina TB, Shamrov II, Kolesova GE (1982) Embryology of the Nymphaeales and Nelumbonales II. The development of the female embryonic structures. *Botanicheskii Zhurnal* 67: 117S–119S.

Bliss BJ, Wanke S, Barakat A, *et al* (2013) Characterization of the basal angiosperm *Aristolochia fimbriata*: a potential experimental system for genetic studies. *BMC Plant Biol* 13: 13. doi:10.1186/1471-2229-13-13.

Bonilla-Barbosa J, Novelo A, Orozco YH, Márquez-Guzmán J (2000) Comparative seed morphology of Mexican *Nymphaea* species. *Aquat Bot* 68: 189–204.

Borsch T, Löhne C, Mbaye MS, Wiersema J (2011) Towards a complete species tree of *Nymphaea*: shedding further light on subg. Brachyceras and its relationship to the Australian water-lilies. *Telopea* 13: 193–217.

Borsch T, Löhne C, Wiersema J (2008) Phylogeny and evolutionary patterns in Nymphaeales: integrating genes, genomes and morphology. *Taxon* 57: 1052–1081.

Brook BW, Tonkyn DW, Q´Grady JJ, Frankham R (2002) Contribution of inbreeding depression to extinction risk in threatened species. *Conserv Ecol* 6(1): 16.

Čapek, M., J. Janáček, Kubìnová L (2006) Methods of compensation of the light attenuation with depth of images captured by a confocal microscope. *Microsc Res Tech* 69: 624-635.

Capperino ME, Schneider EL (1985) Floral biology of *Nymphaea Mexicana* Zucc (Nymphaeaceae). *Aquat Bot* 23: 83–93.

Chanderbali AS, Yoo M, Zahn LM, *et al* (2010) Conservation and canalization of gene expression during angiosperm diversification accompany the origin and evolution of the flower. *Proc Natl Acad Sci U S A* 107: 22570-22575.

Chiflot JBJ (1902) Contributions a l'etude de la classe des Nympheinees. *Annales de L'Université de Lyon, nouvelle série.* 10: 1–294.

Conard HS (1905) *The water lilies: A monograph of the genus Nymphaea*. Washington: Carnegie Institution of Washington.

Cook MT (1902) Development of the Embryo-Sac and Embryo of *Castalia odorata* and *Nymphaea advena* Author. *Bull Torrey Bot Club* 29: 211–220.

Cook MT (1906) The embryogeny of some Cuban Nymphaeaceae. *Bot Gaz* 42: 376–392.

Cook MT (1909) Notes on the embryology of Nympaeaceae. *Bot Gaz* 48: 56-59.

Currier HB (1957) Callose substance in plant cells. *Am J Bot* 44: 478–488.

Dahiya P, Brewin NJ (2000) Immunogold localization of callose and other cell wall components in pea nodule transfer cells. *Protoplasma* 214: 210–218.

Davis CC, XI Z, Mathews S (2014) Plastid phylogenomics and green plant phylogeny: almost full circle but not quite there. *BMC Biol* 12:11.

Dornier A, Cheptou P (2012) Determinants of extinction in fragmented plant populations: *Crepis sancta* (asteraceae) in urban environments. *Oecologia* 169: 703–712.

Doyle JA, Endress PK (2014) Integrating early Cretaceious fossils into the phylogeny of living angiosperms: ANITA lines and relatives of Chloranthaceae. *Int J Plant Sci* 175: 555–600.

Dresselhaus T, Doughty J (2014) Regulation of fertilization and early seed development. *Biochem Soc Trans* 42: 309-312.

Endress PK (2001) The flowers in extant basal angiosperms and inferences on ancestral flowers. *Int J Plant Sci* 162: 1111–1140.

Endress PK (2005) Carpels in *Brasenia* (Cabombaceae) are completely ascidiate despite a long stigmatic crest. *Ann Bot* 96: 209–215.

Endress PK (2010) The evolution of floral biology in basal angiosperms. *Philos Trans of the R Soc B Biol Sci* 365: 411–421.

Feder N, O'Brien TP (1968) Plant microtechnique: some principles and new methods. *Am J Bot* 55: 123–142.

Fischer E, Magdalena-Rodriguez C (2010) *Nymphaea thermarum* (Nymphaeaceae). *Curtis Bot Mag* 27:318–327.

Fischer, E (1988) Beitr¨age zur Flora Zentralafrikas I. Eine neue *Nymphaea* sowie ein neuer *Streptocarpus* aus Rwanda. *Feddes Repert* 99: 385–390.

Floyd SK, Friedman WE (2000) Evolution of endosperm developmental patterns among basal flowering plants. *Int J Plant Sci* 16: S57–S81.

Floyd SK, Friedman WE (2001) Developmental evolution of endosperm in basal angiosperms: Evidence from *Amborella* (Amborellaceae), *Nuphar* (Nymphaeaceae), and *Illicium* (Illiciaceae). *Plant Syst Evol* 228: 153–169.

Frankham R (2005) Genetics and extinction. *Biol Conserv* 126(6): 131–140.

Friedman WE, Bachelier JB, Hormaza JI (2012) Embryology in *Trithuria submersa* (Hydatellaceae) and relationships between embryo, endosperm, and perisperm in early-diverging flowering plants. *Am J Bot* 99: 1083–1095.

Friedman WE, Gallup WN, Williams JH (2003) Gametophyte development in *Kadsura*: implications for Schisandraceae, Austrobaileyales, and the early evolution of flowering plants. *Int J PLant Sci* 164: S293–S305.

Friedman WE, Ryerson KC (2009) Reconstructing the ancient female gametophyte in angiosperms: insights from *Amborella* and other ancient lineages of flowering plants. *Am J Bot* 96: 129–143.

Friedman WE, Williams JH (2003) Modularity of the angiosperm female gametophyte and its bearing on the early evolution of endosperm in flowering plants. *Evolution* 57: 216–230.

Friedman WE (2006) Embryological evidence for developmental labiality during early angiosperm evolution. *Nature* 441: 337–340.

Friedman, WE (2008) Hydatellaceae are water lilies with gymnospermous tendencies. *Nature* 453: 94 – 97.

Friis EM, Crane PR, Pedersen KR (2011) *Early flowers and angiosperm evolution.* Cambridge: Cambridge University Press.

Friis EM, Pedersen KR, Crane PR (2006) Cretaceous angiosperm flowers: innovation and evolution in plant reproduction. *Palaeo* 232: 251–293.

Friis EM, Pedersen KR, Crane, PR (2001) Fossil evidence of water lilies (Nymphaeales) in the Early Cretaceous. *Nature* 410: 357–360.

Grob V, Moline P, Pfeifer E, Novelo AR, Rutishauser R (2006) Developmental morphology of branching flowers in *Nymphaea prolifera*. *J Plant Res* 119: 561–570.

Heslop-Harrison Y (1955*a*) Biological flora of the British Isles. Nuphar Sm. *J Ecol* 43: 342–364.

Heslop-Harrison Y (1955*b*) Biological flora of the British Isles. *J Ecol* 42: 719–734.

Hu GW, Lei LG, Liu KM, Long CL (2009) Floral development in *Nymphaea tetragona* (Nymphaeaceae). *Bot J Linn Soc* 159: 211–221.

Hughes J, McCully ME (1975) The use of an optical brightener in the study of plant structure. *Stain Technol* 50: 319–329.

Iles WD, Lee C, Sokoloff DD, *et al* (2014) Reconstructing the age and historical biogeography of the ancient flowering-plant family Hydatellaceae (Nymphaeales). *BMC Evol Biol* 14:120. doi:10.1186/1471-2148-14-102.

Kadono Y, Schneider EL (1987) The life history of *Euryale ferox* Salisb. In Southwestern Japan with special reference to reproductive ecology. *Plant Species Biol* 2: 109–115

Khanna P (1964a) Some interesting observations in *Euryale ferox* Salisb. *Curr Sci* 33: 152.

Khanna P (1964b) Morphological and embryological studies in Nymphaeaceae. I. *Euryale ferox* Salisb. *P Indian Acad Sci Plant Sci* 59: 237–244.

Khanna P (1965) Morphological and embryological studies in Nymphaeaceae II. *Brasenia scherebei* Gmel. and *Nelumbo nucifera* Gaertin. *Aust J Bot* 13: 379–387.

Khanna P (1967) Morphological and embryological studies in Nymphaeaceae III. *Victoria cruziana* D´Orb., and *Nymphaea stellate* Willd. *Bot Mag Tokyo* 80: 305–312.

Lafon-Placette C, Köhler C (2014) Embryo and endosperm, partners in seed development. *Curr Opin Plant Biol* 17: 64–69.

Landon K, Nozaic PI, Edwards RA (2007) A new species of water lily (*Nymphaea minuta*: Nymphaeaceae) from Madagascar. *Water Garden Journal* 22: 5–10.

Litt A, Kramer, EM (2010) The ABC model and the diversification of floral organ identity. *Semin Cell Dev Biol* 21: 129–137.

Magallón S, Hilu KW, Quandt D (2013) Land plant evolutionary timeline: gene effects are secondary to fossil constraints in relaxed clock estimation of age and substitution rates. *Am J Bot* 100: 556–573.

Maheshwari P (1950) *An introduction to the embryology of angiosperms.* Mc Graw Hill Book Company, New York.

Maia VH, Gitzendanner MA, Soltis PA, Wong GK, Soltis DE (2014) Angiosperm Phylogeny Based on 18S/26S rDNA Sequence Data: Constructing a Large Data Set Using Next-Generation Sequence Data. *Int J Plant Sci* 75: 613–650.

Martin AC (1946) The comparative internal morphology of seeds. *Am Midland Natur* 36: 513–660.

Meyer KI. 1960. On the embryology of *Nuphar luteum* SM. *Bull of Moscow Soc Natur Biol Series* 65: 48–60.

Moseley MF, Mehta IJ, Williamson PS, Kosakai H (1984) Morphological Studies of the Nymphaeaceae (Sensu Lato). XIII. Contributions to the Vegetative and Floral Structure of *Cabomba*. *Am J Bot* 71: 902–924.

Moseley MF (1961) Morphological studies of the Nymphaeaceae II. The flower of *Nymphaea*. *Bot Gaz* 122: 233–259.

Nierbauer KU, Kanz B, Zizka G (2014) The widespread naturalization of Nymphaea hybrids is masking the decline of wild-type *Nymphaea alba* in Hesse, Germany. Flora - Morphology, Distribution, Functional *Ecol Plants* 209: 122–130.

Ó'Maoiléidigh DS, Graciet E, Wellmer F (2014) Gene networks controlling *Arabidopsis thaliana* flower development. *New Phytol* 201: 16–30.

Offler CE, McCurdy DW, Patrick JW, Talbot MJ (2003) Transfer cells: cells specialized for a special purpose. *Ann Rev Plant Biol* 54: 431–454.

Okada Y, Otaya T (1930) Study of *Euryale ferox* Salisb. VI. Cleistogamous versus chasmogamous flower. *Bot Mag Tokyo* 44: 369–373.

Okada, Y (1938) On chasmogamous flowers of *Euryale ferox* Salisb. *Eco Rev* 4: 159–163.

Orban I, Bouharmont J (1995) Reproductive biology of *Nymphaea capensis* Thunb. var. *zanzibariensis* (Casp.) Verdc (Nymphaeaceae). *Bot J Linn Soc* 119: 35–43.

Orban I, Bouharmont J (1998) Megagametophyte development of *Nymphaea nouchali* Burm. F (Nymphaeaceae). *Bot J Linn Soc* 126: 339–348.

Pang C, Saunders RMK (2014) The evolution of alternative mechanisms that promote outcrossing in Annonaceae, a self-compatible family of early-divergent angiosperms. *Bot J Linn Soc* 174: 93–109.

Pellicer J, Kelly LJ, Magdalena C, Leitch IJ (2013) Insights into the dynamics of genome size and chromosome evolution in the early diverging angiosperm lineage Nymphaeales (water lilies). *Genome* 56: 1–13.

Prance GT, Anderson AB (1976) Studies of the floral biology of tropical Nymphaeaceae. *Acta Amazonica* 6: 163–170.

Qiu YL, Lee J, Bernasconi-Quadroni F, *et al* (1999) The earliest angiosperms: evidence from mitochondrial, plastid and nuclear genomes. *Nature* 402: 404–407.

Ramji MV, Padmanabhan D (1965) Developmental studies on *Cabomba caroliniana* Gray I. Ovule and carpel. *Proc Indian Acad Sci Section B* 62: 215–223.

Reed DH (2005) Relationship between Population Size and Fitness. *Conserv Biol* 19:563–568.

Ruan Y, Patrick JW, Bouzayen M, Fernie AR (2012) Molecular regulation of seed and fruit set. *Trends Plant Sci* 17:656–665

Rudall PJ, MV Remizowa, A. S. Beer, E. Bradshaw, D.W. Stevenson, T. D. Macfarlane, R. E. Tuckett , *et al (*2008) Comparative ovule and megagametophyte development in Hydatellaceae and water lilies reveal a mosaic of features among the earliest angiosperms. *Ann Bot* 101: 941–956 .

Rudall PJ, Eldridge T, Tratt J *et al* (2009) Seed fertilization, development, and germination in Hydatellaceae (Nymphaeales): implications for endosperm evolution in early angiosperms. *Am J Bot* 96: 1581–1593.

Rudall PJ, Sarkoloff DD, Remizowa MV, *et al* (2007) Morphology of Hydatellaceae, an anomalous aquatic family recently recognized as an early-divergent angiosperm lineage. *Am J Bot* 94: 1073–1092.

Ruhfel BR, Gitzendanner MA, Soltis PS, Soltis DE, Burleigh JG (2014) From algae to angiosperms–inferring the phylogeny of green plants (Viridiplantae) from 360 plastid genomes. *BMC Evol Biol* 14: 23.

Saarela JM, Rai HS, Doyle JA, *et al* (2007) Hydatellaceae identified as a new branch near the base of the angiosperm phylogenetic tree. *Nature* 446: 312–315.

Schneider EL, Chaney T (1981) The floral biology of *Nymphaea odorata* (Nymphaeaceae). *The Southwestern Nat* 26: 159–165.

Schneider EL, Ford EG (1978) Morphological studies of the Nymphaeacee. X. The seed of *Ondinea purpurea* Den Hartog. *Bull Torrey Bot Club* 105: 192–200.

Schneider EL, Jeter JM (1982) Morphological studies of the Nymphaeaceae XII. The Floral Biology of *Cabomba caroliniana*. *Am J Bot* 69: 1410–1419.

Schneider EL, Moore LA (1977) Morphological studies of the Nymphaeaceae. VII. The floral biology of *Nuphar lutea* subsp. *Macrophylla*. *Brittonia* 29: 88–99.

Schneider EL, Tucker SC, Williamson PS (2003) Floral development in the Nymphaeales. *Int J Plant Sci* 164: S279–S292.

Schneider EL (1976) The floral anatomy of *Victoria* Schomb (Nymphaeaceae). *Bot J Linn Soc* 72: 115–148.

Schneider EL (1978) Morphological studies of the Nymphaeaceae IX. The seed of *Barclaya longifolia* Wall. *Bot Gaz* 139: 223–230.

Schneider EL (1983) Gross morphology and floral biology of *Ondinea purpurea* den Hartog. *Aust J Bot* 31: 371–382.

Schneider, EL (1982) Observations on the pollination biology of *Nymphaea gigantea* WJ Hooker (Nymphaeaceae). *West Aust Nat* 15: 71–72.

Seaton S (1908) The development of the embryo-sac of *Nymphaea advena*. *Bull Torrey Bot Club* 35: 283–290.

Sokoloff DD, Remizowa MV, Briggs BG, *et al (*2009) Shoot architecture and branching pattern in perennial Hydatellaceae (Nymphaeales). *Int J Plant Sci* 170: 869–884.

Sokoloff DD, Remizowa MV, Yadav SR, *et al (*2010) Development of reproductive structures in the sole Indian species of Hydatellaceae, *Trithuria konkanensis*, and its morphological differences from Australian taxa. *Aust Syst Bot* 23: 217–228.

Soltis DE, Chanderbali AS, Kim S, Buzgo M, Soltis PS (2007) The ABC model and its applicability to basal angiosperms. *Ann Bot* 100: 155–163.

Stevens PF (2001) *Angiosperm Phylogeny Website*. http://www.mobot.org/MOBOT/research/APweb/. 16 July 2014.

Talbot MJ, Wasteneys GO, Ofler CE, McCurdy DW (2007) Cellulose synthesis is required for deposition of reticulate wall ingrowths in transfer cells. *Plant Cell Physiol* 48: 147–158.

Thiel J, Riewe D, Rutten T, *et al* (2012) Differentiation of endosperm transfer cells of barley: a comprehensive analysis at the micro-scale. *Plant J* 71: 639–655.

Thiel J (2014) Development of endosperm transfer cells in barley. *Front Plant Sci* 5: 108. doi: 10.3389/fpls.2014.00108

Thien LB, Bernhardt P, Devall MS, *et* al (2009) Pollination biology of basal angiosperms (ANITA grade). *Am J Bot* 96: 166–182.

Tobe H, Kimoto Y, Prakash N (2007) Development and structure of the female gametophyte in *Austrobaileya scandens* (Austrobaileyaceae). *J PLant Res* 120: 431–436.

Valtzeva OV, Savich EI (1965) Development of embryo in *Nymphaea candida* Presl. and *N. tetragona* Georgi. *Botanicheskii Zhurnal* 50: 1323–1326.

Van Miegroet F, Dujardin M (1992) Cytologie et histolgie de la reproduction chez le *Nymphaea heudelotii*. *Canad J Bot* 70: 1991–1996.

Vialette-Guiraud ACM, Alaux M, Legeai F, *et al* (2011) *Cabomba* as a model for studies of early angiosperm evolution. *Ann Bot* 108: 589–598.

Wiersema JH (1988) Reproductive biology of *Nymphaea* (Nymphaeaceae). *Ann Missouri Bot Gard* 75: 795–804.

Williams JH , Friedman WE (2002) Identification of diploid endosperm in an early angiosperm lineage. *Nature* 415: 522–526.

Williams JH, Friedman WE (2004) The four-celled female gametophyte of Illicium (Illiciaceae; Austrobaileyales): Implications for understanding the origin and early evolution of monocots, eumagnoliids, and eudicots. *Am J Bot* 91: 332–357.

Williams JH, McNeilage RT, Lettre MT, *et al* (2010) Pollen tube growth and the pollen-tube pathway of

Nymphaea odorata (Nymphaeaceae). *Bot J Linn Soc* 162: 581–593.

Williamson PS, Moseley MF (1989) Morphological Studies of the Nymphaeaceae Sensu Lato. XVII. Floral Anatomy of *Ondinea purpurea* Subspecies *Purpurea* (Nymphaeaceae). *Am J Bot* 76: 1779–1794.

Williamson PS, Schneider EL (1994) Floral aspects of *Barclaya* (Nymphaeaceae): pollination, ontogeny and structure. *Plant Syst Evol* 8: 159–173.

Winter AN, Shamrov II (1991) Megasporogenesis and embryo sac development in representatives of the genera *Nymphaea* and *Victoria* (Nymphaeaceae). *Botanicheskii Zhurnal* 76: 1716–1728.

Yamada T, Imaichi R, Kato, M (2001) Developmental morphology of ovules and seeds of Nymphaeales. *Am J Bot* 88: 963-974.

Zanis MJ (2007) Grass spikelet genetics and duplicate gene comparisons. *Int J Plant Sci* 168:93–110.

Zheng Y, and Wang Z (2011) Contrast observation and investigation of wheat endosperm transfer cells and nucellar projection transfer cells. *Plant Cell Rep* 30: 1281–1288.

Zhou Q, Fu D (2007) Floral biology of *Nuphar pumila* (Timm) DC (Nymphaeaceae) in China. *Plant Syst Evol* 264: 101–108.

Zhou Q, Fu D (2008) Reproductive morphology of *Nuphar* (Nymphaeaceae), a member of basal angiosperms. *Plant Syst Evol* 272: 79–96.

Funding Information

This work was supported by a grant from the NSF [grant number IOS-S-0919986] to W.E.F.

Acknowledgements

We thank Ekaterina Morozova for help with sectioning, and the staff of Botanische Gärten der Universität Bonn for providing plant material for propagation.

Chapter 2

Title: Reciprocal interploidy crosses in *Nymphaea thermarum*: a new perspective on interparental conflict and flowering plant evolution

Authors: Rebecca Povilus[a], Pamela K. Diggle[b], William E. Friedman[a,c]

[a] Department of Organismic and Evolutionary Biology, Harvard University, 26 Oxford Street, Cambridge, MA 02138, USA; [b] Department of Ecology and Evolutionary Biology, University of Connecticut, Storrs, CT 06269-3043, USA [c] Arnold Arboretum of Harvard University, 1300 Centre Street, Boston, MA 02131, USA

Manuscript in review at the Proceedings of the Royal Society of London B - Biological Sciences.

Abstract

Endosperm is a genetically biparental product of a second fertilization event that is unique to angiosperms (flowering plants). Because endosperm separates its compatriot embryo from the maternal sporophyte for most of seed development, it is a *de facto* mediator of nutrient dynamics within a seed. Furthermore, experimental and theoretical studies have demonstrated that endosperm, as a biparental entity, is central to understanding how conflicting parental interests in resource distribution can affect offspring development. While these studies draw from a range of monocot and eudicot taxa, they have not included members of any of the early-diverging angiosperm lineages, nor do they span the full developmental and structural diversity of seeds. We performed reciprocal interploidy crosses in the experimentally tractable water lily *Nymphaea thermarum*, a member of the Nymphaeales, one of the most ancient angiosperm lineages. Seed component sizes and embryo morphogenesis were compared between crosses of diploid and tetraploid parents over the course of ovule maturation and seed development. Changes to maternal and paternal genome dosage altered the development of offspring tissues, but had little impact on nutrient allocation into the seed. Rather, the size of the perisperm (a maternally-derived nutrient storage tissue) was exclusively influenced by maternal ploidy. Altogether, we provide the first evidence that parent-of-origin effects on offspring development may date to the evolutionary origin of flowering plants and their unique embryo-nourishing tissue, endosperm. We also demonstrate that that the evolutionary transfer of embryo-nourishing function from a genetically biparental endosperm to a genetically maternal perisperm can function as a maternal strategy to recapture control of resource distribution among progeny.

Keywords: Interparental conflict, Endosperm, Perisperm, Interploidy crosses, Seed development

Significance Statement

Almost a century of research connects the origin of double fertilization, a major evolutionary innovation of flowering plants, to conflicting parental interests over offspring provisioning. We sought to provide additional insights from within one of the most ancient flowering plant lineages, and characterized parent-of-origin effects in interploidy crosses in the waterlily *Nymphaea thermarum*. We find that relative dosage of parental genome complements does indeed affect offspring development in this

species. However, exclusive maternal control of resource allocation into seeds is uniquely established by storing nutrients in a tissue derived from the mother. We propose that the evolution of such a nutrient storage strategy in this lineage may represent an alternative maternal response to the origin of double fertilization and the introduction of a paternal genome into the embryo-nourishing tissue of angiosperms.

Introduction:

Seeds of flowering plants (angiosperms) are distinguished from those of their closest relatives (gymnosperms) by the presence endosperm, a product of a second fertilization event that occurs at the inception of each angiosperm seed. In gymnospermous seeds, embryos depend directly on nourishment from the female gametophyte. The evolutionary origin of endosperm, a genetically biparental entity, represents the insertion of a paternal genome into a part of a seed that can act as the site of nutrient acquisition and storage.

Endosperm has consequently been viewed as an arena for interparental conflict over how maternal resources are distributed among offspring (Charnov 1979; Haig 1987; Haig and Westoby, 1991). The theory of interparental conflict proposes that, when mothers (maternal sporophytes) use limited resources to support the growth of offspring with multiple fathers, the parents of individual embryos may have different genetic interests with respect to nutrient investment in offspring development. Assuming that the fathers of each embryo on a maternal plant are unrelated, individual paternal fitness will be maximized by increasing maternal investment in its own offspring. Conversely, maternal fitness will be maximized by strategically distributing these resources among offspring to maximize their collective (rather than individual) fitness. Therefore, the effect of greater paternal control over seed development should be to produce more assertive offspring that draw more resources, while greater maternal control should restrict excessive resource investment into any single seed. (Smith and Fretwell, 1974; Trivers 1974; Queller 1983; Wu et al, 2012)

The discussion of interparental conflict in angiosperms has historically focused on endosperm because of the results of reciprocal interploidy crosses. In these experiments, diploid (2n) and tetraploid (4n) individuals of the same species are reciprocally crossed to create embryos and endosperms that have different ratios of maternal and paternal genome complements than are found in homoploid

(2x2 and 4x4) crosses. If the parental origin of a genome complement matters, the potential for greater maternal or paternal control over offspring development is introduced. Results of interploidy crosses are remarkably consistent across a diversity of angiosperm species: in maternal-excess crosses (4x2), endosperm proliferation is suppressed, while in paternal-excess crosses (2x4), endosperm proliferation is promoted (Haig and Westoby, 1991). Specifically, changes to the timing of endosperm cellularization (Lafon-Placette and Köhler, 2014) and/or changes to the rates of nuclear or cellular divisions in the endosperm (von Wagenheim 1957; von Wagenheim 1962) result in the observed parent-of-origin effects on development. Because endosperm plays a significant role in the regulation of embryo development (Lafon-Placette and Köhler, 2014), seed coat development (Ingouff *et al.*, 2006), and resource acquisition from the maternal sporophyte (Zhang *et al.*, 2007), changes to endosperm development have far-reaching consequences for seed development as a whole. In many cases, particularly with paternal-excess crosses, endosperm development is sufficiently perturbed that seeds abort (Haig and Westoby, 1991).

The consistency of parent-of-origin effects on endosperm proliferation across a wide diversity of monocot and eudicot angiosperms has led to the suggestion that interparental conflict has affected the evolution of seeds ever since the origin of angiosperms (Haig 1987; Friedman *et al.*, 2008). However, interploidy crosses have not been performed with any species from clades whose origins predate the divergence of monocots and eudicots. This perhaps is not surprising, as robust interploidy crosses require genetically homogeneous lines of multiple ploidy levels, as well as reproductive systems and growing conditions in which controlled cross-pollinations are possible. The vast majority of early-diverging angiosperm species are long-lived trees, lianas, or aquatic plants, and do not satisfy these requirements.

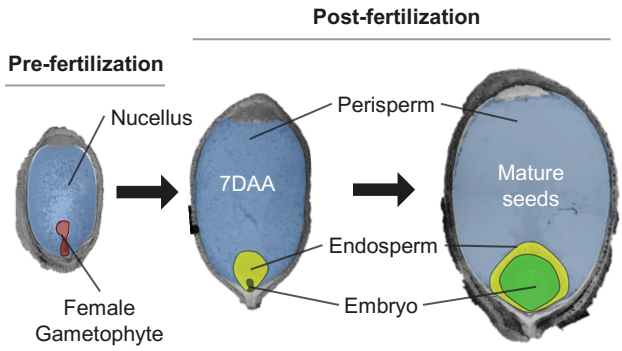

Figure 2.1: Seed development in *Nymphaea thermarum*

Ovule and seed components in longitudinal section in *N. thermarum* before fertilization, at 7DAA (days after anthesis), and at seed maturity.

Nymphaea thermarum is a member the Nymphaeales, one of one of the most ancient lineages of flowering plants. As a diminutive waterlily that prefers very shallow water and has a short generation time, it is a uniquely tractable experimental system. Seed development has been comprehensively documented, and is generally typical of Nymphaeaceae (Povilus *et al.*, 2015) (Figure 2.1). Seeds of *N. thermarum* are primarily composed of perisperm, a nutrient storage and embryo-nourishing tissue derived from the nucellus (part of the maternal sporophyte). In mature seeds, the embryo is small, but morphologically well developed (in that cotyledons, and even the first few epicotylar leaves, are present). The endosperm of *N. thermarum* is diploid, undergoes *ab initio* cellular development, and persists at seed maturity as a single layer of cells that separates the embryo from the surrounding perisperm. Diploid, cellular endosperm is distinct from the vast majority of angiosperms, where endosperm is triploid (due to an additional maternal genomic complement) and undergoes an initial stage of free-nuclear development (Maheshwari 1950; Friedman *et al.*, 2008). However, diploid, cellular endosperms are found in most members of early-diverging angiosperm lineages and are thought to be ancestral for angiosperms as a whole (Floyd and Friedman, 2000; Geeta 2002; Williams and Friedman, 2002; Friedman and Ryerson, 2009). While most interploidy crosses have been performed using species with triploid, free-nuclear endosperm, a small number of species characterized by diploid or cellular endosperm (not both) have

been similarly studied (Cooper and Brink, 1945; Håkansson 1952). Some of these crosses displayed reciprocal modifications to endosperm and embryo development (Cooper and Brink, 1945), so neither triploid nor free-nuclear endosperm are strictly required for parent-of-origin effects on endosperm development to occur.

The unique seed biology of *Nymphaea* none-the-less raises several questions about how, and even whether, parent-of-origin effects on seed development are expressed in this lineage. Because the nutrient storage tissue (perisperm) is derived from the maternal sporophyte, the effect of higher paternal ploidy on nutrient investment into seeds might be predicted to be minimal. However, the fact that endosperm remains at the physiological and structural interface between an embryo and the perisperm means that endosperm must still have an important role in mediating nutrient dynamics within the seed.

In a broader context, determination of the presence or absence of parent-of-origin effects in the Nymphaeales will provide a much-needed perspective on the question of whether interparental conflict within seeds influenced the early evolution of flowering plants. We therefore created autotetraploid lines of *Nymphaea thermarum* and used them for homoploid and reciprocal interploidy crosses with diploid lines. We analyzed the development of resulting ovules/seeds from just before fertilization through seed maturity, and found that endosperm, embryo, and perisperm development differ between cross types – ways that match and also uniquely differ from the results of previous studies in eudicots and monocots.

Materials and Methods:

Creation and verification of autotetraploid lines of *Nymphaea thermarum*

Nymphaea thermarum seeds from the Botanische Gärten der Universität Bonn (Bonn, Germany) were sown and plants grown at the greenhouses of the Arnold Arboretum of Harvard University, according to established protocols (Fisher and Magdalena-Rodriguez, 2010). Seeds from a single fruit of *Nymphaea thermarum* were surface sterilized (Clough and Bent, 1998) and placed in a sterile dish with water. Once seedlings began to germinate, they were immersed in solutions of either 0.25% colchicine, 0.005% Silwet L-77 or 0.025% colchicine, 0.005% Silwet L-77 for 16-72 hours, rinsed, and transferred to a sterile dish with water to monitor viability.

Surviving seedlings were selected for propagation and ploidy assessment via either flow cytom-

etry and/or chromosome counting, as were embryos from some of the subsequent interploidy crosses (SI Materials and Methods) (Doležel *et al.*, 2007; Povilus *et al.*, 2015). Tetraploid individuals were allowed to self-fertilize to produce additional tetraploid plants to act as parents for the interploidy crosses.

Crosses and Collection of plant material

Multiple controlled crosses were performed for each cross type (2x2, 2x4, 4x2, 4x4), from July 2014 to November 2015 (SI Materials and Methods) and fruits were collected at 7 DAA (days after anthesis), at 13 DAA, and at seed maturity (25-32 DAA). In addition, flowers of diploid and tetraploid individuals were allowed to self-pollinate, and fruits were collected at seed maturity (SI Materials and Methods). Diploid and tetraploid flowers were collected the day before anthesis. Material collected for microscopy was fixed in 4% v/v acrolein (Polysciences, New Orleans, Louisiana, USA) in 1X PIPES buffer (50 mmol/L PIPES, 1 mmol/L MgSO4, 5 mmol/L EGTA) pH 6.8, for 24 hours. Fixed material was then rinsed three times (one hour per rinse) with 1X PIPES buffer, dehydrated through a graded ethanol series, and stored in 70% ethanol.

Seed Counts and Seed Germination

For mature fruits, seeds were removed from surrounding fruit tissues and counted. Seeds that were not fixed for histological analysis were surface sterilized (Clough and Bent, 1998) and placed in a dish with water. Seed germination was monitored weekly for up to a month after collection. Once additional seeds no longer germinated, the numbers of germinated and ungerminated seeds were counted.

Microscopy for Seed Tissue Measurements and Embryo Morphology

Samples were prepared for confocal microscopy and imaged according to Povilus *et al*, 2015 (SI Materials and Methods) (Povilus *et al.*, 2015). Measurements (maximum area of the nucellus, female gametophyte, perisperm, endosperm, and embryo in longitudinal section) and descriptions of embryo morphology were made from either single optical sections, 3D projections, or from digital median longitudinal sections produced by digital re-cutting of z-stacks. Measurements of at least 10 ovules/seeds per fruit were attempted, but in cases where 10 healthy-looking ovules/seeds were not available, as many seeds as possible were processed and measured.

Data analysis

We took a conservative approach to assessing the significance of results. Developmentally anomalous outliers were defined as being greater than 3 standard deviations from the grand mean (calculated using all data points per tissue type), and omitted from subsequent analysis (Baker *et al.*, 2017). Average endosperm cell size at 7 DAA was calculated for each seed by dividing the endosperm size (maximum area in longitudinal section) by the number of endosperm cells. Significance level $\alpha = 0.05$ was used to assess effect p-values. Datasets are available in Datasets S1.

The number of 4x4 fruits that set enough mature seed to test both seed germination efficiency and perform histological analysis was too low to allow for conclusions about that cross type. However, seeds from self-fertilized diploid and tetraploid plants were readily available, and were not significantly different from seeds produced via cross-pollination (or the magnitude of the difference was very small, < 5%), for seed germination and for all seed component measurements (SI Materials and Methods). We therefore included measurements from 2n and 4n self-fertilized seeds in (respectively) the 2x2 and 4x4 datasets for seed germination and seed component sizes.

Mixed linear effect models, generalized linear effect models, or zero-inflated generalized linear models were used to fit data on (respectively) ovule or seed component sizes, embryo morphological development, seed germination, and number of seeds per fruit. For each model, either cross type or parental ploidies and their interaction were used as fixed effects. When components from multiple individual seeds from the same fruit were measured, fruit ID was included as a random effect. Full descriptions of models are provided in SI Materials and Methods (Fournier *et al.*, 2012; Zeileis *et al.*, 2008; Bates *et al.*, 2015). For all mixed or general linear models, visual inspection of residual plots did not reveal any obvious deviations from homoscedasticity or normality. Average effect sizes were calculated from the intercept and effect estimates from the model outputs.

Results

External appearance of mature seeds does not differ between cross types, but number of seeds per fruit and seed viability does

Mature seeds from the four cross types (2x2, 2x4, 4x2, 4x4) displayed no obvious differences in external appearance (Figure S2.1). Cross type also did not significantly affect whether whole fruits abort-

ed (produced no seeds). For fruits that did not abort, however, the number of mature seeds per fruit was significantly lower in 2x4, 4x2, and 4x4 crosses, as compared with 2x2 crosses (Table S2.1). Seeds derived from 4x2 and 4x4 crosses that reached maturity were less likely to germinate than seeds of 2x2 crosses (Table S2.1).

Seed component sizes in mature seeds

In mature seeds (Figure 2.2A, FigureS2.2,Table S2.2), perisperm size was not significantly different between 2x2 crosses and any other cross type. Endosperms of 2x4 and 4x2 crosses were significantly larger (by 21% and 19%, respectively) than endosperms of 2x2 crosses. Endosperms of 4x4 crosses were not significantly different from endosperms of 2x2 crosses. Embryos of 2x4 crosses were larger than embryos of 2x2 crosses (by 19%), while 4x2 and 2x2 embryos were not significantly different. Embryos of 4x4 crosses were not significantly different from embryos of 2x2 crosses or 4x2 crosses.

Seed component sizes and endosperm characters during early seed development

Because offspring size varied between cross types at maturity, we wanted to understand how and when during development these patterns were initiated. We analyzed seeds at 7 DAA, when the endosperm is proliferating (Figure 2.2A, Figure S2.2, Table S2.4). At this early stage, all seed components (perisperm, endosperm, and embryo) from 4x2 crosses were significantly larger than their counterparts in 2x2 crosses (by, respectively, 11%, 63%, and 22%). At 7 DAA, seed components of 2x4 crosses were not significantly different than those from 2x2 crosses, nor were seed components of 4x4 crosses (4x4 seed component sizes also had relatively high variation, as evidenced by high standard errors for model coefficients in Table S2.4).

As the data suggested that maternal ploidy, distinct from cross type (a combination of maternal and paternal ploidy), may influence seed component sizes at 7DAA, we fitted a model to test whether maternal ploidy, paternal ploidy, or the interaction of maternal and paternal ploidy had an effect on the sizes of seed components (Figure 2.2B, Table S2.6). Seed components with tetraploid mothers were larger by 11% (perisperm), 63% (endosperm), and 22% (embryo) when compared to tissues from seeds with diploid mothers. Paternal ploidy alone was not a significant factor for the size of any tissue at 7 DAA, nor was the interaction of maternal and paternal ploidy.

A

Significance of differences: p > 0.1 | p < 0.1 | p < 0.05

	Paternal-excess cross (2x4)		Maternal-excess cross (4x2)		4n homoploid cross(4x 4)	
	7 DAA	Mature	7 DAA	Mature	7 DAA	Mature
Perisperm	+2%	+7%	**+11%**	+3%	**+11%**	-6%
Endosperm	+8%	**+21%**	**+63%**	**+19%**	**+39%**	+2%
Embryo	+3%	**+19%**	**+22%**	+9%	+10%	+2%

B

		Higher Maternal Ploidy	Higher Paternal Ploidy	Interaction (Higher Ploidies)
7 DAA	Perisperm	**+11%**	+2%	+11%
	Endosperm	**+63%**	+8%	+39%
	Embryo	**+22%**	+3%	+10%
	Av. Endosperm Cell Size	**+22%**	+12%	+22%
	Number of Endosperm Cells	+12%	-15%	-13%
Before Anthesis	Nucellus	**+10%**	n/a	n/a
	Female Gametophyte	**+25%**	n/a	n/a

Figure 2.2: Effects of Cross Type and Parental Ploidy on Seed Development

A) Summary of seed component size differences between 2x4, 4x2, 4x4 crosses and 2x2 crosses at 7DAA and at seed maturity. B) Summary of effects of maternal ploidy, paternal ploidy, and the interaction of maternal and paternal ploidy on seed component sizes at 7DAA and on ovule component sizes one day before anthesis. For A and B, percents indicate differences relative to 2x2 crosses, and box shading reflects α at which differences are significant. See Tables S2-S9 for linear effect model descriptions and outputs. Number of seeds measured for seed component sizes: 7DAA (2x2 = 200, 2x4 = 182, 4x2 = 112, 4x4 = 26), maturity (2x2 = 313, 2x4 = 123, 4x2 = 57, 4x4 = 96). Number of seeds measured for endosperm cell size and cell number: (2x2 = 65;88, 2x4 = 50;65, 4x2 = 50;59, 4x4 = 24;19). Number of seeds measured for ovule component sizes: (2n maternal sporophyte = 29, 4n maternal sporophyte = 25)

Differences in endosperm cell size, but not cell number

Differences in endosperm size were observed at 7 DAA; we tested whether these differences were driven by changes in endosperm cell number or endosperm cell size. Endosperm cell number was not significantly affected by maternal or paternal ploidy, nor their interaction (Figure 2.2B, Table S2.7). Higher maternal ploidy alone had a significant, positive effect on average endosperm cell size. The effect of higher maternal ploidy on endosperm cell size was not dependent on paternal ploidy (Figure 2.2B, Table S2.8). Thus, endosperm produced from crosses with a tetraploid mother had larger cells than endosperm from crosses with diploid mothers, but not more cells.

Sizes of Ovule Components, Prior to Fertilization

In light of our findings of the effects of maternal ploidy on seed component size at 7 DAA, we tested for the effect of maternal ploidy, just prior to fertilization, on the size of nucellus (progenitor of the perisperm) and size of the female gametophyte (progenitor of the embryo and endosperm). Increased maternal ploidy had a significant positive effect on sizes of both the nucellus and female gametophyte: 4n maternal sporophytes produced 10% larger nucellus, and 25% larger female gametophytes, as compared to counterparts from 2n maternal sporophytes. (Figure 2.2B, Table S2.9).

Early embryo morphogenetic transitions differ in timing between cross types

We characterized embryo developmental stages in each cross type at two time points (Figure 2.3, Table S2.10): at 7 DAA (when the embryo typically transitions from filamentous to globular development in 2x2 crosses) and 13 DAA (when embryos typically initiate cotyledons in 2x2 crosses). At 7 DAA, embryos of both interploidy crosses are as likely to have progressed from filamentous to globular development as were embryos of 2x2 crosses, while embryos of 4x4 crosses were significantly more likely to be developmentally retarded. At 13 DAA the homoploid crosses had similar proportions of embryos that had initiated cotyledons, while fewer 4x2 embryos had cotyledons. All of the 2x4 embryos examined had initiated cotyledons. The slowing of embryo development in maternal-excess crosses was significant, relative to 2x2 crosses.

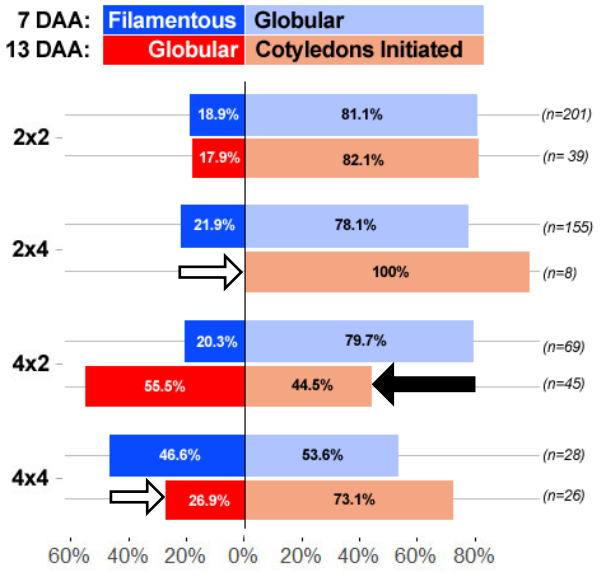

Figure 2.3: Rates of Morphogenetic Transitions of Embryo Development

Proportions of embryos in each cross type that achieved a specific morphological transition at 7DAA and 13 DAA. At 7DAA, embryos were either filamentous or globular. At 13DAA, embryos were either globular or had initiated cotyledons. Arrows represent rate shifts between 7 and 13 DAA, relative to the 2x2 cross type; white arrows are non-significant shifts, black arrow is a significant shift. Description and output of the model used to test for significance of shifts is available in Supplementary Table 8.

Discussion

Overview

The present study of reciprocal interploidy crosses in *Nymphaea thermarum* provides the first evidence of both parent-of-origin effects on offspring development, and of interparental conflict during seed development in an early-diverging angiosperm lineage. Similar to what has been seen in other angiosperms (Haig and Westoby, 1991), we find an excess of paternal genome complements in *N. thermarum* leads to larger endosperms and larger embryos at seed maturity. Meanwhile, an excess of maternal genome complements retards the pace of embryo development with respect to key morphogenetic transitions (which differs from what has been observed in other angiosperms).

Importantly, we found that paternal ploidy does not influence the size of the nutrient storage tissue (perisperm), while maternal ploidy does. Exclusive maternal control of nutrient allocation is consistent with the prediction that maternal fitness benefits from the ability to restrict paternal strategies to selfishly increase resource investment into any particular seed. This study therefore provides the first experimental demonstration that the response of maternal sporophytes to the insertion of an additional paternal genome into the seed need not operate only through modifications of offspring development, but rather can involve tissues derived from the maternal sporophyte.

Ovule and Early Seed Development are Affected by Maternal Ploidy

In order to accurately assess how seeds differ between cross types at maturity, it is essential to understand whether early development differs between cross types. In *N. thermarum*, ovules and female gametophytes of 4n maternal sporophytes are larger than those of 2n maternal sporophytes at the time of pollination. A positive relationship between ploidy and cell/tissue/organ size is widely observed among plants (Kondorosi *et al.*, 2000; Mizukami 2001), so we interpret the positive effect of higher maternal ploidy on ovule size as an effect of ploidy '*per se*'. The positive effects of maternal ploidy *per se* are still readily apparent 7 days after anthesis for all seed components (perisperm being 11% larger, endosperm being 63% larger, and the embryo being 25% larger, when the mother is a tetraploid). The continued relationship between ploidy of the maternal sporophyte and perisperm size might be expected, as the perisperm is derived from the maternal sporophyte. Additionally, the endosperm and embryo develop within a space initially blocked out by the female gametophyte; the size of the primary endosperm cell is *de facto* related to female gametophyte size. Accordingly, we note that early differences in endosperm size between cross types were driven by differences in cell size, but not cell number – again, suggesting that effects of maternal ploidy *per se* are not modifications of endosperm developmental processes (such as rate of cell division or differentiation), but rather, are residual effects of the positive relationship between female gametophyte size and ploidy.

Maternal and Paternal Effects on Endosperm Development

Mature 3n endosperms of *N. thermarum* derived from reciprocal interploidy crosses (4x2 and 2x4) are each ~20% larger than the 2n endosperms of 2x2 crosses. Endosperm growth, however, does

not simply scale with endosperm ploidy, as the 4n endosperms of 4x4 crosses were no larger than the 2n endosperms of 2x2 crosses. Similarly, there is no simple relationship between mature endosperm size and the ratio of maternal and paternal genome complements: endosperms of 4x2 crosses (which has a 2:1 m:p ratio) and 2x4 crosses (1:2 m:p ratio) were both larger than endosperm of the homoploid 2x2 crosses (1:1 m:p ratio).

Here it is essential to consider mature endosperm size within the context of early endosperm development. While endosperms of maternal excess 4x2 crosses are larger than endosperms of 2x2 crosses at seed maturity (a 19% difference), the difference is much less than what was observed at 7DAA (a 63% difference). Higher maternal ploidy therefore has a negative effect on endosperm growth rate, even though it only acts relatively late in development. Meanwhile, 2x4 endosperms are 21% larger at maturity than 2x2 endosperms, even though sizes of endosperm from 2x4 and 2x2 crosses were not significantly different at 7 DAA. An excess of paternal genome complements therefore increases endosperm growth rate.

Maternal and Paternal Effects on Embryo Development

Paternal-excess embryos of *N. thermarum* are significantly larger than embryos of homoploid or maternal-excess crosses. As the embryo eventually displaces the majority of the endosperm chamber in *N. thermarum*, larger paternal-excess embryos may be a result of the previously discussed positive effect of paternal-excess on endosperm size. Maternal-excess embryos, however, are not larger than 2x2 embryos, despite being similarly accompanied by relatively larger endosperms. Accordingly, we show that the ontogenetic progression of maternal-excess embryos slows between 7 and 13 DAA, relative to the rate of embryo development in 2x2 crosses during the same time frame. Thus, while paternal-excess embryos are able to utilize the additional space afforded by larger endosperms, the more slowly-developing maternal-excess embryos do not.

In interploidy crosses performed with other angiosperms, changes in embryo development are tightly linked to modifications of endosperm proliferation (Lafon-Placette and Köhler, 2014), either in terms of maximum embryo size (if the embryo fills most of the mature seed) or ontogenetic progression. In *Arabidopsis* and other species with an initial phase of free-nuclear endosperm development, embryo development generally does not proceed beyond the heart or globular stages until the endosperm cel-

lularizes (Scott *et al.*, 1998). In maternal-excess crosses in rice (in which embryos do not displace the majority of the endosperm at seed maturity), precocious cellularization of the free nuclear endosperm is correlated with larger embryos at seed maturity, suggesting that embryo growth is accelerated or prolonged (Zhang *et al.*, 2016). In *Solanum*, which is similar to *Nymphaea* in that it has *ab initio* cellular endosperm that is mostly displaced by embryo growth, there was a positive correlation between endosperm size and embryo size (both being smaller in maternal-excess crosses) (Cooper and Brink, 1945). The effect of maternal-excess in *N. thermarum* is therefore unique, as both embryo developmental rate is slowed (not accelerated), and changes in endosperm size do not necessarily coincide with changes in embryo size.

Perisperm Size does not Differ among Cross Types

At seed maturity, perisperm size does not differ between 2x2 crosses and any other cross type. As the perisperm is the primary site of nutrient acquisition and storage within *N. thermarum* seeds, investment of maternal resources into seeds is also ultimately similar across all cross types. The lack of a positive relationship between maternal ploidy and perisperm size, however, represents a negation of a relationship present earlier in development (when perisperms from 4n maternal sporophytes were significantly larger than perisperms from 2n maternal sporophytes). Thus, perisperm size and nutrient investment into any particular seed are negatively, albeit subtly, affected by higher maternal ploidy - suggesting an important maternal control on resource allocation during seed development.

Meanwhile, perisperm growth is not affected by paternal ploidy: mature perisperm size does not differ between 2x2 and 2x4 crosses. Furthermore, at 7DAA paternal ploidy has no significant effect on perisperm size, nor does it modulate the effect of maternal ploidy. That paternal ploidy does not affect perisperm development is not unexpected, as perisperm is a maternal tissue that does not receive a paternal genome contribution from the fertilization process. The fact that paternal genome dosages in the embryo and endosperm also have no effect on perisperm size confirms that the father cannot influence the bulk of nutrient acquisition into *Nymphaea* through the modification of offspring development. In *N. thermarum,* having nutrient acquisition and storage occur in a maternal tissue (as opposed to endosperm) therefore establishes exclusive maternal control over resource allocation into mature seeds.

Interparental Conflict and Evolution of Angiosperm Seeds: Maternal Control via Endosperm or Perisperm

The peculiar seed biology and ~139 million years (Magallón *et al.*, 2015) of independent evolutionary history of the Nymphaeales present a unique perspective on how the relationships between seed components have evolved among flowering plants (Figure 2.4). In angiosperms, enhanced maternal control over seed development can be interpreted as an evolved developmental reaction to the origin of double fertilization (Westoby and Rice, 1982). In the last common ancestor of angiosperms and their closest gymnospermous relatives, nutrients were likely stored in a large haploid female gametophyte. The origin of endosperm (in the last common ancestor of angiosperms) inserted a paternal genome complement into a seed tissue that separates the embryo from the maternal nutrient source, and therefore provided an additional opportunity for paternal interests in offspring development to enact. Consistent with this conceptual framework, we observe that higher paternal genome dosage has a positive effect on endosperm growth in *N. thermarum*.

Increased paternal control over resource investment in a seed, however, can be detrimental to maternal fitness if unchecked. The predicted maternal response to the presence of a paternal genome in the embryo-nourishing tissue (endosperm) is to reduce paternal influence on resource allocation (Charnov 1979; Haig 1987; Haig and Westoby, 1991). This can be accomplished by increasing maternal control of gene expression during endosperm development, and/or transferring the function of nutrient acquisition back to a maternal tissue. Most angiosperm taxa appear use the first strategy, and increase maternal influence of gene expression via two mechanisms. One mechanism has been to increase absolute maternal genome dosage, as is seen with the addition of maternal complement(s) in triploid or higher ploidy endosperm (Friedman *et al.*, 2008). The second mechanism involves increasing the effective maternal genetic dosage through genetic imprinting of chromatin methylation patterns. Several genes critical for offspring (and specifically endosperm development) are imprinted, and expressed differentially depending on the parent of origin (Dilkes and Comai, 2004; Patten *et al.*, 2014; Gehring and Satyaki, 2017).

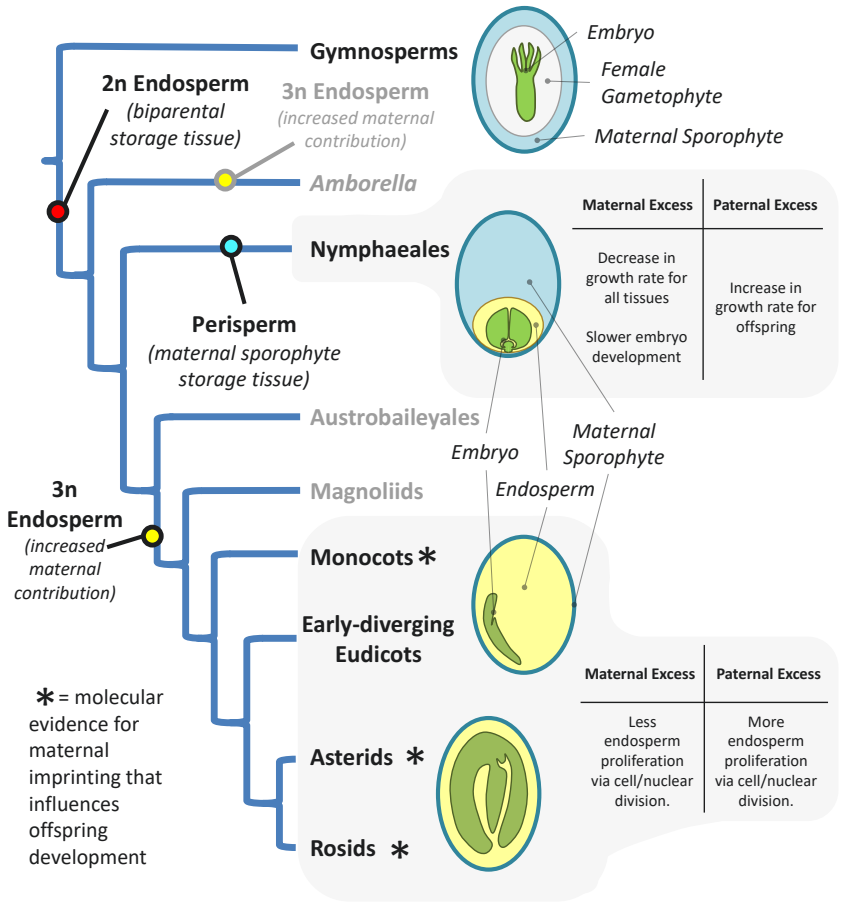

Figure 2.4: Evolution of Maternal and Paternal Genome Dosage Effects on Seed Development in Angiosperms

Key events in the evolution of endosperm ploidy, endosperm development, and seed storage strategies are noted, for relevant angiosperm lineages. Common types of seed structure are illustrated for gymnosperms, Nymphaeales, and monocots + eudicots (early-diverging, rosids and asterids), although they do not represent the full diversity of seed bauplans within these groups. Results of interploidy crosses are summarized for the Nymphaeales, and monocots + eudicots.

Higher maternal genome dosage affects embryo and endosperm development in *Nymphaea thermarum*. As the Nymphaeales have diploid endosperm (and thus do not have higher absolute maternal genome dosage), the effective maternal genetic dosage is likely being altered via imprinting. If so, the question arises: does imprinting in *N. thermarum* share the same underlying mechanisms, and thus potentially a common origin, with imprinting in other angiosperms?

Even though offspring development is subject to maternal and paternal parent-of-origin effects in *N. thermarum*, maternal control of resource allocation is clearly established by having nutrient acquisition and storage occur in a tissue of the maternal sporophyte (perisperm). While it has been proposed that other maternal seed tissues could participate in interparental conflict (Westoby and Rice, 1982), we provide the first experimental evidence involving perisperm. Perisperm has evolved in multiple, distantly related angiosperm lineages (Povilus *et al.*, 2015; Lersten 2004), and this homoplasy is suggestive of some adaptive value. To date there has been no discussion as to why storing nutrients in a non-biparental seed tissue would be advantageous. We propose that, at least in the Nymphaeales, the evolution of perisperm represents a maternal response to the increase of paternal influence over resource distribution that is inherent to the origin and establishment of endosperm as a major arbiter of offspring interactions with the mother. That the mechanism of maternal control in *N. thermarum* does not rely solely on modifications to endosperm development means that interparental conflict has influenced the evolution of not just endosperm development since the origin of angiosperms, but the evolution of seed biology as a whole.

References

Baker RL, Yarkhunova Y, Vidal K, Ewers BE, Weinig C (2017) Polyploidy and the relationship between leaf structure and function: implications for correlated evolution of anatomy, morphology, and physiology in *Brassica. BMC Plant Biol* 17:3-15

Bates D, Maechler M, Bolker B, Walker S (2015) Fitting linear mixed-effects models using lme4. *J Stat Softw 67(1):1-48.*

Charnov EL (1979) Simultaneous hermaphroditism and sexual selection. *Proc Natl Acad Sci U S A* 76: 2480-2484.

Clough SJ, Bent AF (1998) Floral dip: a simplified method for *Agrobacterium*-mediated transformation of *Arabidopsis thaliana*. *Plant J* 16:735-743.

Cooper DC, Brink RA (1945) Seed collapse following matings betweteen diploid and tetraploid races of *Lycopersicon pimpinellifolium*. *Genetics* 30:376-401.

Dilkes BP, Comai L (2004) A differential dosage hypothesis for parental effects in seed development. *Plant Cell* 16: 3174–3180 .

Doležel J, Greilbufer J, Suda J (2007) Estimation of nuclear SNA content in plants using flow cytometry. *Nat Protoc* 2:2233-2244.

Fischer E, Magdalena-Rodriguez C (2010) *Nymphaea thermarum* (Nymphaeaceae). *Curtis Bot Mag* 27:318–327.

Floyd SK, Friedman WE (2000) Evolution of Endosperm Developmental Patterns among Basal Flowering Plants. *Int J Plant Sci* 161(S6)S57-S81.

Fournier DA, Skaug HJ, Ancheta J, Ianelli J, Magnusson A, Maunder M, Neilsen A, Silbert J (2012) AD model builder: using automatic differentiation for statistical inference of highly parameterized complex nonlinear models. *Optim Methods Softw* 27(233-249)

Friedman WE, Madrid EN, Williams JH (2008) Origin of the fittest and survival of the fittest: relating female gametophyte development to endosperm genetics. *Int J Plant Sci* 169(1):79-92.

Friedman WE, Ryerson KC (2009) Reconstructing the ancestral female gametophyte of angiosperms: Insights from *Amborella* and other ancient lineages of flowering plants. *Am J Bot* 96(1):129-43.

Geeta R (2002) The origin and maintenance of nuclear endosperms: viewing development through a phylogenetic lens. *Proc R Soc Lond B* 270:29-35.

Gehring M, Satyaki PR (2017) Endosperm and imprinting, inextricably linked. *Plant Physiol* 173:143-154.

Haig D (1987) Kin conflict in seed plants. *Trends Ecol Evol* 2(11):337–340.

Haig D, Westoby M (1991) Genomic imprinting in endosperm: its effects on seed development in crosses between species and between different ploidies of the same species, and its implications for the evolution of apomixis. *Phil Trans R Soc B* 333:1–13.

Håkansson A (1952) Seed development after 2x, 4x crosses in *Galeopsis pubescens*. *Hereditas* 38:425-448.

Ingouff M, Jullien PE, Berger F (2006). The Female Gametophyte and the Endosperm Control Cell Proliferation and Differentiation of the Seed Coat in Arabidopsis. *Plant Cell* 18(12):3491-3501.

Kondorosi E, Roudier F, Gendreau E (2000) Plant cell-size control: growing by ploidy. *Curr Opin Plant Biol* 3(6):488-492.

Lafon-Placette C, Köhler C (2014) Embryo and Endosperm, partners in seed development. *Curr Opin Plant Biol* 17:64-69.

Lersten NR (2004) Endosperm. *Flowering Plant Embryology* (Blackwell Publishing), pp 161-163.

Magallón A, Gómez-Acevedo S, Sánchez-Reyes LL, Hernández-Hernández T (2015) A metacalibrated time-tree documents the early rise of flowering plant phylogenetic diversity. *New Phytol* 207(2):437-453

Maheshwari P (1950) *An Introduction to the Embryology of Angiosperms* (McGraw-Hill Book Company, New York).

Mizukami Y (2001) A matter of size: developmental control of organ size in plants. *Curr Opin Plant Biol* 4:533-539.

Patten MM, Ross L, Curley JP, Queller DC, Bonduriansky R, Wolf JB (2014) The evolution of genomic imprinting: theories, predictions and empirical tests. *Heredity (Edinb)* 113: 119–128.

Povilus RA, Losada JM, Friedman WE (2015) Floral biology and ovule and seed ontogeny of *Nymphaea thermarum*, a water lily at the brink of extinction with potential as a model system for basal angiosperms. *Ann Bot* 115:211-226

Queller DC (1983) Kin selection and conflict in seed maturation. *J Theor Biol* 100(1):153–172.

Scott RJ, Spielman M, Baily J, Dickinson HG (1998) Parent-of-origin effects on seed development in *Arabidopsis thaliana*. *Development* 125:3329-3341.

Smith CC, Fretwell, SD (1974) The optimal balance between size and number of offspring. *Am Nat* 108:499-506.

Trivers RL (1974) Parent-offspring conflict. *Am Zool* 14:249-264.

von Wangenheim KH (1957) Untersuchungen über den Zusammenhang zwischen Chromosomenzhal und Kreuzbarkeit bei *Solanum*-Arten. *Z induct Abstamm u Vererb Lehre* 88:21-37.

von Wangenheim KH (1962) Zur Ursache der Abortion von Samenanlagen in Diploid-Polyploid-Kreuzungen: II. Untershiedliche Differenzierung von Endospermen mit glechem Genom. *Z Vererb Lehre* 93:319-334.

Westoby M, Rice B (1982) Evolution of the seed plants and inclusive fitness of plant tissues. *Evolution* 36(4):713–724.

Williams JH, Friedman WE (2002) Identification of diploid endosperm in an early angiosperm lineage. *Nature* 415(6871):522-526.

Wu CC, Diggle PK, Friedman WE (2012) Kin recognition within a seed and the effect of genetic relatedness of an endosperm to its compatriot embryo on maize seed development. *Proc Natl Acad Sci U S A* 110(6):2217-2222

Zeileis A, Kleiber C, Jackman S (2008) Regression Models for Count Data in R. *J Stat Softw* 27(8).

Zhang H, Luo M, Johnson SD, Zhu X, Liu L, Huang F, Liu Y, Xu P, Wu X (2016) Parental genome imbalance causes post-zygotic lethality and deregulates imprinting in rice. *Rice* 9:43-55

Zhang WH, Zhou Y, Dibley KE, Tyerman SD, Furbank RT, Patrick JW (2007) Nutrient loading of developing seeds. *Funct Plant Biol* 34:314-331.

Funding Information

This work was supported by funds from the Department of Organismic and Evolutionary Biology, at Harvard University.

Acknowledgments

We thank Grace Yu for help with crossing experiments and seed imaging, Dr. David Haig for helpful discussions, and the staff of Botanische Gärten der Universität Bonn for providing plant material for propagation.

Chapter 3

Title: RNA-seq of seed development in the water lily *Nymphaea thermarum* (Nymphaeales), and the expression of imprinting-related and non-imprinting-related chromatin methylation regulators.

Authors: Rebecca Povilus[a], William E. Friedman[a,b]

[a] Department of Organismic and Evolutionary Biology, Harvard University, 26 Oxford Street, Cambridge, MA 02138, USA; [b] Arnold Arboretum of Harvard University, 1300 Centre Street, Boston, MA 02131, USA

Abstract

RNA-seq datasets offer unparalleled opportunities to discover genes and processes that are important for seed development. Such datasets have already been generated for a growing collection of species from a phylogenetically broad sampling of flowering plants (angiosperms). However, information on gene expression during seed development is minimal for those angiosperm lineages whose origins predate the divergence of monocots and eudicots. In order to provide a new perspective on the early evolution of seed development in flowering plants, we sequenced transcriptomes of whole ovules and seeds from three key stages of reproductive development in the waterlily *Nymphaea thermarum*, an experimentally-tractable member of one of the earliest-diverging angiosperm lineages. We first explore general patterns of gene expression, beginning with mature ovules and continuing through fertilization into early- and mid-seed developmental stages. We then examine the expression of genes associated with DNA and histone methylation – processes known to be essential for seed development, but mechanistically variable in distantly-related monocots and eudicots. Around 60% of transcripts putatively homologous to chromatin methylation modifiers are differentially expressed during seed development in *N. thermarum*, suggesting that the importance of dynamic chromatin methylation during seed development dates to the earliest phases of angiosperm evolution. However, genes involved in establishing, maintaining, and removing methylation marks associated with genetic imprinting show a mix of conserved and unique expression patterns between *N. thermarum* and other flowering plants. Our data suggests that the regulation of imprinting has likely changed throughout angiosperm evolution, and furthermore identifies genes that merit further characterization in any angiosperm model system.

Introduction

Fertilization and seed development are critical parts of plant development that require extensive transcriptional reprogramming. Seed development in flowering plants (angiosperms) is of particular interest, as it uniquely involves two separate fertilization events that produce two distinct offspring. Double fertilization in angiosperms occurs when a pollen tube successfully reaches a mature ovule and delivers two sperm cells into the female gametophyte. Each sperm cell fuses with one of the two female gametes, the egg cell and the central cell, to produce (respectively) the embryo and the embryo-nourishing endosperm. While endosperm does not necessarily persist past seed germination, it surrounds the

embryo throughout seed development, and is a crucial mediator of the relationship between an embryo and its maternal sporophyte.

Given that seeds, and specifically endosperm, are the cornerstone of human diets, there has been much effort to understand the dynamic transcriptional landscape of seed development in a variety of economically important (maize (Li *et al.*, 2014; Chen *et al.*, 2014), rice (Xu *et al.*, 2014; Gao *et al.*, 2013), soybean (Jones and Vodkin, 2013), peanut (Zhang *et al.*, 2011), camelina (Nguyen *et al.*, 2013), *Brassica* (Gao *et al.*, 2014)) or model system (*Arabidopsis* (Girke *et al.*, 2000)) plants. Yet little information exists from within early diverging angiosperm lineages, hindering any understanding the evolution of processes involved in seed development. While this undoubtedly is related to the difficulty of working with the vast majority of species within these lineages (e.g., *Amborella*, Nymphaeales, Austrobaileyales, Chloranthales, Ceratophyllales, magnoliids, which are typically long-lived trees, shrubs, lianas, or aquatic plants), a genetically and experimentally tractable species from within one of the most-early diverging lineages has recently been identified (Povilus *et al.*, 2015). *Nymphaea thermarum* (Nymphaeales) is a minute waterlily with a relatively short generation time, simple erect growth habit, and a growing toolkit of genetic resources – as such, it is poised to help illuminate questions about the evolution of flowering plant reproduction.

A common thread has emerged from studies of seed development in a wide variety of angiosperms: imprinting is important for seed development, and particularly for endosperm development (Haig and Westoby, 1991; Haig 2013; Gehring and Satyaki, 2017). Imprinting is an epigenetic phenomenon that results in alleles with identical nucleotide sequences that have different expression patterns, depending on which parent the allele was inherited from (a “parent-of-origin” effect). In flowering plants, imprinting is largely understood to occur via the establishment of chromatin methylation patterns during gamete and seed development. Because methylation of DNA or histones can affect how a locus is expressed, different methylation patterns established during the development of different gametes can mean that certain loci are expressed only from the maternally- or paternally-inherited copy of the allele (Zilberman *et al.*, 2006). Imprinting has been noted to be particularly important for the ability of endosperm to function as a nutritional mediator between the embryo and maternal sporophyte (Haig and Westoby, 1991; Gehring and Satyaki, 2017). However, some of the mechanisms that control chromatin methylation patterns appear to differ between monocots and eudicots (Gleason and Kramer, 2012;

Köhler *et al.*, 2012; Nalaamilli 2013; Furihata *et al.*, 2016), leading to the question of how and when imprinting and chromatin methylation became important aspects of seed development in flowering plants.

Chromatin methylation during reproductive development is best understood in *Arabidopsis*, and involves the coordination of DNA methylation/demethylation, histone methylation, and RNA-dependent DNA methylation (Gehring and Satyaki, 2017). Members of the DNA METHYLTRANSFERASE family (MET) maintain CG methylation, while CHROMOMETHYLASE proteins (CMT) establish or maintain CNG methylation. METs and CMT are known to be expressed both in developing female gametophytes of *Arabidopsis*, as well as in offspring tissues after fertilization (Jullien 2012; Köhler *et al.*, 2012). DEMETER (DME) is a DNA glycosylase that removes methylation established by MET1 and is active mostly during female gametophyte development. DME activity determines expression of some of the components of the POLYCOMB REPRESSIVE COMPLEX 2 (PRC2) (Hsieh *et al.*, 2012). PRC2 is comprised of MEDEA (MEA), FERTILIZATION-INDEPENDENT SEED2 (FIS2), FERTILIZATION-INDEPENDENT ENDOSPERM (FIE), and MULTICOPY SUPRESSOR OF IRA1 (MSI1), and is active in both the central cell of the female gametophyte and in endosperm (Furihata *et al.*, 2016). The PRC2 complex participates in histone methylation, and in doing so regulates the expression of several genes known to be important for seed development (Hsieh *et al.*, 2012). Together, METs, CMTs, DME, and PRC2 regulate methylation patterns necessary for imprinting of parent-or-origin specific expression patterns. Methylation processes not necessarily associated with imprinting, such as RNA-directed DNA methylation (RdDM), are also active during reproductive development and have been tied to repression of transposon activity in the egg cell and embryo (Köhler *et al.*, 2012; Ingouff *et al.*, 2017).

In order to shed light on whether imprinting via chromatin methylation could be responsible for recently discovered parent-of-origin effects on endosperm and embryo development in *N. thermarum* (Povilus *et al.*, 2015), we examined the expression patterns of genes involved in DNA and histone methylation, and in particular those known to be important for imprinting. By obtaining comprehensive libraries of gene expression during important stages of seed development in the water lily *Nymphaea thermarum*, we provide the first such dataset from within any early-diverging angiosperm lineage. We compare the expression profiles of chromatin methylation regulators in *N. thermarum* with those of their homologs in monocots and *Arabidopsis*. In doing so, we identify processes of chromatin methylation that have likely been involved in seed development since the earliest stages of angiosperm evolution, and demonstrate

that all of the molecular processes known to be involved in imprinting are indeed expressed before and after fertilization – meaning that imprinting is certainly possible in *N. thermarum*, even if its regulation likely varies from the current *Arabidopsis*-based model.

Materials and methods

Plant Material and Sequencing

The *Nymphaea thermarum* plants sampled for this study were grown in a greenhouse at the Arnold Arboretum of Harvard University (Boston, MA, United States) according to previously established protocols (Fischer and Magdalena-Rodriguez, 2010). Flowers were allowed to self-fertilize. All samples were collected between 10 and 11 am on their respective collection days. Ovules and seeds were quickly dissected from surrounding carpel or fruit tissue, weighed, then immediately frozen in liquid nitrogen, and stored at -80 C. For 0 DAA (days after anthesis), each biological replicate represents material from 3-4 individual flowers from different plants. For 7 and 15 DAA, each biological replicate includes material from a single fruit.

RNA extractions were performed with modified protocol, originally developed for use on maize kernels (Wang *et al.*, 2012)(Supplementary Materials and Methods 3). RNA seq libraries were prepared by the Whitehead Genome Sequencing Core, according to the manufacturer protocols of the Illumina Standard mRNA-seq library preparation kit (Illumina), using poly A selection, and were sequenced at the Baur Core of Harvard University to generate 125-bp, paired-end reads on a Illumina HiSeq Platform. All 12 libraries were multiplexed and sequenced on 3 lanes.

Read mapping and differential expression analysis

For each sample, kallisto (Bray *et al.*, 2016) was used to pseudo-align reads to the *Nymphaea thermarum* genome (manuscript in preparation) and quantify transcript abundances. 100 mapping boot-straps were performed, using default parameters for paired-end reads. Kallisto reports both estimated number of transcript reads per sample (EST), as well as transcript abundance per million reads (TPM, normalized for transcript length and number of reads per sample)(Supplemental Dataset 3.1). Transcripts that are differentially expressed (DE) between time points were identified using sleuth (Pimentel *et al.*, 2017)(Supplemental Dataset 3.2). The primary DE analysis modeled the effect of time, for all time points,

on transcript abundance. Subsequent DE analysis was conducted for pair-wise comparisons between time points (for this analysis, multiple testing was accounted for by requiring transcripts to be significantly DE according to the primary DE analysis). Sleuth incorporates information from bootstraps performed by kallisto to estimate the inferential variance of each transcript; the adjusted variances were used to determine differential expression for each transcript. Transcripts were considered differentially expressed if time point (DAA) was a significant factor for transcript abundance, according to both a conservative likelihood ratio test and a Wald test (multiple-testing corrected p-value < 0.01).

PCA and Clustering of Biological Replicates

Analyses were performed with R (version 3.4.0, (R Core Team, 2017)). To assess similarity of biological replicates, EST values for each transcript that was differentially expressed were centered and scaled (according to transcript means across all samples), using the scale function. Dimensional expression data was reduced to two dimensions by PCA using the prcomp function. K-means clustering within PCA space was performed by the kmeans function, with cluster number set to 3 (number chosen to reflect the number of sampled time points).

Expression pattern cluster definition and analysis

Analyses were performed with R (version 3.4.0, (R Core Team, 2017)). K-means clustering of gene expression patterns was performed with sample TPM values, using the kmeans function. The cluster number was set to 9, as the use of higher cluster numbers failed to identify additional unique expression patterns. Only transcripts that were differentially expressed were used for k-means clustering. The z-score was calculated for each gene per sample, using the scale function. Only genes whose expression patterns correlated with the average profile of each cluster (Pearson correlation > 0.9) were used in further analysis (Supplementary Dataset 3.3).

GO (molecular function) enrichment for each expression pattern cluster was performed with agriGO (Tian *et al.*, 2017), using *Arabidopsis thaliana* TAIR 10 annotation as the background, with hypergeometric or chi-squared tests (chi-squared was only performed if the query list had relatively few intersections with the reference list, and is noted separately), Yekutieli (FDR under dependency) multiple corrections testing adjustment, and significance level = 0.1. Putative *A. thaliana* homologs of *N. ther-*

marum transcripts were identified via BLASTX for each *N. thermarum* transcript against a database of all TAIR 10 *Arabidopsis* transcript amino acid sequences (downloaded from Phytozome (Goodstein *et al.*, 2012)), using the hit with the lowest e-value as the putative homolog match (e-value cutoff = 1e-15).

Identification and analysis of transcription factors

Putative transcription factors (and their respective family type) were identified from the *Nymphaea thermarum* genome using the 'Prediction' tool available from the Plant Transcription Factor Database v4.0 (Jin *et al.*, 2017). Enrichment analysis for TF families among the set of DE TFs in each expression cluster was performed in R with Fisher's exact test; adjusted p-values (FDR) <0.1 and <0.05 are noted.

Identification of genes involved in histone and DNA methylation

To comprehensively identify putative homologs of genes known to be involved in regulation of DNA and chromatin methylation during seed development in other angiosperms, we estimated gene-family phylogenies for gene families of particular interest (CMT, MET, DME, components of the PCR2 complex). For each gene family, amino acid sequences for *Arabidopsis* members were aligned with MUSCLE (Edgar 2004) and used as the input for HMMER searches (e-value cutoff = 1e-15) (Eddy, 2011) to identify putative homologs from the genomes of *Physcomitrella patens (Physcomitrella patens* v3.3, DOE-JGI, http://phytozome.jgi.doe.gov/), *Amborella trichopoda* (Amborella Genome Project 2013), *Nymphaea thermarum* (manuscript in preparation), *Aquilegia coerulea (Aquilegia coerulea* Genome Sequencing Project, http://phytozome.jgi.doe.gov/), *Oryza sativa* (Ouyang *et al.*, 2007), *Zea mays (*Hirsch *et al.*, 2016), *Arabidopsis thaliana* (Lanesch *et al.*, 2012), and *Solanum lycopersicum* (Tomato Genome Consortium 2012). The latest versions of all annotated genome datasets, except for *N. thermaurm*, were downloaded from Phytozome (Goodstein *et al.*, 2012). Putative homologs were also identified from within the de-novo assembled, immature-ovule and non-seed transcriptomes of *N. thermarum* (which includes tissues from roots, floral buds, leaves, and pre-meiotic ovules)(manuscript in preparation). The amino acid sequences for the set of all putative homologs for a gene family were aligned with MUSCLE (Edgar, 2004), alignments were manually trimmed to represent highly conserved regions, and phylogenetic tree estimation and bootstrapping (n=100) was performed with RAxML under the PROTGAMMAGTR amino-

acid substitution model (Stamataki, 2014). During further discussion we took a conservative approach, using a relatively broad definition as to which members were included in particular gene sub-families of interest.

All *Arabidopsis* genes annotated as being involved with either DNA methylation (GO:0006306) and histone methylation (GO:0016571) were collected using QuickGO (http://www.ebi.ac.uk/). Putative *N. thermarum* homologs of *A. thaliana* transcripts were identified via BLASTX for each *N. thermarum* transcript against a database of all TAIR 10 *Arabidopsis* transcript amino acid sequences (Lanesch *et al.*, 2012), using the hit with the lowest e-value as the putative homolog match (e-value cutoff = 1e-15).

Histology and Microscopy

Material collected for microscopy was fixed in 4% v/v acrolein (Polysciences, New Orleans, Louisiana, USA) in 1X PIPES buffer (50 mmol/L PIPES, 1 mmol/L MgSO4, 5 mmol/L EGTA) pH 6.8, for 24 hours. Fixed material was then rinsed three times (one hour per rinse) with 1X PIPES buffer, dehydrated through a graded ethanol series, and stored in 70% ethanol. Samples were prepared for confocal microscopy and imaged according previously established protocols (Povilus *et al.*, 2015). Briefly: tissues were stained according the Fuelgen method, and then infiltrated with and embedded in JB-4 glycol methacrylate (Electron Microscopy Sciences, Hatfield, PA, USA). Blocks were cut by hand with razor blades to remove superfluous tissue layers. Samples were mounted in a drop of Immersol 518f (Zeiss, Oberkochen, Germany) on custom well slides and imaged with a Zeiss LSM700 Confocal Microscope, equipped with an AxioCam HRc camera (Zeiss, Oberkochen, Germany). Excitation/emission detection settings: excitation at 405 and 488 nm, emission detection between 400-520 nm (Channel 1) and 520-700 (Channel 2).

Results

Generation and analysis of RNA-seq Data

In order to investigate the transcriptional landscape of seed development in *N. thermarum*, we generated RNA-seq libraries of whole ovules or seeds at 3 times points. The three stages sampled represent unique suites of developmental processes (Figure 3.1)(Povilus *et al.*, 2015). The first stage (0 DAA) consists of whole, unfertilized ovules. The second stage is whole seeds at 7 DAA, when the endosperm is expanding but the embryo is relatively quiescent. Nutrients are actively being acquired by, and stored

in, a tissue called the perisperm (which is a maternal sporophyte tissue derived from the nucellus). The third stage sampled is whole seeds at 15 DAA, when endosperm expansion and differentiation is nearly complete. The embryo begins to undergo significant growth and morphogenesis, displacing space occupied by degenerating endosperm cells. The perisperm continues to acquire and store nutrient reserves. Thus, while seed components were not spatially dissected from each other, the selected time points capture different developmental landmarks.

Between 66 and 100 million high quality reads were generated for each sample, for a total of 940 million reads. 76.2% of the reads pseudo-mapped to the *Nymphaea thermarum* genome, and uniquely mapped reads were used to estimate normalized transcript abundance as TPM (transcripts per million) (Supplementary Table 3.1). Biological replicates of each time point clustered with each other (and not with samples of other time points) during PCA and k-means analysis of expression patterns of the 4000 most highly expressed transcripts, except for one sample of 0 DAA seeds that clustered instead with 7 DAA samples (Figure 3.2A). This sample was removed from further analysis. When PCA and k-means clustering were performed with the remaining 11 samples, samples clustered according to collection time point.

In total, 19,412 unique transcripts with at least a minimum abundance of 1 TPM were present during the sampled time points (Supplemental Dataset 3.1). This represents 74.4% of the 25,760 genes identified from the *Nymphaea thermaurm* genome (Figure 3.2B). 16,329 transcripts were present at all three ovule/seed developmental stages. 0 DAA had the most unique transcripts, and 7 DAA had the fewest. Among transcripts present in two stages, 0 DAA and 7 DAA shared the most transcripts, while 7 DAA and 15 DAA shared the fewest. The majority of transcript expression levels fell within a similar range across all three stages (Figure 3.2C). However, the expression levels of the 0.1% most highly expressed transcripts increased significantly over time (Supplementary Table 3.2).

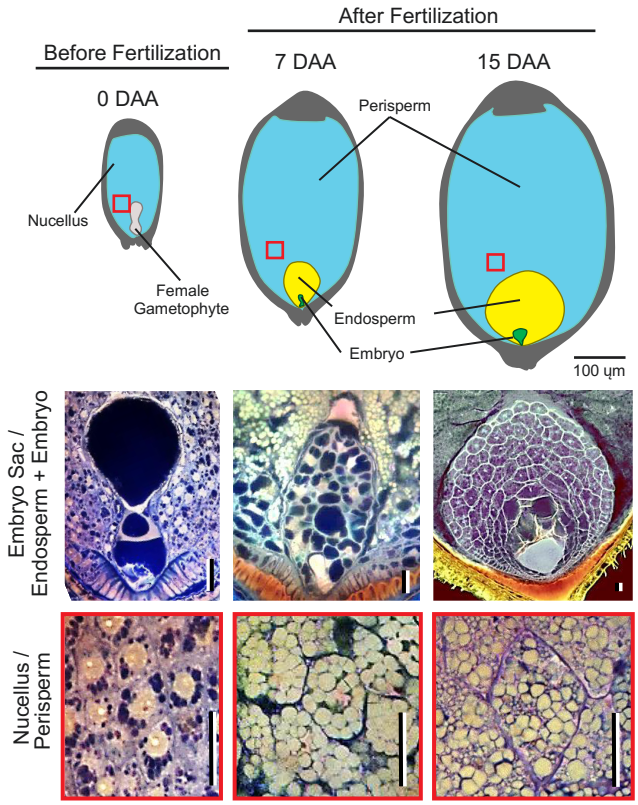

Figure 3.1: Stages of ovule and seed development in *N. thermarum* sampled for RNA-seq.

Top row: Diagrams of the internal structure of ovules (before fertilization, 0 days before anthesis (DAA)) and seeds (after fertilization) at 7 DAA and 15 DAA, with key components labeled. Red boxes indicate location of corresponding image of the nucellus/perisperm (featured in the bottom row). Scale bar = 100 µm. Middle and bottom rows: Confocal images of key ovule or seed components at each stage. Scale bars = 20 µm.

Besides differences in TPM values among the most highly expressed transcripts, the types of genes represented by the 10 most highly expressed transcripts varied with time point (Table 3.1). At 0 DAA, most of the 10 most highly expressed transcripts coded for structural components of histones or ribosomes. Notably, a putative homolog to an arabinogalactan peptide (AGP16) was the third most highly expressed transcript at 0 DAA. Arabinogalactans are known to regulate female gametophyte development and function in pollen tube interactions in other angiosperms (Pereira *et al.*, 2016). At 7 DAA, ribosome components again featured prominently among the 10 most highly expressed transcripts. A lipid transfer protein, WAXY starch synthase, and TPS10 terpene synthase were also highly expressed at 7 DAA, likely in relation to the initiation of nutrient import and storage in the seed, and seed coat differentiation. At 15 DAA, several transcripts involved with terpene synthesis or modification were among the 10 most highly expressed transcripts, coincident with continued maturation of the seed coat. A WAXY starch synthase, highly expressed at 7 DAA, continued to be highly expressed at 15 DAA.

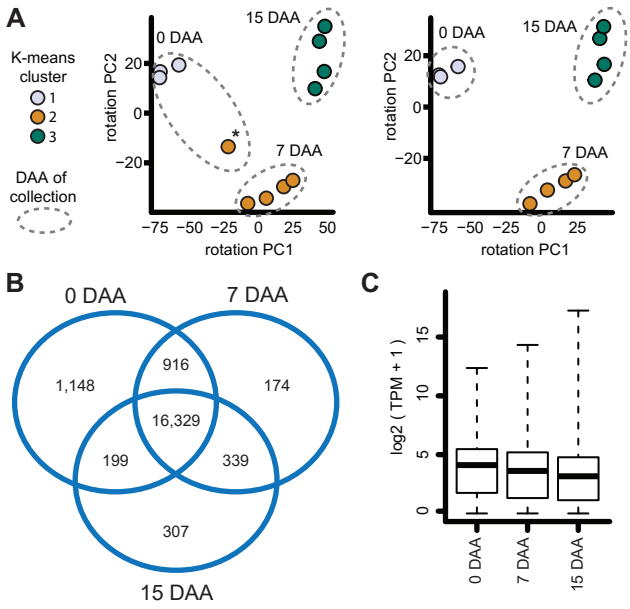

Figure 3.2: Basic Analysis of Transcriptomes of Reproductive Development

General characteristics of transcription in all samples. A) PCA of K-means clustering of biological replicates. Dot color indicates cluster identity, while inclusion within dashed outline indicates which DAA the sample was collected. Left graph: One 0 DAA sample clustered with 7 DAA samples (*). This sample was considered developmentally anomalous and removed from further analysis. Right graph: PCA without the anomalous sample. B) Venn diagram of unique transcripts with a TPM > 1 at each stage, and present in multiple stages. C) Distribution of TPM values for all transcripts (TPM >1) at each stage. Median values are indicated with bold horizontal lines, bottom and top of boxes indicate 25th and 75th percentile, and dashed lines indicate minimum and maximum values.

	TPM	ID	Putative Homology
0 DAA	4966.98	NYTH03818-RA	Ubiquitin (*Triticum aestivum*)
	4640.607	NYTH03847-RA	Histone H4 (*Glycine max*)
	4466.02	NYTH43515-RA	AGP16 Arabinogalactan peptide 16 (*Arabidopsis thaliana*)
	4220.917	NYTH18212-RA	RPS30A 40S ribosomal protein S30 (*Arabidopsis thaliana*)
	3675.603	NYTH26983-RA	Os01g0645000 Zinc finger CCCH domain-containing protein 9 (*Oryza sativa* subsp. *japonica*)
	3509.973	NYTH40689-RA	RPL29A 60S ribosomal protein L29-1 (*Arabidopsis thaliana*)
	3436.017	NYTH51439-RA	Defensin J1-2 (*Capsicum annuum*)
	3241.97	NYTH00189-RA	At4g30220 Probable small nuclear ribonucleoprotein F (*Arabidopsis thaliana*)
	3104.7	NYTH38977-RA	Protein of unknown function
	3056.18	NYTH00233-RA	H2B Histone H2B.6 (*Arabidopsis thaliana*)
7 DAA	19593.65	NYTH51439-RA	Defensin J1-2 (*Capsicum annuum*)
	8724.83	NYTH16912-RA	Non-specific lipid-transfer protein 1 (*Lens culinaris*)
	8283.093	NYTH03818-RA	Ubiquitin (*Triticum aestivum*)
	6436.833	NYTH18212-RA	RPS30A 40S ribosomal protein S30 (*Arabidopsis thaliana*)
	6126.765	NYTH40689-RA	RPL29A 60S ribosomal protein L29-1 (*Arabidopsis thaliana*)
	6077.737	NYTH45457-RA	HSP22 Small heat shock protein (*Glycine max*)
	4974.465	NYTH18464-RA	WAXY Granule-bound starch synthase 1(*Antirrhinum majus*)
	4805.542	NYTH27985-RA	Protein of unknown function
	4318.512	NYTH59946-RA	TPS10 Terpene synthase 10 (*Ricinus communis*)
	4024.218	NYTH38580-RA	RPL37C 60S ribosomal protein L37-3 (*Arabidopsis thaliana*)
15 DAA	102890.9	NYTH59946-RA	TPS10 Terpene synthase 10 (*Ricinus communis*)
	26734.5	NYTH51439-RA	Defensin J1-2 (*Capsicum annuum*)
	18853.65	NYTH44750-RA	(-)-alpha-terpineol synthase (*Vitis vinifera*)
	18529.12	NYTH18464-RA	WAXY Granule-bound starch synthase 1(*Antirrhinum majus*)
	13610.54	NYTH45457-RA	HSP22 Small heat shock protein, (*Glycine max*)
	9038.013	NYTH16912-RA	Non-specific lipid-transfer protein 1 (*Lens culinaris*)
	8806.638	NYTH28556-RA	Protein of unknown function
	8389.802	NYTH59911-RA	Alpha-terpineol synthase, chloroplastic (*Magnolia grandiflora*)
	6565.69	NYTH03818-RA	Ubiquitin (*Triticum aestivum*)
	6242.847	NYTH59528-RA	TPS10 Terpene synthase 10 (*Ricinus communis*)

Table 3.1: TPM, Identifier, and Putatative Homology of the 10 Transcripts with the Highest Abundances at each Stage. Putative homology information was collected from the annotated genome of *N. thermarum* (manuscript in progress).

Analysis of Differential Gene Expression

Out of the 19,412 unique transcripts expressed during seed development in *N. thermarum*, 10,933 were significantly differentially expressed (DE) (Supplementary Dataset 3.2). A stringent definition of differential expression was used: transcripts had to pass both a Wald and LRT test ($p < 0.01$) to test for DE according to the factor of time (i.e. developmental stage) The set of DE transcripts was used to perform hierarchical clustering of all transcripts in all samples (Figure 3.3A). The three main 'clades' identified by hierarchical clustering of samples correlated with the three sampling time points. 7 DAA samples and 15 DAA samples were more closely related to each other, than to 0 DAA samples.

Two sets of differentially expressed (DE) transcripts were considered during further analysis: a set of all DE transcripts ("all-DE"), and a set of DE transcripts with very high relative changes in expression ("highly-DE"). For the latter set, an absolute b-value > 2 for the expression change(s) was used as the filtering criteria. B-values are reported by sleuth as part of differential gene expression analysis, and are analogous to fold-change in what a positive or negative value means for the direction of expression change (Pimentel *et al.*, 2017). However, b-values are derived from the effect size of time point on the log10-transformed transcript abundances – a b-value is therefore not equivalent to the same value fold-change (ie: a b-value of 2 does not imply a fold-change of 2).

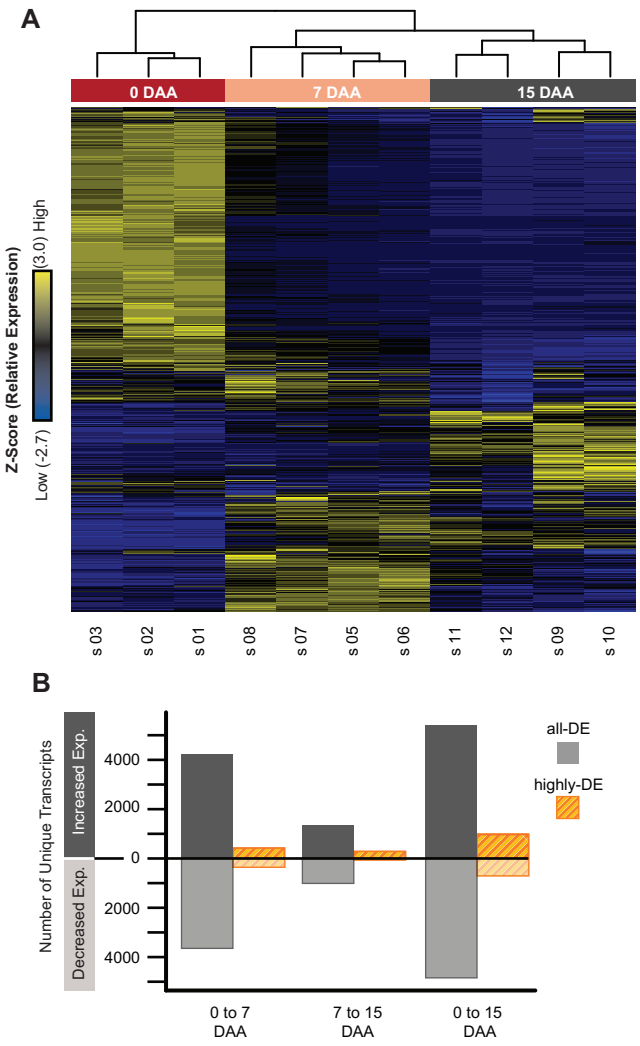

Figure 3.3: Differential Expression of Transcripts During Seed Development in *N. thermarum.*

Basic analysis of differentially expressed (DE) transcripts. A) Heatmap of the relative expression (Z-scores of the mean TPM of all biological replicates at each stage) for each of 10,933 DE transcripts. Each row represents a single unique transcript; transcript identifies are not included. Rows are hierarchically clustered (dendrogram not included). Each column represents a single sample, and are hierarchically clustered (top dendrogram). B) Number of unique, DE transcripts that showed either an increase or decrease in expression between time points. Results from the set of all-DE or highly-DE transcripts are shown separately.

Among the set of all DE transcripts (10,933 transcripts), more than three times more transcripts were differentially expressed between 0-7DAA, than between 7-15 DAA, while the number of transcripts differentially expressed between 0-7 DAA and 0-15 DAA was more similar (Figure 3.3B). For each time-point comparison in the all-DE set, between 53 and 58% of the significant changes in expression were due to increases in expression (as opposed to decreases in expression). The set of highly-DE transcripts was smaller, consisting of 1,865 unique transcripts. The 7-15 DAA transition had the fewest highly-DE transcripts, with 0-7 DAA having about 2.5 times as many, and 0-15 DAA having about twice as many as 0-7DAA. While the proportion of transcripts that increased expression between 0-7DAA and 0-15 DAA was similar to what was seen in the set of all DE transcripts (between 54-58%), for 7-15DAA the proportion of highly-DE transcripts that increased expression was much higher (80%, as compared to 58% for the set of all DE transcripts).

Analysis of transcripts grouped by expression pattern

The expression patterns of all DE transcripts were associated with 9 expression pattern types (or 'clusters') using a K-means clustering approach (Figure 3.4A) (Supplementary Table 3.3). The expression patterns represented by the 9 clusters include: increased or decreased expression across the entire time sampled (respectively, Clusters A and B), as well as increased or decreased expression to produce a minimum or maximum at each of the 3 time points (increase and decrease, respectively, 0 DAA = Clusters C,D; 7 DAA = E,F; 15DAA = G,H). The final cluster (cluster I) represented transcripts that, while differentially expressed, displayed a relatively small magnitude of change. 10,450 transcripts (96% of DE transcripts) were strongly correlated with the average profile of their respective clusters (Pearson correlation > 0.9) and were considered for further analysis.

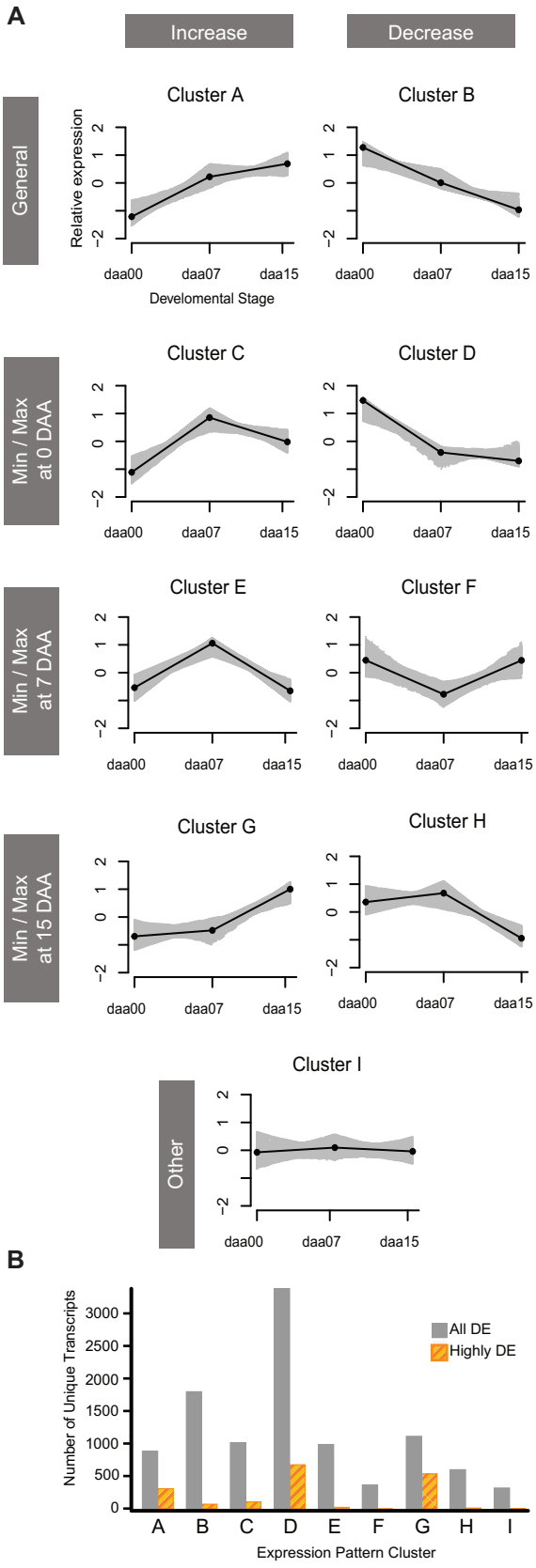

Figure 3.4: Expression Pattern Clusters for DE Transcripts

A) 9 expression pattern clusters, which contain 96% of all transcripts differentially expressed during the sampled stages of reproductive development. Mean TPM values of biological replicates at each stage were centered and scaled, relative to the mean transcript expression value over all stages. Clusters are organized by whether they represent initial increases or decreases (columns) to achieve consistent increase or decreased expression, minimum or maximum expression at each stage (rows). Grey areas represent expression of each transcript in a cluster (only includes transcripts whose expression patterns correlated with the average profile of each cluster (Pearson correlation > 0.9)), while black lines represent the median expression pattern for each cluster. B) Number of unique transcripts in each cluster. Results from sets of all-DE and highly-DE transcripts are shown separately.

In addition to the set of 10,450 DE transcripts represented in the expression pattern clusters ("all-DE"), a subset of "highly-DE" transcripts (b-value > 2 for at least one time point transition: 1,783 transcripts) was considered during further analysis of expression clusters (Figure 3.4B). For the cluster pairs that represent general change (A,B) or minimum/maximum expression at 0 DAA (C,D), more transcripts showed expression decreases. In contrast, in the cluster pairs that represent minimum/maximum expression at 7 DAA (E,F) and 15 DAA (G,H), more transcripts showed increased expression. The clusters with the highest proportion of highly-DE transcripts were Cluster A (consistent expression increase) and G (maximum expression at 15 DAA).

Functional enrichment of expression pattern clusters

Each cluster was tested for significant enrichment of GO molecular function terms, based on the TAIR 10 annotations for the putative *A. thaliana* homolog of each *N. thermarum* transcript. All significantly enriched child terms (ie: the most specialized of a hierarchy) are reported for each cluster, and terms of particular interest are further discussed (Figure 3.5).

Clusters with general or time-point-specific increases in expression were found to be generally enriched for functions related to various types of transmembrane transporter activity. For the set of all-DE transcripts, Cluster G (maximum at 15 DAA) was additionally enriched for functions that appear to be related to chloroplast activity (chlorophyll-binding). While it seems unlikely that seeds at this stage (which are enclosed within opaque fruit walls) would be carrying out photosynthesis, the analogous stage of embryo development in *Arabidopsis* is associated with the formation of chloroplasts within embryo tissues (Mansfield and Briarty, 1991). Among the set of highly-DE transcripts, various transmembrane transporter activities were again enriched in Clusters A (general increase) and G (maximum at 15DAA). Cluster C (increase after 0 DAA) was enriched for lipid binding, and Cluster E (maximum at 7DAA) was enriched for transcription factor activity.

Clusters associated with general or time-point-specific decreases in expression prominently featured significantly enriched terms related to DNA or chromatin binding and modification. For the set of all-DE transcripts, Cluster B (general decrease) was enriched for terms related to methyltransferase activity and Cluster D (decrease after 0 DAA) was enriched for transcription factor activity. Among the set of highly-DE transcripts, Cluster D (decrease after 0 DAA) was enriched for transcription factor activity.

	Cluster	All DE/ highly DE	All DE transcripts	Highly DE transcripts
Increased Expression	A	909 **316** (35%)	• **Amino acid transmembrane transporter activity** • **Phosphate transmembrane transporter activity** • **P-P-bond-hydrolysis protein transmembrane transporter** Oxioreductase, acting on CH-CH group of donors • Transaminase activity • Vitamin binding • Fe-S cluster binding • Metal ion binding • Lyase activity • Protein binding	• **Amino acid transmembrane transporter activity** • Transferase activity, acyl groups other than amino-acyl • Cation binding • Oxidoreductase activity
	C	1062 **105** (6%)	• Translation elongation factor activity • Cu ion binding • Fe-S cluster binding • Structural constituent of ribosome • Disulfide oxioreductase activity • Hydro-lyase activity • Threonine-type endopeptidase activity	*(chi square test)* • Lipid binding
	E	1036 **22** (2%)	• Translation elongation factor activity • Structural constituent of ribosome • NAD or NADH binding • GTP binding • **P-P-bond-hydrolysis protein transmembrane transporter activity** • Nucleobase, nucleoside, nucleotide kinase activity • acyltransferase activity • Phosphotransferase activity, phosphate group as acceptor • GTPase activity • Ligase activity, forming C-S bonds • Metalloendopeptidase	*(chi square test)* • **Transcription factor activity**
	G	1129 **546** (48%)	• Chlorophyll binding • Cu ion binding • Heme binding • Cofactor binding • Lipid binding • **Transition metal ion transmembrane transporter activity** • **K ion transmembrane transporter activity** • **ATPase activity, transmembrane movement of substances** • **symporter activity** • Hydrolase activity • NADH dehydrogenase (ubiquinone) activity • Lyase activity • Electron carrier activity	• Chlorophyll binding • Oxygen binding • Heme binding • **Metal ion transmembrane transporter activity** • **Hydrogen ion transmembrane transporter activity** • **Secondary active transmembrane transporter** • **ATPase, transmembrane movement of substances** • Electron carrier activity • Lyase activity • Monooxygenase activity • NADH dehydrogenase (ubiquinone) activity • Peroxidase activity
Decreased Expression	B	1879 **69** (4%)	• Mismatched DNA binding • Damaged DNA binding • Zn ion binding • ATP binding • **S-adenosylmethionine-dependent methyltransferase** • **N-methyltransferase activity** • DNA-directed DNA polymerase activity • DNA-directed RNA polymerase activity • Protein serine/threonine kinase activity • Small conjugating protein-specific protease activity • 3'-5' exonuclease activity • Hydrolase activity, C-N (not peptide) bonds • ATP-dependent DNA helicase activity	*(chi square test)* • DNA binding
	D	3537 **715** (20%)	• Microtubule motor activity • Microtubule binding • DNA helicase activity • DNA-dependent ATPase activity • Hydrolase activity, O-glycosyl compounds • UDP-glycosyltransferase activity • Transferase activity, hexosyl groups • DNA-directed DNA polymerase activity • Protein serine-threonine kinase activity • Protein tyrosine kinase activity • Transmembrane receptor protein kinase acitivity • **Transcription factor activity** • **Sequence-specific DNA binding** • Protein self-association • Protein homodimerization activity • Identical protein binding • Chromatin binding • ATP binding	• Signal transducer activity • **Transcription factor activity** • Protein kinase binding • Heme binding • Cyclin-dependent protein kinase regulator activity • Protein serine-threonine kinase activity • Monooxygenase activity • ATP binding • **ATPase activity, transmembrane movement of substances** • Oxygen binding • Electron carrier activity
	F	234 **0** (0%)	• (none)	• (none)
	H	605 **9** (1%)	• Catalytic activity • Nucleotide binding	*(chi square test)* • Hydrolase activity
Other	I	59 **1** (2%)	(chi square test) • Ligase activity	*(chi square test)* • (none)

(Previous page) Figure 3.5: Summary of putative molecular functioned enriched in each expression pattern cluster.

All significantly enriched child terms (ie: the most specialized of a hierarchy) are reported for each cluster. Unless otherwise noted, molecular function enriched was tested with hypergeometric test, using Yekutieli (FDR under dependency) multiple corrections testing adjustment, and significance level = 0.1. Molecular function in bold indicate functions of particular interest during discussion.

TF expression during seed development

The fact that clusters that represent both increases and decreases in expression were enriched for transcription factors merited further investigation of transcription factor activity. Of the 1,268 putative transcription factors identified from the *N. thermaurm* genome, 1,039 were expressed during the sampled stages (with a TPM > 1), and 719 were significantly differentially expressed. Among the set of DE transcription factors, we examined whether expression pattern clusters were significantly enriched for any of 58 transcription factor families (Figure 3.6). For the all-DE transcription factor dataset, Cluster B (general decrease) was enriched for FAR1, Cluster D (decrease after 0 DAA) was enriched for GRF, and Cluster E (maximum at 7 DAA) was enriched for MYB transcription factors. When only highly-DE transcription factors were considered (b > 2), Cluster C (increase after 0 DAA) was enriched for WRKY, Cluster D (decrease after 0 DAA) was enriched for ZF-HD and GRF, and cluster E (maximum at 7 DAA) was enriched for MYB activity.

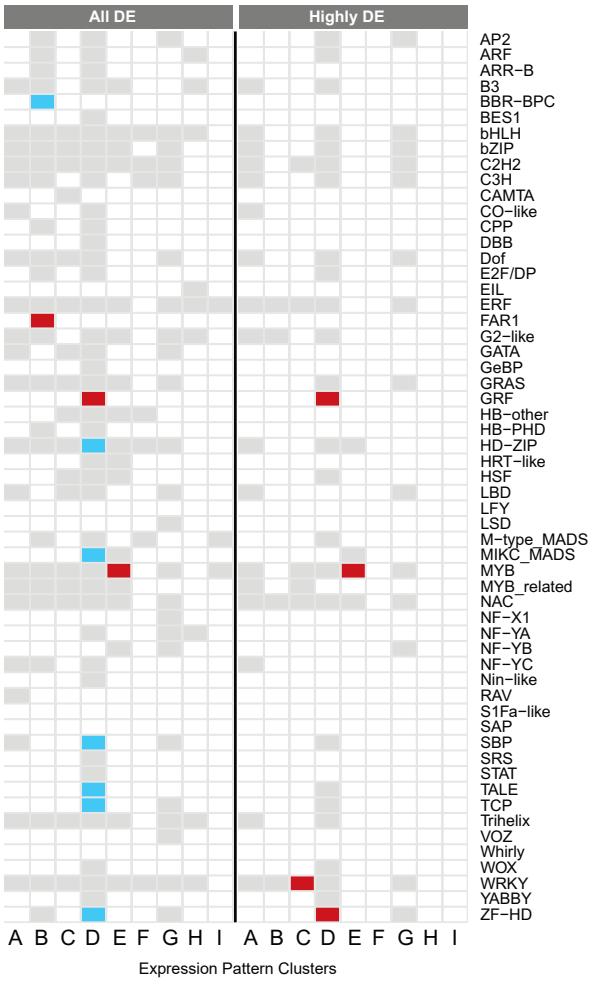

Figure 3.6: Enrichment of differentially-expressed transcription factor families.

Enrichment analysis for TF families among the set of DE TFs in each expression cluster, performed with Fisher's exact test; adjusted p-values (FDR) <0.1 (light blue) and <0.05 (dark red) are noted. Boxes in grey indicate at least one member of a TF family is present in an expression cluster, white indicates that no member of a TF family is present. Results for TFs from the sets of all-DE and highly-DE transcripts are reported separately.

Activity of genes associated with imprinting via DNA and histone methylation

Methyltransferase-related terms were enriched in cluster B (consistent decrease in expression), already hinting at a dynamic chromatin methylation landscape during reproductive development in *N. thermarum*. We constructed gene family phylogenies for genes that are known to regulate imprinted patterns in other angiosperms (CMT, MET, DME, and the PCR2 components MEA, FIS, FIE, and MSI), using sequences from species that represent a wide phylogenetic diversity of angiosperms. Many of the relationships between gene family members corroborates previous studies (Furihata *et al.*, 2016; Bewick *et al.*, 2017).

First, we examined genes involved in the establishment or maintenance of imprinting-related DNA methylation patterns: CMT and MET. Although there are 4 MET homologs in *Arabidopsis*, they appear to be the result of clade-specific gene duplications; the two *N. thermarum* MET homologs are similarly the result of a clade-specific gene duplication (Figure 3.7A). Only one *N. thermarum* CMT homolog was identified, although it's affinity for either of the [CMT2] or [CMT1, CMT3] clades was poorly resolved (Figure 3.7B). All *N. thermarum* homologs of CMT and MET were differentially expressed during reproductive development in *N. thermarum*, and belonged to expression Cluster D (decrease after 0DAA) (Figure 3.9).

DME, on the other hand, removes certain types of methylation marks from DNA. We find that angiosperm DME genes were divided into two poorly-supported clades: one with DME and DML1, and one with DML2 and DML3 (Figure 3.7C). The *N. thermarum* DME homologs formed a single well-supported clade, suggesting clade-specific gene duplication events, that was placed (with poor support) within the [DME, DML1] clade. Three of the four *N. thermarum* DME homologs were in expression Cluster D (decrease after 0 DAA). The fourth and most highly expressed DME homolog, while in expression Cluster H (minimum at 15 DAA), did in fact display a significant increase in expression after 0 DAA (Figure 3.9).

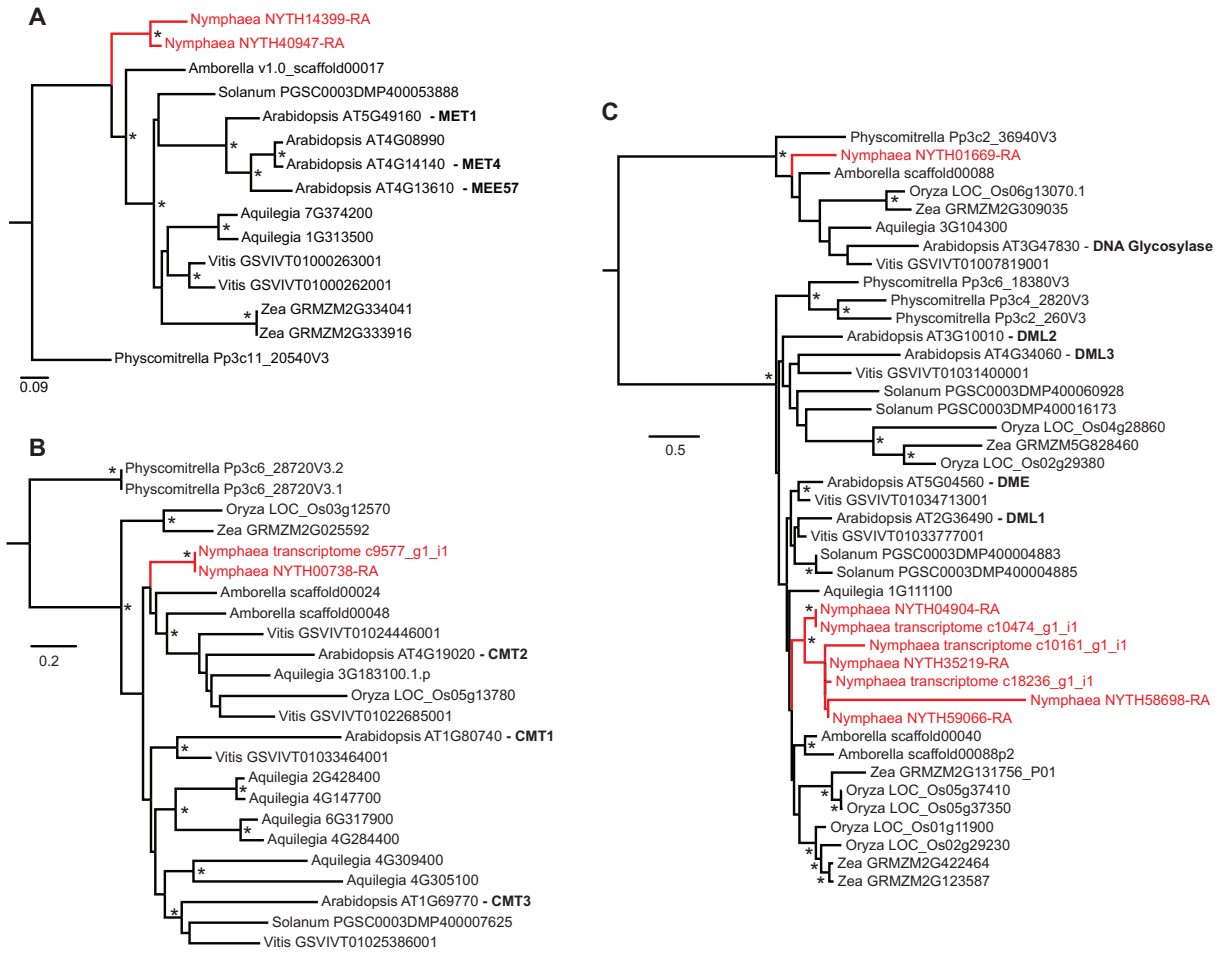

Figure 3.7: Gene family evolution for imprinting-related genes involved in the regulation of DNA methylation patterns.

All gene family phylogenies were calculated with RAxML, from trimmed amino acid alignments. Bootstrap support (n=100) > 0.75 indicated by an asterisk. For each included sequence, the organism (genus name) and transcript identifier are noted. The gene names for *Arabidopsis* copies of interest are included in bold text. *Nymphaea* sequences and sequence lineages are colored red. A) MET gene family. B) CMT gene family. C) DME (and DML) gene family.

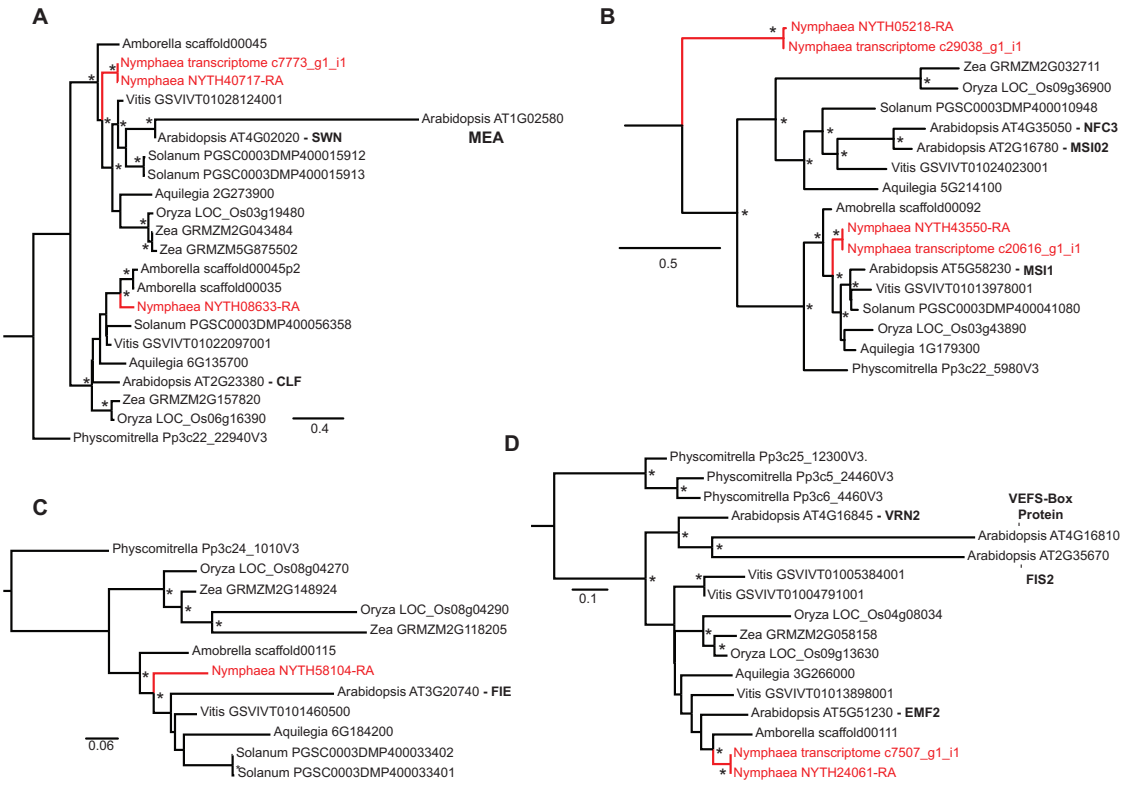

Figure 3.8: Gene family evolution for PRC2 components.

All gene family phylogenies were calculated with RAxML, from trimmed amino acid alignments. Bootstrap support (n=100) > 0.75 indicated by an asterisk. For each included sequence, the organism (genus name) and transcript identifier are noted. The gene names for *Arabidopsis* copies of interest are included in bold text. *Nymphaea* sequences and sequence lineages are colored red. A) MEA (and CLF) gene family. B) MSI1 (and MSI02, NFC3) gene family. C) FIE gene family. D) FIS2 (and VRN2 and EMF2) gene family.

N. thermarum homologs were also identified for all components of PRC2, and all were expressed during reproductive development. Angiosperm homologs of MEA formed two well-supported clades: one with MEA and SWN, and one with CLF (Figure 3.8A). Two *N. thermarum* MEA homologs were identified, with one present in each of the MEA clades. The *N. thermarum* homolog within the [MEA, SWN] clade was expressed during reproductive development, but not differentially expressed; the *N. thermarum* homolog of CLF associated with expression cluster D (decreased expression after 7 DAA) (Figure 3.9). Two *N. thermarum* homologs of MSI1 were identified, and both associated with expression cluster B (consistent decreased expression) (Figures 3.8B, 3.9). The FIE gene family appeared to be relatively simple, with little indication of gene duplications outside of monocots – one copy of FIE was identified from *N. thermarum* (Figure 3.8C). Angiosperm FIS2 genes formed two well-supported clades: one appeared to be specific to *Arabidopsis* (and included VRN2 and FIS2), while the other included EMF2. Only one homolog was identified from *N. thermarum*, and its placement within the EMF2 clade was poorly supported (Figure 3.8D). The FIE and FIS2 homologs in *N. thermarum* were expressed during reproductive development, but not differentially (Figure 3.9).

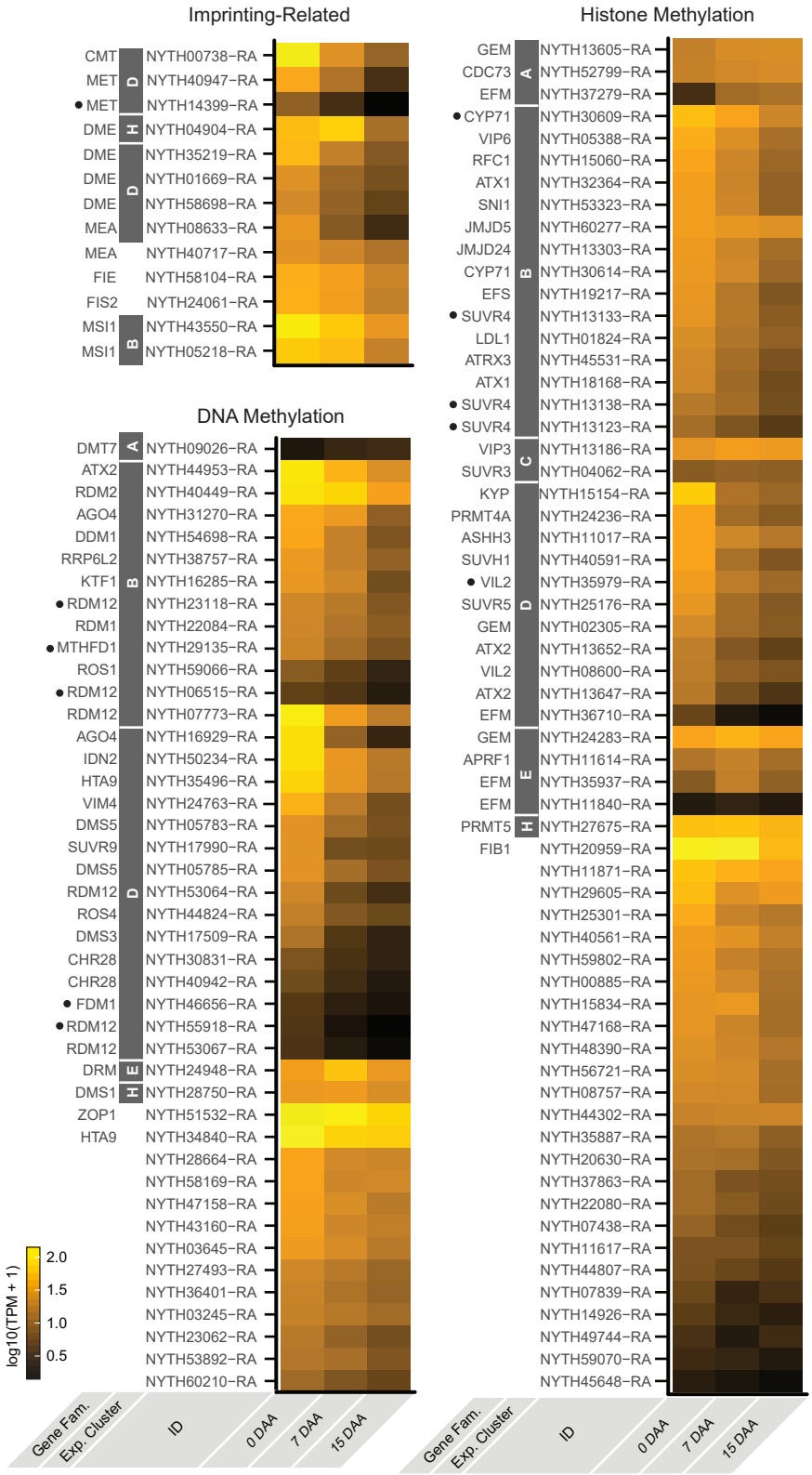
Imprinting-Related
CMT D NYTH00738−RA
MET NYTH40947−RA
● MET NYTH14399−RA
DME H NYTH04904−RA
DME NYTH35219−RA
DME D NYTH01669−RA
DME NYTH58698−RA
MEA NYTH08633−RA
MEA NYTH40717−RA
FIE NYTH58104−RA
FIS2 NYTH24061−RA
MSI1 B NYTH43550−RA
MSI1 NYTH05218−RA
DNA Methylation
DMT7 A NYTH09026−RA
ATX2 NYTH44953−RA
RDM2 NYTH40449−RA
AGO4 NYTH31270−RA
DDM1 NYTH54698−RA
RRP6L2 NYTH38757−RA
KTF1 B NYTH16285−RA
● RDM12 NYTH23118−RA
RDM1 NYTH22084−RA
● MTHFD1 NYTH29135−RA
ROS1 NYTH59066−RA
● RDM12 NYTH06515−RA
RDM12 NYTH07773−RA
AGO4 NYTH16929−RA
IDN2 NYTH50234−RA
HTA9 NYTH35496−RA
VIM4 NYTH24763−RA
DMS5 NYTH05783−RA
SUVR9 NYTH17990−RA
DMS5 NYTH05785−RA
RDM12 D NYTH53064−RA
ROS4 NYTH44824−RA
DMS3 NYTH17509−RA
CHR28 NYTH30831−RA
CHR28 NYTH40942−RA
● FDM1 NYTH46656−RA
● RDM12 NYTH55918−RA
RDM12 NYTH53067−RA
DRM E NYTH24948−RA
DMS1 H NYTH28750−RA
ZOP1 NYTH51532−RA
HTA9 NYTH34840−RA
NYTH28664−RA
NYTH58169−RA
NYTH47158−RA
NYTH43160−RA
NYTH03645−RA
NYTH27493−RA
NYTH36401−RA
NYTH03245−RA
NYTH23062−RA
NYTH53892−RA
NYTH60210−RA
log10(TPM + 1)
2.0
1.5
1.0
0.5
Gene Fam.
Exp. Cluster
ID
0 DAA
7 DAA
15 DAA
Histone Methylation
GEM A NYTH13605−RA
CDC73 NYTH52799−RA
EFM NYTH37279−RA
● CYP71 NYTH30609−RA
VIP6 NYTH05388−RA
RFC1 NYTH15060−RA
ATX1 NYTH32364−RA
SNI1 NYTH53323−RA
JMJD5 NYTH60277−RA
JMJD24 NYTH13303−RA
CYP71 B NYTH30614−RA
EFS NYTH19217−RA
● SUVR4 NYTH13133−RA
LDL1 NYTH01824−RA
ATRX3 NYTH45531−RA
ATX1 NYTH18168−RA
● SUVR4 NYTH13138−RA
● SUVR4 NYTH13123−RA
VIP3 C NYTH13186−RA
SUVR3 NYTH04062−RA
KYP NYTH15154−RA
PRMT4A NYTH24236−RA
ASHH3 NYTH11017−RA
SUVH1 NYTH40591−RA
● VIL2 NYTH35979−RA
SUVR5 D NYTH25176−RA
GEM NYTH02305−RA
ATX2 NYTH13652−RA
VIL2 NYTH08600−RA
ATX2 NYTH13647−RA
EFM NYTH36710−RA
GEM NYTH24283−RA
APRF1 E NYTH11614−RA
EFM NYTH35937−RA
EFM NYTH11840−RA
PRMT5 H NYTH27675−RA
FIB1 NYTH20959−RA
NYTH11871−RA
NYTH29605−RA
NYTH25301−RA
NYTH40561−RA
NYTH59802−RA
NYTH00885−RA
NYTH15834−RA
NYTH47168−RA
NYTH48390−RA
NYTH56721−RA
NYTH08757−RA
NYTH44302−RA
NYTH35887−RA
NYTH20630−RA
NYTH37863−RA
NYTH22080−RA
NYTH07438−RA
NYTH11617−RA
NYTH44807−RA
NYTH07839−RA
NYTH14926−RA
NYTH49744−RA
NYTH59070−RA
NYTH45648−RA
Gene Fam.
Exp. Cluster
ID
0 DAA
7 DAA
15 DAA

(Previous page) Figure 3.9: Expression of N. thermarum transcripts putatively involved in DNA and histone methylation.

Transcripts putatively related to imprinting are noted separately from all other transcripts putatively involved in DNA or histone methylation. For each transcript, the following information is included (from left to right): gene family the transcript is associated with or the gene name of the most closely-related *Arabidopsis* homolog; whether the transcript is present in a DE expression pattern cluster; transcript identifier; expression at each of the sampled stages of reproductive development. Black dots indicate transcript is not expressed in roots, leaves, floral buds, or pre-meiotic ovules.

Activity of genes associated with DNA and histone methylation

We next used a broader approach to examine the expression of any transcript that could be involved in regulation of methylation patterns (Figure 3.9). 121 loci in *Arabidopsis* thaliana are annotated as being involved in DNA or histone methylation; 125 putative homologs were identified from within the *N. thermarum* genome using pair-wise blast comparisons. 112 of the *Nymphaea* methyltransferase-related homologs were expressed in mature ovules or during seed development with a TPM >1, and of those 73 were significantly differentially expressed. Of the 112 putative DNA or histone methyltransferase-related homologs in *N. thermarum* expressed in mature ovules or developing seeds, 20 of them were not present in transcriptomes of root tips, leaves, young floral buds, or young ovules (data not shown). 11 of the mature ovule/seed-development-specific homologs were differentially expressed, including putative homologs of RDM12, MTHFD1, MET, FDM1, CYP71, SUVR4, and ATX2; all were in the expression-pattern clusters that represented either general expression decrease (Cluster B), or decreased expression after 0 DAA (Cluster D).

Most of the *Nymphaea* chromatin methylation-associated transcripts were in expression-pattern clusters that represented decreased expression or expression minima (Clusters B,D,F,H). Only 11 transcripts were among the increased-expression clusters (A,C,E,G). This included homologs of DTM7, DRM, GEM, CDC73, EFM, VIP3, SUVR3, and APRF1. Among the set of non-DE transcripts, a few were present with fairly high abundance, including homologs of ZOP1, HTA9, and FIB1.

Discussion

Overview

RNA-seq has proved to be a powerful tool for understanding the genes and processes important for development. We leverage its ability to move beyond a candidate gene approach, to study seed development in the water lily *Nymphaea thermarum*, and specifically the processes involved in regulating imprinting-related and non-imprinting-related chromatin methylation. However, we first assess the quality of the produced RNA seq libraries, and address possible caveats that arise from whole ovule or seed sampling. We then highlight broad-scale patterns in transcript abundance, expression, and functional enrichment. Methylation-realted activity is enriched among a certain subset of differentially expressed genes, supporting the need for further exploration of chromatin-methylation activity.

We describe the activity of both imprinting-related and non-imprinting-related genes involved in chromatin methylation. In one approach, gene family phylogenies are constructed to identify all putative homologs of genes known to be involved in regulating imprinting in other angiosperms, and to understand the evolutionary relationships of those homologs. In a second, broader approach, we assess the expression of putative homologs of all 121 Arabidopsis genes known to be involved in DNA or histone methylation. We find that all components of known imprinting mechanisms are expressed during reproductive development in *N. thermarum*, and that many other chromatin methylation regulators are differentially expressed (with some increasing expression after fertilization). This indicates that not only is imprinting possible *in N. thermarum*, but that the chromatin methylation landscape is almost certainly dynamic throughout reproductive development. Comparisons with the expression of imprinting regulation in other angiosperms suggests that the current model for how imprinting is regulated, mostly based on in *Arabidopsis*, is likely a mix of deeply conserved and eudicot-specific processes. Finally, we are able to suggest that the function several histone-methylation genes merit further investigation during seed development in not only *N. thermarum*, but any model system.

Quality of transcriptomes

A common benchmark for the completeness of RNA seq datasets is their ability to document the expression of genes with low expression. Achieving sufficiently high sequencing depth, however, often comes as a trade-off with the inclusion of biological replicates that are necessary for rigorous differential

expression analysis (Conesa *et al.*, 2016). We balanced these concerns by using 3-4 biological replicates, sequenced at high depth, for a small number of developmental stages. Previous studies have suggested accurate recovery of genes expressed at low levels can require up to 80 million reads per sample (Sims *et al.*, 2014); the current study generated 66-100 million reads per sample. Transcription factors, which are regulatory genes that can have relatively large biological effects at relatively low expression levels, require high sequencing depth to accurately capture. We documented the expression of 1,039 putative transcription factors (82% of all putative transcription factors in the *N. thermarum* genome) which belong to 55 out of the 58 land plant transcription factor families. Importantly, we find that expression clusters that represent increased expression during key points during early embryo development were enriched for MYB or WKRY transcription factors. Both MYB and WKRY transcription factors have been associated with early embryogenesis in *Arabidopsis* and other angiosperms (Lagacé *et al.*, 2004; Luo *et al.*, 2005; Dubos *et al.*, 2010; Wickramasuriya and Dunwell, 2015), and the fact that their enrichment temporally coincides with the initiation of embryo development in *N. thermarum* suggests that our dataset accurately captures genes with low expression.

Whole seeds were sampled for this study, however, and it is therefore possible that the expression of embryo- or endosperm-development-related genes are not accurately represented over time. The embryo and endosperm represent far less than half of the total volume of a seed of *Nymphaea thermarum*. After fertilization, the perisperm constitutes most of the seed volume, and becomes metabolically active in terms of nutrient transport, processing, and storage – high levels of gene expression related to these perisperm-specific processes could be 'drowning out' transcriptional information from the embryo and endosperm. However, three lines of evidence suggest that the relative transcriptional presence of the embryo and endosperm does not significantly change during seed development. First, the proportion of the ovule/seed occupied by the perisperm remains fairly constant throughout development (Povilus *et al.*, 2015). Second, studies of seed development in other species found that the distribution of embryo-specific and endosperm-specific gene expression levels are fairly constant across time, relative to the distribution of transcript expression levels from a whole-seed samples (Chen *et al.*, 2014). Finally, we recover patterns of increased expression for genes whose homologs are known to be important for and/or expressed in the embryo or endosperm in other species (for example: putative homologs of TITAN-LIKE (Lu *et al.*, 2012) and TOPLESS (Long *et al.*, 2006) are found in expression Cluster E (maxi-

mum expression at 7 DAA)(Supplementary Dataset 3.3)). However, further investigation specifically of embryogenesis and endosperm-development gene networks in *N. thermarum* should consider physical dissection of seeds, to separate offspring components from the perisperm.

Patterns of gene expression during reproductive development

We find that a large proportion of genes is expressed during reproductive development in *N. thermarum*: 74% of the total number of genes predicted from the *N. thermarum* genome. Furthermore, 56% of the expressed transcripts are differentially expressed. The proportion of genes expressed (either differentially expressed or not) during reproductive development is similar what has been described in other species (Chen *et al.*, 2014). The number of unique transcripts in *N. thermarum* suggests that the transitions from female gametophyte maturation, through fertilization, and into mid-seed development require substantial transcriptional reprogramming (Figure 3.2B). While female gametophyte and ovule maturation involve relatively high numbers of unique genes (1,148), the expression of almost as many genes (916) appears to carry over into early seed development. 7 and 15 DAA shared the expression of far fewer genes (339; other than those shared by all three stages) – a surprising result given that 7 and 15 DAA are understood to share more developmental processes than 0 and 7 DAA. However, a previous study provided evidence for a lingering maternal influence on early seed development in *N. thermarum* (Chapter 2 of this dissertation), which is supported by the relatively large number of transcripts shared between 0 and 7 DAA. Furthermore, when expression pattern (not just presence/absence of transcripts) is taken into account, 7 and 15 DAA samples were more similar to each other than either were to 0 DAA samples (Figure 3.3A).

When DE transcripts are clustered by expression pattern, there are clear similarities among the enriched putative molecular functions for clusters that represent increases or decreases in expression. As could be predicted by the onset of nutrient import and storage after fertilization, most of the "increased-expression" clusters were enriched for transporter activities, and a homolog of WAXY starch synthase 1 was among the 10 most highly expressed genes at 7 and 15 DAA. However, we also note patterns of gene expression associated with the onset of embryogenesis and/or endosperm development: highly-DE transcripts in Cluster E (maximum expression at 7 DAA) were enriched for transcription factor activity. Furthermore, the set of DE transcription factors in Cluster C and E were enriched for (respectively) WRKY

and MYB genes, which have been associated with embryo and endosperm development in both *Arabidopsis* and *Zea mays* (Lagacé *et al.*, 2004; Luo *et al.*, 2005; Dubous 2010; Wickramasuriya and Dunwell, 2015).

Expression pattern clusters that represent a decrease in expression were enriched with an altogether different set of molecular functions. DNA/chromatin binding, transcription factor activity, and control of DNA polymerase are featured prominently in both the all-DE and highly-DE datasets. Intriguingly, expression Cluster D (decrease after 0 DAA) was enriched for GRF and ZF-HD transcription factors, which are associated with, among other things, cell division and floral development (Omidbakhshfard 2015). We therefore attribute the pattern of decreased DNA-related functions to either the cessation of cell proliferation and differentiation associated with ovule development, and/or the de-repression of seed development programs.

Evidence for dynamic methylation landscape during reproductive development

In *N. thermarum*, 125 genes putatively share homology with *Arabidopsis* genes involved in DNA or histone methylation. A remarkable 89% of these *N. thermarum* homologs are expressed in mature ovules or during seed development (at TPM > 1), with 58% being differentially expressed, suggesting a dynamic methylation landscape during reproductive development. Most of the DE methylation-related genes belonged to either expression cluster B (consistent decrease in expression) or expression cluster D (decreased expression after 0 DAA), which is further supported by the enrichment of methylation-related activity in expression cluster B.

Among the gene families known to specifically regulate imprinting-related methylation patterns, MET and CMT homologs were recovered in expression Cluster D (decreased expression after 0 DAA), as were three-quarters of the DME homologs. Furthermore, one of the MET homologs appears to be specifically expressed during seed development. The fourth *N. thermarum* DME, while associated with expression cluster H (decreased expression after 7 DAA), did in fact display a significant increase in expression after 0 DAA. All components of PRC2 were expressed during reproductive development.

Putative homologs of other chromatin methylation-related genes were also found to be expressed during reproductive development in *N. thermarum*. Many components of the RdDM pathway were present during the sampled developmental stages in *N. thermarum*. Most fell into expression-pat-

tern clusters B and D (consistent decrease in expression, or decreased expression after 0 DAA). Interestingly, most of the chromatin methylation-related homologs expressed only during seed development are components of the RdDM pathway (RDM12, FDM1), are known to be involved in chromatin remodeling (CYP71), and/or have been specifically tied to transposon repression (SUVR4, MTHFD1). In addition, DRM, an important component of the RdDM pathway, showed increased expression after fertilization. Homologs of several genes involved in histone methylation (GEM, CYP71, EFM, VIP3, SUVR3, APRF1) showed increased expression after fertilization, although they have not previously been associated with seed development.

Altogether, our data suggests that DNA methylation patterns are being established, maintained, and removed before fertilization in *N. thermarum*. After fertilization, DNA methylation maintenance (CMT, MET) decreases, while the expression of some genes involved in DNA demethylation (DME) and de novo methylation (DRM and other RdDM components) increases. The components of PRC2, which establish loci-specific histone methylation patterns associated with imprinting, all decrease in expression over time. By the time that the embryo typically initiates cotyledons, the expression of nearly all chromatin methylation-related genes has decreased, relative to pre-fertilization levels.

Comparison of DNA and histone methylation activity with other angiosperms

DNA and histone methylation has been studied for a small handful of distantly-related angiosperms. Many studies are fragmentary and only address a subset of chromatin methylation-related genes. The most complete models for chromatin methylation dynamics come from the eudicot *Arabidopsis* and the monocot *Oryza* (rice)(Köhler *et al.*, 2012). Importantly, chromatin methylation has been shown to be dynamic and important for seed development in every taxon which has been studied. The molecular/genetic evidence for imprinting (which depends on chromatin methylation) is less consistent (Gleason and Kramer, 2012), although there is wide-spread phenotypic evidence for parent-of-origin effects on seed development (Haig and Westoby, 1991). It must be noted, however, that developmental stage sampling is inconsistent in many studies of gene expression during seed development (due in part to fundamental differences in how seeds develop), so comparisons should be approached with caution. In addition, complex, lineage-specific histories of gene duplication and loss can make it difficult to assess specific homology relationships within gene families.

	Nymphaea	Monocots (mostly *Oryza*)	*Arabidopsis*	Summary
CMT	***1 copy*** • Decreases	***2 copies*** • 1 copy decreases • 1 copy increases, then decreases (Sharma 2006)	***3 copies*** • 1 copy decreases (Sharma 2006)(Julien 2012)	Fairly consistent expression patterns, for the copies expressed during seed development.
MET	***2 copies*** • Both decrease	***2 copies*** (Sharma 2009) • 1 copy constant • 1 copy increases, then decreases	***4 copies*** • 1 copy increases (Sharma 2006)(Julien 2012)	Lineage-specific duplications. *Nymphaea* copies have opposite expression patterns than what is seen in Arabidopsis and Oryza.
DME*	***4 copies*** • 3 copies decrease • 1 copy increases, then decreases	***6 copies?*** • Most copies decrease (Jiang 2016) • In barely, one MET copy increases (Kapazoglou 2013)	***4 copies*** • 1 copy decreases (Choi 2002)	Lineage-specific duplication in *Nymphaea* and in monocots. *Nymphaea* expression resembles certain homologs in *Arabidopsis*, or in some monocots.
MEA*	***2 copies*** • Both decrease	***1 copy*** • Low in egg cell (Anderson 2013) • Little change in endosperm (Nallamilli 2013)	***3 copies*** • 1 copy changes little (Sharma 2006)	*Nymphaea* expression decreases, while in *Arabidopsis* and rice, expression changes little.
FIE	***1 copy*** • Decreases (non-significant)	***2 copies*** • Both copies high in egg cell (Anderson 2013) • 1 copy increases in endosperm (Nallamilli 2013) • 1 copy changes little in endosperm	***1 copy*** • Increases, then decreases (Baroux 2006)	*Nymphaea* expression decreases (non-significantly), while expression in *Arabidopsis* and rice increases. Lineage-specific duplication in *Oryza* may have led to functional divergence.
FIS2*	***1 copy*** • Decreases (non-significant)	***2 copies*** • Both copies high in egg cell (Anderson 2013) • Both copies change little in endosperm (Nallamilli 2013)	***4 copies*** • 1 copy decreases (Baroux 2006)	*Nymphaea* expression is similar to the one *Arabidopsis* copy important for seed development.
MSI1*	***1 or 2 copies*** • Decreases	***1 copy*** • High in egg cell (Anderson 2013)	***1 copy*** • Decreases (Baroux 2006)	Fairly consistent expression patterns, for the copies expressed during seed development.

Figure 3.10: Summary and comparison of imprinting-related methylation regulators in *Nymphaea*, monocots (mostly *Oryza*), and *Arabidopsis*, and their expression before and after fertilization.
For each gene family of interest, the number of copies in each species is reported, as well a brief summary of their relative expression before and after fertilization. An asterisk next to the gene family name indicates that a broad definition of gene family was used when assessing copy number (for example, the MEA* gene family includes both the MEA and CLF subfamilies).

A summary of expression patterns, before and after fertilization, in ovules and seeds of *Nymphaea*, monocots (mostly *Oryza*), and *Arabidopsis* is presented in Figure 3.10. The expression of some chromatin-methylation genes appears to be conserved in *N. thermarum*, while others are different than expression patterns observed in *Arabidopsis* or rice. CMT, and MET homologs all show decreased expression after fertilization in *Nymphaea*. While decreased expression of CMT is similar to what is is seen in *Arabidopsis* and rice, the expression pattern of the *Nymphaea* METs is the opposite of those in *Arabidopsis* and rice (Sharma *et al.*, 2009; Julien *et al.*, 2012). The comparison for DME is more complex – one DME copy in *Nymphaea* shares the expression pattern with one barley DME homolog (Kapazoglou *et al.*, 2013). The expression of the second DME copy in *Nymphaea* is more similar to most of the rice DME

homologs and to the *Arabidopsis* DME (Choi *et al.*, 2002; Jiang and Ramachandran, 2016). All copies of PRC2 components decrease in expression after fertilization in *Nymphaea*, while expression patterns of individual components show more variation in *Arabidopsis* and rice (Baroux *et al.*, 2006; Anderson *et al.*, 2013; Nallamilli *et al.*, 2013).

Based on the complexity of DNA methylation-related activity, we conclude that DNA methylation is likely as dynamic during reproductive development in *N. thermarum*, as it is in other angiosperms. Maintenance of CG methylation by MET may, however, be relatively less important after fertilization, compared to the role that MET is understood to play during seed development in *Arabidopsis*. In contrast, de novo CG methylation by DRMs may be relatively more important during seed development (as evidenced by the expression maximum at 7 DAA for a highly-expressed DRM copy). Histone methylation is also clearly a dynamic process after fertilization in *Nymphaea*, although it may largely be regulated by genes other than those of the PRC2 – such as GEM, CYP71, EFM, VIP3, SUVR3, and/or APRF1 (all of which show increased expression after fertilization).

Could imprinting occur during reproductive development in an early diverging angiosperm lineage?

We conclude that chromatin methylation is actively regulated during reproductive development in *N. thermarum*. Importantly, homologs of all of the genes known to be involved in imprinting via chromatin methylation are expressed in mature ovules or developing seeds. If imprinting occurs, however, its regulation is likely different than what is known for *Arabidopsis* – particularly with respect to the roles of MET and PRC2. Interestingly, there is little evidence that PRC2 as a whole is important for seed development in rice (Luo *et al.*, 2009). Yet imprinting occurs in monocots, and impacts endosperm development – other molecular machinery must be responsible for regulating and responding to imprinting-related methylation patterns. Until the functions of the *Nymphaea* PRC2 homologs can be determined, we suggest that the role of the PRC2 as whole in regulating imprinting may represent a derived condition within eudicots.

Finally, this study reveals a list of histone-methylation related genes that show increased expression after fertilization, but have not before been described as being important for seed development. We suggest that the functions of these genes (GEM, CYP71, EFM, VIP3, SUVR3, and/or APRF1) deserve further investigation in not just *N. thermaurm*, but in model species like *Arabidopsis*, rice, and maize.

The discovery that additional chromatin methylation-related mechanisms may be important for seed development highlights the profound potential of RNA seq datasets to enrich our understanding of seed development.

References

Amborella Genome Project (2013) The *Amborella* genome and the evolution of flowering plants. *Science* 342:6165

Anderson SN, Johnsom CS, Jones DS, Conrad LJ, Gou X, Russell SD, Sundaresan V (2013) Transcriptomes of isolated *Oryza sativa* gametes characterized by deep sequencing: evidence for distinct sex-dependent chromatin and epigenetic states before fertilization. *Plant J* 76(5):729-741.

Baroux C, Gagliardini V, Page DR, Grossniklaus U (2006) Dynamic regulatory interactions of Polycomb group genes: MEDEA autoregulation is required for imprinted gene expression in *Arabidopsis*. *Genes Dev* 20(9)1081-1086.

Bewick AJ, Niederhuth CE, Ji L, Rohr NA, Griffin PT, Leebens-Mack J, Schmitz RJ (2017) The evolution of CHROMOMETHYLASES and gene body DNA methylation in plants. *Genome Biol* 18:65.

Bray NL, Pimentel H, Melsted P, Pachter L (2016) Near-optimal probabilistic RNA-seq quantification. *Nat Biotech* 34:525–527.

Butenko Y, Ohad N (2011) Polycomb-group mediated epigenetic mechanisms through plant evolution. *Biochim Biophys Acta, Gen Regul Mech* 1809(8):395-406.

Chen J, Zeng M, Xie S, Wang G, Hauck A, Lai J (2014) Dynamic transcriptome landscape of maize embryo and endosperm development. *Plant Physiol* 166:252-264.

Choi Y, Gehring M, Johnson L, Hannon M, Harada JJ, Goldberg RB, Jacobsen SE, Fischer RL (2002) DEMETER, a DNA glycosylase domain protein, is required for endosperm gene imprinting and seed viability in *Arabidopsis*. *Cell* 110(11):33-42.

Conesa A, Madrigal P, Tarazona S, Gomez-Cabrero D, Cervera A, McPherson A, Szcześniak MW, Gaffney DJ, Elo L, Zhang X, Mortazavi A (2016) A survey of best practices for RNA-seq data analysis. *Genome Biol* 17:13.

Dubos C, Stracke R, Grotewold E, Weisshaae B, Martin C, Lepiniec L (2010) MYB transcription factors in *Arabidopsis*. *Trends Plant Sci* 15(10):573-581.

Eddy SR (2011) Accelerated profile HMM searches. *PLoS Comp Biol* 7:e1002195

Edgar RC (2004) MUSCLE: multiple sequence alignment with high accuracy and high throughput. *Nucleic Acids Res* 32(5), 1792-97.

Fischer E, Magdalena-Rodriguez C (2010) *Nymphaea thermarum* (Nymphaeaceae). *Curtis Bot Mag* 27:318–327.

Furihata HY, Suenaga K, Kawanabe T, Yoshida T, Kawabe A (2016) Gene duplication, silencing, and expression alteration govern the molecular evolution of PRC2 genes in plants. *Genes Genet Syst* 91(2):85-95.

Gao Y, Xu H, Shen Y, Wang J (2013) Transcriptome analysis of rice (*Oryza sativa*) developing endosperm using the RNA-Seq technique. *Plant Mol Biol* 81(4-5):363-378.

Gao J, Yu X, Ma F, Li J (2014) RNA-seq analysis of transcriptome and glucosinolate metabolism in seeds and sprouts of broccoli (*Brassica oleracea var. italic)*. *PLoS ONE* 9(2):e88804.

Gehring M, Satyaki PR (2017) Endosperm and imprinting, inextricably linked. *Plant Physiol* 173:143-154

Girke T, Todd J, Ruuska S, White J, Benning C, Ohirogge J (2000) Microarray analysis of developing *Arabidopsis* seeds. *Plant Physiol* 124:1570-1581.

Gleason EJ, Kramer EM (2012) Characterization of *Aquilegia* Polycomb Repressive complex 2 homologs reveals absence of imprinting. *Gene* 507(1):54–60.

Goodstein DM, Shu S, Howson R, Neupane R, Hayes RD, Fazo J, Mitros T, Dirks W, Hellsten U, Putnam N, Rokhsar DS (2012) Phytozome: a comparative platform for green plant genomics. *Nucleic Acids Res* 40(Database issue):D1178-1186.

Haig D, Westoby M (1991) Genomic imprinting in endosperm: its effects on seed development in crosses between species and between different ploidies of the same species, and its implications for the evolution of apomixis. *Phil Trans R Soc B* 333:1–13.

Haig D (2013) Kin conflict in seed development: an interdependent but fractious collective. *Annu Rev Cell Dev Biol* 29:189-211.

Hirsch C, Hirsch CD, Brohammer AB, Bowman MJ, Soifer I, Barad O, Shem-Tov D, Baruch K, Lu F, Hernandez AG, Fields CJ, Wright CL, Koehler K, Springer NM, Buckler ES, Buell CR, de Leon N, Kaeppler SM, Childs K, Mikel MA (2016) Draft assembly of elite inbred line PH207 provides insights into genomic and transcriptome diversity in maize. *Plant Cell* 28(11)2700-2714.

Hsieh TF, Shin J, Uzawa R, Silva P, Cohen S, Bauer MJ, Hashimoto M, Kirkbride RD, Harada JJ, Ziberman D, Fischer RL (2012) Regulation of imprinted gene expression in *Arabidopsis* endosperm. *Proc Natl Acad Sci U S A* 108(5):1755-1762.

Jiang SY, Ramachandran S (2016) Expansion mechanisms and evolutionary history on genes encoding DNA glycosylases and their involvement in stress and hormone signaling. *Genome Biol Evol* 8(4):1165-1184.

Jin JP, Tian F, Yang DC, Meng YQ, Kong L, Luo JC and Gao G. (2017). PlantTFDB 4.0: toward a central hub for transcription factors and regulatory interactions in plants. *Nucleic Acids Res* 45(D1):D1040-D1045.

Jones SI, Vodkin LO (2013) Using RNA-seq to profile soybean seed development from fertilization to maturity. *PLoS ONE* 8(3):e59270.

Julien PE, Susaki D, Yelagandula R, Higashiyama T, Berger F (2012) DNA methylation dynamics during sexual reproduction in *Arabidopsis thaliana*. *Curr Biol* 22(19):1825-1830.

Kapazoglou A, Drosou V, Argiriou A, Tsaftaris AS (2013) The study of a barley epigenetic regulator, HvDME, in seed development and under drought. *BMC Plant Biol* 13:172.

Köhler C, Wolff P, Spillane C (2012) Epigenetic mechanisms underlying genomic imprinting in plants. *Ann Rev Plant Biol* 63:331-352.

Lagacé M, Matton DP (2004) Characterization of a WRKY transcription factor expressed in late torpedo-stage embryos of *Solanum chacoense*. *Planta* 219(1):185-189.

Lamesch P, Berardini TZ, Li D, Swarbreck D, Wilks C, Sasidharan R, Muller R, Dreher K, Alexander DL, Garcia-Hernandez M, Karthikeyan AS, Lee CH, Nelson WD, Ploetz L, Singh S, Wensel A, Huala E (2012) The Arabidopsis Information Resource (TAIR): improved gene annotation and new tools. *Nucleic acids res* 40(Database issue):D1202-D1210.

Li G, Wang D, Yang R, Logan K, Zhang S, Skaggs M, Lloyd A, Burnette WJ, Laurie JD, Hunter BG, Dannenhoffer JM, Larkins BA, Drews GN, Wang X, Yadegari R (2014) Temporal patterns of gene expression in developing maize endosperm identified through transcriptome sequencing. *Proc Natl Acad Sci U S A* 111(21):7582-7587.

Long JA, Ohno C, Smith ZR, Meyerowitz EM (2006) TOPLESS regulates apical embryonic fate in *Arabidopsis*. *Science* 312(5779):1520-1523.

Lu X, Li Y, Su Y, Liang Q, Meng H, Li S, Shen S, Fan Y, Zhang C (2012) An *Arabidopsis* gene encoding a C2H2-domain protein with alternatively spliced transcripts is essential for endosperm development. *J Exp Bot* 63(16):5935-5944.

Luo M, Dennis ES, Berger F, Peacock WJ, Chaudhury A (2005) *MINISEED2* (*MINI3*), a WRKY family gene, and *HAIKU2* (*IKU2*), a leucine-rich repeat (*LRR*) *KINASE* gene, are regulators of seed size in *Arabidopsis*. *Proc Natl Acad Sci U S A* 102(48):17531-17536.

Luo M, Platten D, Chaudhury A, Peacock WJ, Dennis ES (2009) Expression, imprinting, and evolution of rice homologs of the polycomb group genes. *Mol Plant* 2:711–723

Mansfield SG, Briarty LG (1991) Early embryogenesis in *Arabidopsis thaliana*. II. The developing embryo. *Canad J Bot* 69(3):461-476.

Nallamilli BRR, Zhang J, Mujahid H, Malone BM, Bridges SM, Peng Z (2013) Polycomb group gene OsFIE2 regulates rice (*Oryza sativa*) deed development and grain filling via a mechanism distinct from *Arabidopsis*. *PLoS Genet* 9(3):e1003322.

Nguyen HT, Silva JE, Podicheti R, Macrander J, Yang W, Nazerenus TJ, Nam JW, Jaworski JG, Lu C, Scheffler BE, Mackaitis K, Cahoon EB (2013) Camelina seed transcriptome: a tool for meal and oil improvement and translational research. *Plant Biotech J* 11(6):759-769.

Ouyang S, Zhu W, Hamilton J, Lin H, Campbell M, Childs K, Thibaud-Nissen F, Malek RL, Lee Y, Zheng L, Orvis J, Haas B, Wortman J, Buell CR (2007)The TIGR Rice Genome Annotation Resource: improvements and new features. *Nucleic Acids Res* 35(Database issue):D883-D887.

Pereira AM, Lopes AL, Coimbra S (2016) Arabinogalactan proteins as interactors along the crosstalk between the pollen tube and the female tissues. *Front Plant Sci* 7:1895.

Pimentel HJ, Bray N, Puente S, Melsted P, Pachter L (2017) Differential analysis of RNA-Seq incorporating quantification uncertainty. *Nat Methods* (2017), advanced access http://dx.doi.org/10.1038/nmeth.4324.

Povilus RA, Losada JM, Friedman WE (2015) Floral biology and ovule and seed ontogeny of *Nymphaea thermarum*, a water lily at the brink of extinction with potential as a model system for basal angiosperms. *Ann Bot* 115:211-226

R Core Team (2017). *R: A language and environment for statistical computing*. R Foundation for Statistical Computing, Vienna, Austria. URL https://www.R-project.org/.

Sharma R, Mohan Singh RK, Malik G, Deveshwar P, Tyagi AK, Kapoor S, Kapoor M (2009) Rice cytosine DNA methyltransferases - gene expression profiling during reproductive development and abiotic stress. *FEBS J* 276(21):6301-6311.

Sims D, Sudbery I, Ilott NE, Heger A, Ponting CP (2014) Sequencing depth and coverage key considerations in genome analyses. *Nat Rev Genet* 15:121-132.

Springer NM, Danilevskaya ON, Hermon P, Helentjaris TG, Phillips RL, Kaeppler HF, Kaeppler SM (2002) Sequence relationships, conserved domains, and expression patterns for maize homologs of the polycomb group genes *E(z)*, *esc*, and *E(Pc)*. *Plant Physiol* 128(4):1332-1345.

Stamatakis A (2014) RAxML Version 8: A tool for phylogenetic analysis and post-analysis of large phylogenies. *Bioinformatics* 30(9):1312-1313.

Tian T, Liu T, Yan H, You Q, Yi X, Du H, Xu W, Su Z (2017) agriGO v2.0: a GO analysis toolkit for the agricultural community, 2017 update. *Nucleic Acids Res* 45(W1):W122-W129

Tomato Genome Consortium (2012) The tomato genome sequence provides insights into fleshy fruit evolution. *Nature* 485(7400): 635-641.

Wang G, Wang G, Zhang X, Wang F, Song R (2012) Isolation of high quality RNA from cereal seeds containing high levels of starch. *Phytochem Anal* 23(2):159-163.

Wickramasuriya AM, Dunwell JM (2015) Global scale transcriptome analysis of *Arabidopsis* embryogenesis *in vitro*. *BMC Genomics* 16(1):301.

Xu H, Gao Y, Wang J (2014) Transcriptome analysis of rice (*Oryza sativa*) developing embryos using the RNA-Seq technique. *PLoS ONE* 7(2):e30646.

Zhang J, Shan L, Duan J, Wang J, Chen S, Cheng Z, Zhang Q, Liang X, Li Y (2011) *De novo* assembly and characterization of the transcriptome during seed development, and generation of genic-SSR markers in peanut (*Arachis hypogaea L.*). *BMC Genomics* 13:90-96.

Zilberman D, Gehring M, Tran RK, Ballinger T, Henikoff S (2006) Genome-wide analysis of *Arabidopsis thaliana* DNA methylation uncovers an interdependence between methylation and transcription. *Nature Genet* 39:61-69.

Funding Information

This work was supported by a NSF Doctoral Dissertation Improvement Grant (Grant number 1500963; Evolution of Angiosperm Seed Development: perspectives from *Nymphaea thermarum* (Nymphaeales).

Acknowledgments

We thank the staff of Harvard FAS Informatics for assistance with development of data analysis strategy, and Morgan Moglein and Johan Jaenisch for their work in key developing aspects of the RNA extraction protocol used in this study.

Appendix: Supplementary Material

Page

112 **Chapter 2 Supplementary Material**

113 **Supplementary Materials and Methods**

116 **Supplementary Figures S2.1-S2.2**

118 **Supplementary Tables S2.1-S2.10**

123 **List of Supplementary Dataset 2.1**

124 **Chapter 3 Supplementary Material**

124 **Supplementary Materials and Methods**

125 **Supplementary Table S3.1-S3.2**

126 **List of Supplementary Datasets 3.1-3.3**

Chapter 2 Supplementary Information

Supplementary Materials and Methods

Flow Cytometry Chromosome Counts in Whole Mounts

For flow cytometry, prepared samples (Doležel *et al.*, 2007) were analyzed at the Baur Core Facility of Harvard University on a BD LSR II flow cytometer, using the settings for the Pacific-Blue-A fluorochrome, and resulting data were analyzed with BD FACSDiva7.0. Samples from a known diploid individual of *Nymphaea thermarum* were used as the control.

For chromosome counting, 2-3 clean, healthy root tips or young shoot apical meristems (including young leaf primordia) were collected per plant, incubated in a saturated solution of 1-Bromonapthalene for 4 or more hours at room temperature, transferred to a solution of 3:1 95% ethanol and glacial acetic acid, fixed overnight, and stored at -20 C°. Prior to staining, the clear outer root caps were removed and remaining root tips stained with the Feulgen reaction, cleared, and imaged (Povilus *et al.*, 2015) with a 63x lens on a Zeiss LSM700 Confocal Microscope, equipped with an AxioCam HRc camera (Zeiss, Oberkochen, Germany) (excitation = 405 nm and 488 nm, detection = 405-700 nm, pinhole = 60 ųm). Chromosome counts were performed on z-stacks of complete nuclei in ImageJ or Zeiss LSM Image Browser, and 3D models of nuclei were created using the 3D Viewer plugin in ImageJ.

Chromosome counts of all samples were within (+/- 1) of expected values for either diploid (2n = 28) or tetraploid (2n = 56) individuals. The +/-1 uncertainty of chromosome number is due to the very small size of chromosomes in *N. thermarum*, combined with the somewhat large number of chromosomes. For chromosome counts, multiple cells were counted for each individual; both root tips and shoot apical meristems cells were observed.

When both methods were used for a single individual, they always gave the same result for the ploidy of that individual. Similarly, when multiple cells from multiple tissues from the same individual were analyzed via chromosome counts, the same ploidy was recovered (2n = 28, 4n = 56, 3n = 42). The consistency of chromosome number between tissue types means that tetraploid plants are unlikely to be chimeras of diploid and tetraploid cells, and are therefore likely to produce diploid gametes. In order to verify that gametes produced by tetraploid parents were diploid, we assessed the ploidy of embryos that resulted from interploidy crosses. Chromosome number was counted for multiple individuals from

multiple fruits of each interploidy cross type and 2x2 crosses: the number of chromosomes in all counted cells from interploidy offspring was 42 (+/- 1), as expected. For cells from embryos that resulted from the 2x2 crosses, the chromosome number was 28 (+/-1), as expected for diploid individuals.

Cross Fertilizations

Randomly selected, unopened flower buds were emasculated at least 24 hours before the first day of anthesis to generate outcrossing female flowers, and any older flowers or fruits were removed. Pollen (collected the same day from randomly-selected male-phase flowers) was manually added to stigmatic surfaces of female flowers on the first day of anthesis via paint brush and transfer of whole, open anthers; efforts were made to transfer roughly equal amounts of pollen for each cross. Controlled cross-pollinated flowers were bagged with a nylon mesh to prevent spurious cross-pollination from other plants, and the bag was removed at 7 days after anthesis; fruits were re-bagged at 25 days after anthesis to facilitate seed collection. All emasculations, pollen collection, and cross-pollinations occurred between 10 and 11 am on any given day. *N. thermarum* flowers continuously but only supports one open flower at a time. If a flower was used as the female in a cross-pollination, all subsequent floral buds were removed until the fruit of interest was collected.

Self-fertilizations

Flowers were covered with a nylon mesh bag on the morning of the first day of anthesis to prevent cross-pollination, and any older flowers or fruits were removed. The bag was removed at 7 days after anthesis; fruits were re-bagged at 25 days after anthesis to facilitate seed collection. If a flower was allowed to self-pollinate, all subsequent floral buds were removed until the fruit of interest was collected.

Confocal Microscopy of Prepared Samples

Samples were prepared and imaged with previously established methods (Povilus *et al.*, 2015). Briefly: tissues were stained according the Fuelgen method, and then infiltrated with and embedded in JB-4 glycol methacrylate (Electron Microscopy Sciences, Hatfield, PA, USA). Blocks were cut by hand with razor blades to remove superfluous tissue layers. Samples were mounted in a drop of Immersol 518f (Zeiss,

Oberkochen, Germany) on custom well slides and imaged with a Zeiss LSM700 Confocal Microscope, equipped with an AxioCam HRc camera (Zeiss, Oberkochen, Germany). One of two excitation/detection settings was used for any given sample: 1) excitation at 405 and 488 nm, emission detection between 400-520 nm (Channel 1) and 520-700 (Channel 2) and 2) excitation at 638 nm, emission detection between 520-700 nm (Channel 1). Z-stacks of optical sections were collected to include the maximum longitudinal section of a seed. Zeiss LSM Image Browser was used to obtain seed component measurements.

Data Analysis

Comparisons of cross- and self-fertilized seeds from diploid parents

Germination rates of seeds from diploid self-fertilizations and 2x2 crosses were not significantly different (t-test, t = 0.3717, df = 35, p-value = 0.7124). Measurements of perisperm and the endosperm tissues were not significantly different for seeds from diploid self-fertilizations or 2x2 crosses (perisperm: t = -1.324, df = 311, p-value = 0.1865; endosperm: t = -1.1305, df = 242.876, p-value = 0.2594). For the embryo, equality of the means between diploid self-fertilizations and 2x2 crosses could not be rejected (t = -2.6479, df = 248.899, p-value = 0.008617), but the actual difference in means was very small (95% CI = 0.007 - 0.001 mm2, or an average of 4.2% difference).

Linear Effect Modeling

The number of mature seeds per fruit were counted, and these data were fitted with a zero-inflated generalized linear model with a negative binomial distribution (using the glmmadmb package (Fournier *et al.*, 2012) and the hurdle function of the pcs1 package in R (Zeileis *et al.*, 2008); cross type was used as the fixed effect for both components of the zero-inflated model.

The percent of ungerminated seeds was calculated for each fruit, and these data were fitted with a generalized linear model (glm function in R) with a gamma distribution (as data were exponentially distributed), using cross type as the fixed effect.

Mixed linear effect models (lmer function of the lme4 package in R) (Bates *et al.*, 2015) were used to examine the effect of cross type on the sizes of (separately) the perisperm, endosperm, and embryo. For all models, fruit ID was included as a random effect, as multiple seeds per fruit were measured.

Embryo and endosperm measurements were log transformed for 7DAA (untransformed model residual plots displayed obvious skewing; model coefficients were back-transformed before calculation of effect sizes). Seed component sizes at 7 DAA, as well as endosperm cell number and endosperm average cell size, were additionally modeled using maternal ploidy, paternal ploidy, and the interaction of maternal and paternal ploidy as fixed effects. Maternal ploidy was used as the fixed effect to model tissue size in pre-fertilization ovules (nucellus and female gametophyte). Pairwise comparisons between cross types were performed using the summary function in R and manually defining the reference cross type to report all 6 comparisons.

A generalized linear mixed-effect model (glmer function of lme4 package in R) (Bates *et al.*, 2015) was used to test for effects of cross type, time, and their interaction on the proportion of embryos of each cross type that had or had not undergone key morphological transitions at a given time point.

Supplementary Figures:

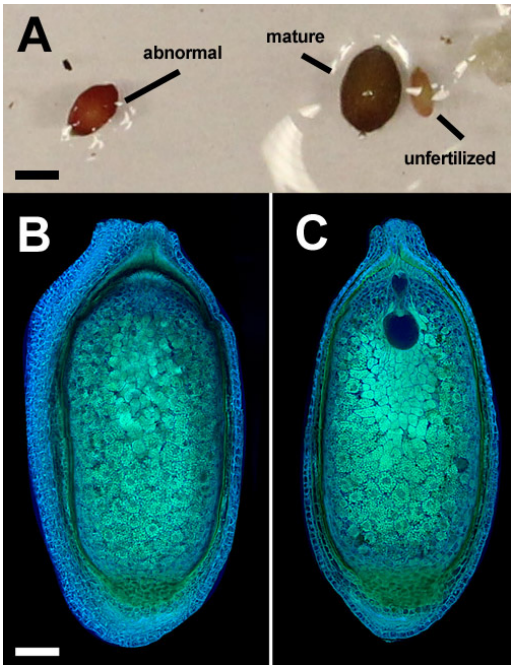

Supplementary Figure 2.1: Types of seeds found in mature fruits

Definition of mature seeds, which were included in further analysis: A) In fruits from cross-pollinated or self-fertilized flowers, typically three types of ovules/seeds could be distinguished by external appearance: 1) mature seeds (brown seed coat, plump), 2) abnormal, 'young-looking' seeds (immature pink seed coat, small size), and 3) unfertilized ovules (pale colored and very small). Abnormal, 'young-looking' seeds were processed for confocal microscopy to see whether they were fertilized but aborted seeds. (Scale bar = 1 mm) B) In all of the abnormal seeds analyzed, starch had accumulated in the perisperm in a pattern similar to ~7 days after anthesis for a normal seed. Many of these "seeds" had not been fertilized, as degenerating female gametophytes were found and no remnants of a pollen tube or pollen tube discharge could be seen at the micropyle. (Scale bar = 0.1 mm) C) Occasionally in abnormal seeds, nuclei or cells were noted in the space normally occupied by offspring tissues, but these were never arranged in a manner that resembled any stage of viable embryo or endosperm development. Because these 'abnormal' seeds were not demonstrably the product of fertilization events, they (and unfertilized seeds) were omitted from further analysis. (Scale bar = 0.1 mm)

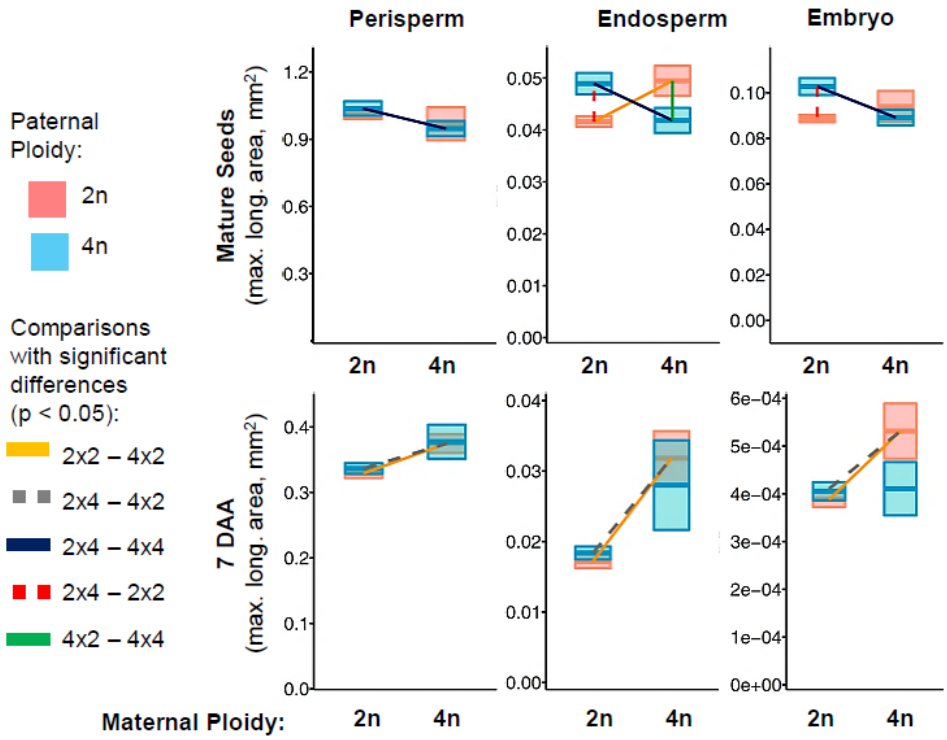

Supplementary Figure 2.2: Summary of seed component size measurements

Sizes of seed components at 7DAA and seed maturity, for each cross type. Boxes represent 95% confidence intervals and dark horizontal lines represent mean tissue size for a cross type. Significant differences between specific cross types are noted by lines (if a comparison between two crosses is not assigned a line color/type, the difference was not significant for any tissue at any time point). See Tables S3, S5 for linear effect model descriptions and outputs. Number of seeds measured for seed component sizes: 7DAA (2x2 = 200, 2x4 = 182, 4x2 = 112, 4x4 = 26), maturity (2x2 = 313, 2x4 = 123, 4x2 = 57, 4x4 = 96).

Supplementary Tables

Supplementary Table 2.1: Effects of Cross type on Seed Set and Seed Germination

Number of Mature Seeds per Fruit,

for Fruits with Non-zero Seed Counts

(Count model coefficients)

Fixed Parts	Estimate	Std. Error	p
(Intercept)	4.9363	0.1907	< 2e-16 ***
2x4	**-0.9292**	**0.2741**	**<0.001*** **
4x2	**-1.3074**	**0.3638**	**<0.001*** **
4x4	**-1.1558**	**0.5341**	**0.030***
Log(theta)	-0.2072	0.1736	0.232

Proportion of Fruits with No Seeds

(Zero hurdle model coefficients)

Fixed Parts	Estimate	Std. Error	p
(Intercept)	0.2072	0.2330	0.374
2x4	0.4205	0.3207	0.190
4x2	0.6305	0.4082	0.122
4x4	0.7688	0.5779	0.183
Observations	236		

Percent of Un-germinated Seeds Per Fruit

Fixed Parts	Estimate	St. Error	P
(Intercept)	4.3960	0.0852	0.002
2x4	-0.1561	0.1196	0.1919
4x2	**-0.3662**	**0.1491**	**0.0141***
4x4	**-1.5628**	**0.3430**	**<0.001*** **
Observations	82		

Supplementary Table 2.2: Effects of cross type on tissue sizes in mature seeds

Mixed Linear Models = tissue size ~ cross type + (1|fruit ID)

Reference level = 2x2 cross

	Perisperm Size			Endosperm Size			Embryo Size		
Fixed Parts	Estimate	Std. Error	p	Estimate	Std. Error	p	Estimate	Std. Error	p
(Intercept)	1.015	0.024	< 0.001	0.042	0.001	<0.001	0.089	0.001	<0.001
2x4	0.067	0.041	0.102	**0.009**	**0.002**	**<0.001 *****	**0.017**	**0.004**	**<0.001 *****
4x2	0.034	0.052	0.522	**0.008**	**0.003**	**<0.004****	0.008	0.005	0.141
4x4	- 0.058	0.049	0.240	0.001	0.004	0.622	0.001	0.005	0.809
Random Parts									
$N_{fruit\ ID}$		75			75			75	
$ICC_{fruit\ ID}$		0.579			0.606			0.606	
Observations		582			584			584	

Supplementary Table 2.3: Pairwise comparisons of different cross types in mature seeds

Mixed Linear Models = tissue size ~ cross type + (1|fruit ID)

	Perisperm Size			Endosperm Size			Embryo Size		
Fixed Parts	Estimate	Std. Error	p	Estimate	Std. Error	p	Estimate	Std. Error	p
2x2 – 2x4	0.067	0.041	0.102	**0.009**	**0.002**	**<0.001 *****	**0.017**	**0.004**	**<0.001 *****
2x2 – 4x2	0.034	0.052	0.522	**0.008**	**0.003**	**0.004 ****	0.008	0.005	0.141
2x2 – 4x4	-0.058	0.049	0.240	0.001	0.002	0.622	0.001	0.005	0.809
2x4 – 4x2	-0.033	0.058	0.558	-0.002	0.003	0.501	-0.009	0.006	0.107
2x4 – 4x4	**-0.125**	**0.054**	**0.022***	**-0.008**	**0.003**	**0.003****	**-0.016**	**0.005**	**0.004 ****
4x2 – 4x4	-0.092	0.063	0.150	**-0.006**	**0.003**	**0.042***	-0.007	0.006	0.299
Random Parts									
$N_{fruit\ ID}$		75			75			75	
$ICC_{fruit\ ID}$		0.579			0.606			0.606	
Observations		582			584			584	

Supplementary Table 2.4: Effects of cross type on tissue sizes in 7DAA seeds

Mixed Linear Models = tissue size ~ cross type + (1|fruit ID)

Reference level = 2x2 cross

	Perisperm Size			log10(Endosperm Size)			log10(Embryo Size)		
Fixed Parts	Estimate	Std. Error	p	Estimate	Std. Error	p	Estimate	Std. Error	p
(Intercept)	0.331	0.009	< 0.001	- 1.800	0.035	<0.001	- 3.427	0.020	<0.001
2x4	0.006	0.013	0.648	0.033	0.048	0.490	0.011	0.027	0699
4x2	**0.038**	**0.016**	**0.017***	**0.212**	**0.060**	**<0.001 *** **	**0.088**	**0.034**	**0.012***
4x4	0.036	0.021	0.095	0.143	0.080	0.079	0.040	0.048	0.400
Random Parts									
$N_{fruit\ ID}$		68			68			68	
$ICC_{fruit\ ID}$		0.512			0.679			0.388	
Observations		517			515			511	

Supplementary Table 2.5: Pairwise comparisons of different cross types in 7DAA seeds

Mixed Linear Models = tissue size ~ cross type + (1|fruit ID)

	Perisperm Size			log10(Endosperm Size)			log10(Embryo Size)		
Fixed Parts	Estimate	Std. Error	p	Estimate	Std. Error	p	Estimate	Std. Error	p
2x2 – 2x4	0.006	0.013	0.648	0.033	0.048	0.490	0.011	0.027	0.700
2x2 – 4x2	**0.038**	**0.016**	**0.017 ***	**0.212**	**0.060**	**<0.001 *** **	**0.088**	**0.034**	**0.012 ***
2x2 – 4x4	0.036	0.021	0.096	0.143	0.080	0.079	0.040	0.048	0.400
2x4 – 4x2	**0.035**	**0.015**	**0.037 ***	**0.180**	**0.059**	**0.003 ** **	**0.077**	**0.033**	**0.024 ***
2x4 – 4x4	0.042	0.021	0.157	0.110	0.080	0.170	0.030	0.047	0.531
4x2 – 4x4	-0.003	0.023	0.911	-0.070	0.087	0.427	-0.048	0.052	0.364
Random Parts									
$N_{fruit\ ID}$		68			68			68	
$ICC_{fruit\ ID}$		0.516			0.679			0.388	
Observations		517			515			511	

Supplementary Table 2.6: Effects of cross type on tissue sizes in 7DAA seeds

Mixed Linear Models = tissue size ~ maternal ploidy * paternal ploidy + (1|fruit ID)

Reference level = 2n maternal ploidy and 2n paternal ploidy

	Perisperm Size			log10(Endosperm Size)			log10(Embryo Size)		
Fixed Parts	Estimate	Std. Error	p	Estimate	Std. Error	p	Estimate	Std. Error	p
(Intercept)	0.331	0.009	< 0.001	- 1.800	0.035	<0.001	- 3.427	0.020	<0.001
Maternal Ploidy (4n)	**0.038**	**0.016**	**0.0168 ***	**0.212**	**0.060**	**<0.001 *** **	**0.088**	**0.034**	**0.012***
Paternal Ploidy (4n)	0.006	0.013	0.6479	0.033	0.048	0.490	0.011	0.027	0.700
Maternal * Paternal Ploidy	-0.008	0.026	0.7504	- 0.103	0.099	0.305	- 0.058	0.058	0.326
Random Parts									
$N_{\text{fruit ID}}$		68			68			68	
$ICC_{\text{fruit ID}}$		0.512			0.679			0.388	
Observations		517			515			511	

Supplementary Table 2.7: Endosperm Cell Number at 7DAA

Model = endosperm cell # ~ maternal ploidy * paternal ploidy +

(1|fruit ID)

Reference level = 2n maternal ploidy and 2n paternal ploidy

	Endosperm Cell Number		
Fixed Parts	Estimate	Std. Error	p
(Intercept)	37.894	1.824	<.001
Maternal Ploidy (4n)	4.671	2.777	0.101
Paternal Ploidy (4n)	-5.574	2.764	0.051
Maternal * Paternal Ploidy	-3.883	4.685	0.412
Random Parts			
$N_{\text{fruit ID}}$		38	
$ICC_{\text{fruit ID}}$		0.534	
Observations		176	

Supplementary Table 2.8: Average Endosperm Cell Size at 7DAA

Models = log10(average endosperm cell size) ~ maternal ploidy *

paternal ploidy + (1|fruit ID)

Reference level = 2n maternal ploidy and 2n paternal ploidy

	Endosperm Cell Number		
Fixed Parts	Estimate	Std. Error	p
(Intercept)	- 3.352	0.018	<.001
Maternal Ploidy (4n)	**0.031**	**0.028**	**0.264**
Paternal Ploidy (4n)	0.078	0.028	0.008**
Maternal * Paternal Ploidy	0.117	0.036	0.002**
Random Parts			
$N_{\text{fruit ID}}$		38	
$ICC_{\text{fruit ID}}$		0.493	
Observations		173	

Supplementary Table 2.9: Unfertilized ovules (one day before anthesis)

Models = tissue size ~ maternal ploidy

Reference level = 2n maternal sporophyte

	Nucellus Size			Female Gametophyte Size		
Fixed Parts	Estimate	Std. Error	p	Estimate	Std. Error	p
(Intercept)	0.071	0.001	<0.001	0.003	0.012	< 0.001
Maternal Ploidy (4n)	**0.007**	**0.002**	**0.004 ****	**0.001**	**0.020**	**< 0.001 *****
Observations		53			53	

Supplementary Table 2.10: Embryo Development Stage

Model = embryo developmental stage ~ cross * daa (day after anthesis),

family = binomial

Reference level = 2x2 cross at 7 DAA

	Endosperm Cell Number		
Fixed Parts	Estimate	Std. Error	p
(Intercept)	- 1.436	0.180	<.001
Cross 2x4	0.187	0.265	0.481
Cross 4x2	0.212	0.329	0.520
Cross 4x4	**1.249**	**0.415**	**0.003 ****
DAA 13DAA	- 0.064	0.454	0.889
Cross 2x4 : DAA 13DAA	- 14.233	514.561	0.978
Cross 4x2 : DAA 13DAA	**1.482**	**0.608**	**0.015 ***
Cross 4x4 : DAA 13DAA	- 0.727	0.739	0.323
Observations		580	

List of Supplementary Datasets

- **Supplementary Dataset 2.1: Measurements of seed number and viability, ovule/seed component size and endosperm cell number**

Chapter 3 Supplementary Information

Supplementary Materials and Methods

RNA extractions:

For RNA extractions, 30-50 mg of tissue was ground in liquid nitrogen with a mortar and pestle before being added to 0.4 mL extraction buffer (100 mM Tris-HCL (pH 9), 2% (v/v) 2-Mercaptoethanol, 2% (w/v) PVP40). 40 µl 10% SDS was added and samples were centrifuged at 12k g for 10 minutes at 4 C. The aqueous phase was transferred to a new tube with 2 volumes of TRIzol (Invitrogen). 1/5 volume chloroform was added, samples were centrifuged at 12k g for 10 min at 4 C, and the aqueous phase was transferred to a new tube. TRIzol extraction was repeated as necessary, up to two more times. An equal volume of cold isopropanol was added to the final aqueous phase, and samples were precipitated at -20 C for 60 min. Pellets were resuspended in H_20, and 2 volumes of saturated acid-phenol:chloroform (5:1) were added. Samples were centrifuged at 12k g for 20 min at 4 C, and the aqueous phase was transferred to a new tube. The acid-phenol extraction was repeated as necessary, up to two more times. If necessary, an additional hot (60 C) acid-phenol phase extraction was performed. For 15 DAA, samples were further purified with a column-based clean-up, using RNeasy Plant Mini Kit (Qiagen) spin columns, according to manufacturer protocol.

Supplemental Table 3.1: Number of reads and proportion of reads mapped for each sample, and for all samples.

Sample	lane 6	lane 7	lane 8	total # reads (paired-end)	reads processed (# read pairs)	reads pseudoaligned (# read pairs)	% reads aligned
1	28,513,314	28,648,800	28,702,606	85,864,720	42,932,360	32,536,875	0.757863649
2	33,267,596	33,432,100	33,489,220	100,188,916	50,094,458	38,815,246	0.774841121
3	23,998,898	24,115,398	24,156,412	72,270,708	36,135,354	28,344,177	0.784389078
4	22,002,490	22,097,360	22,143,926	66,243,776	33,121,888	26,898,197	0.812097336
5	25,246,136	25,382,372	25,411,120	76,039,628	38,019,814	31,515,995	0.828936065
6	23,799,238	23,913,086	23,994,098	71,706,422	35,853,211	29,543,087	0.824001147
7	25,719,940	25,841,438	25,881,410	77,442,788	38,721,394	31,750,444	0.819971616
8	24,241,300	24,331,190	24,425,946	72,998,436	36,499,218	29,397,934	0.805440106
9	24,367,252	24,484,652	24,513,926	73,365,830	36,682,915	26,926,752	0.734040684
10	26,928,802	27,053,360	27,109,876	81,092,038	40,546,019	28,736,670	0.708742084
11	27,721,958	27,863,756	27,890,298	83,476,012	41,738,006	28,537,801	0.683736569
12	26,195,536	26,316,798	26,366,644	78,878,978	39,439,489	24,840,072	0.62982743
				Total number reads:		Total number of reads pairs aligned (and total number reads aligned):	Total % reads aligned:
				939,568,252		357,843,250 (715,686,500 total)	0.761718479

Supplemental Table 3.2: Comparison of linear models, testing for the effect of time (daa) on the mean TPM values (per time point) of the 0.1% most highly expressed transcripts

Analysis of Variance Table

Model 1: log2(meanTPM + 1) ~ 1

Model 2: log2(meanTPM + 1) ~ daa

	Res.Df	RSS	Df	Sum of Sq	F	Pr(>F)
Model 1	74	73.014				
Model 2	72	58.970	2	14.043	8.5732	0.0004573

List of Supplementary Datasets

- **Supplementary Dataset 3.1: Summary of transcript expression values**
- **Supplementary Dataset 3.2: Summary of differential expression analysis**
- **Supplementary Dataset 3.3: Summary of expression pattern clusters**